**UNIVERSIDADE FEDERAL DE PELOTAS**
**Faculdade de Agronomia Eliseu Maciel**
**Programa de Pós-Graduação em Ciência e Tecnologia de Alimentos**

Tese de Doutorado

# Integrating morpho-anatomical insights and innovative technologies to enhance the extraction and application of anthocyanins and antioxidants from purple sweet potato

**Gabriel Laquete de Barros**
Engenheiro Agrônomo

Pelotas, 2025

**Gabriel Laquete de Barros**

# Integrating morpho-anatomical insights and innovative technologies to enhance the extraction and application of anthocyanins and antioxidants from purple sweet potato

Tese de doutorado apresentada ao Programa de Pós-Graduação em Ciência e Tecnologia de Alimentos da Faculdade de Agronomia Eliseu Maciel da Universidade Federal de Pelotas, como requisito parcial à obtenção do título de Doutor em Ciência e Tecnologia de Alimentos.

Orientador: Prof. Dr. Leonardo Nora
Coorientadores: Prof. Cesar Valmor Rombaldi, Ph.D.; Pesq. Márcia Vizzotto, Ph.D., Prof. Ali Ubeyitogullari, Ph.D.

Pelotas, 2025

**Gabriel Laquete de Barros**

**Integrating morpho-anatomical insights and innovative technologies to enhance the extraction and application of anthocyanins and antioxidants from purple sweet potato**

Tese de doutorado aprovada como requisito parcial para a obtenção do grau de Doutor em Ciência e Tecnologia de Alimentos, Programa de Pós-Graduação em Ciência e Tecnologia de Alimentos, Faculdade de Agronomia Eliseu Maciel, Universidade Federal de Pelotas.

Data da defesa: 18 de agosto de 2025.

Banca examinadora:

Prof. Dr. Leonardo Nora, Ph.D. (orientador), Ph.D. em *Plant Molecular Biology*, pela *University of East Anglia*, Inglaterra.

Prof.ª Dr.ª Carmen Luiza Feitosa de Lima Gomes, Ph.D. em *Biological and Agricultural Engineering* pela Texas A&M University, TAMU, Estados Unidos da América.

Prof.ª Dr.ª Helayne Aparecida Maieves, Doutora em Tecnologia de Alimentos pela Universidade Federal do Paraná.

Prof. Dr. Nathan Levien Vanier, Doutor em Ciência e Tecnologia de Alimentos pela Universidade Federal de Pelotas.

Prof.ª Dr.ª Rosane Lopes Crizel, Doutora em Ciência e Tecnologia de Alimentos pela Universidade Federal de Pelotas.

Universidade Federal de Pelotas / Sistema de Bibliotecas
Catalogação da Publicação

B277i Barros, Gabriel Laquete de

Integrating morpho-anatomical insights and innovate technologies to enhance the extraction and application of anthocyanins and antioxidants from purple sweet potato [recurso eletrônico] / Gabriel Laquete de Barros, Leonardo Nora ; Leonardo Nora, orientador ; Cesar Valmor Rombaldi, Márcia Vizzotto, Ali Ubeyitogullari, coorientadores. — Pelotas, 2025.

127 f.

Tese (Doutorado) — Programa de Pós-Graduação em Ciência e Tecnologia de Alimentos, Faculdade de Agronomia Eliseu Maciel, Universidade Federal de Pelotas, 2025.

1. Dióxido de carbono supercrítico. 2. Técnica sustentável. 3. Ferramenta de decisão. 4. Aerogéis bioativos. 5. Encapsulamento. I. Nora, Leonardo. II. Nora, Leonardo, orient. III. Rombaldi, Cesar Valmor, coorient. IV. Vizzotto, Márcia, coorient. V. Título.

CDD 633.492

Elaborada por Ubirajara Buddin Cruz CRB: 10/901

## Dedicatória

**Dedico este trabalho aos meus pais e avós, cujos valores, coragem e sacrifícios foram o alicerce da minha formação e da minha trajetória de vida. Aos meus irmãos, pelo apoio e incentivo constantes, e aos amigos que caminharam comigo, oferecendo força, escuta e amizade nos momentos mais desafiadores. Estendo esta dedicatória a todos os colegas, professores e técnicos da universidade que, de alguma forma, contribuíram para a realização deste trabalho. Em especial, ao meu orientador, por sua orientação generosa, paciência e compromisso com meu crescimento acadêmico. A cada um de vocês, meu mais profundo reconhecimento e gratidão.**

## Dedicatória

Agradeço a Deus pela sua bondade e generosidade comigo, obrigado pelas oportunidades e por ser minha fortaleza em todos os momentos dessa trajetória.

Aos meus pais, Helena e Laquete, que me apoiaram incondicionalmente, acreditaram em mim quando eu não acreditava, sendo fundamentais nesse processo.

À minha família, especialmente meus avós, irmãos, sobrinhos, cunhados, primos e tios, pela compreensão, carinho e torcida de sempre.

À Flávia e Renires, que além de colegas de pós-graduação são grandes amigas, sou muito grato por cada momento que dividimos, todos eles nos fizeram mais fortes. Obrigado por me incentivarem e ajudarem durante esses anos!

À Áuria, pelo companheirismo e força e por cada momento que dividimos, todos eles serviram de motivação, força, coragem e fé de tudo daria frutos prósperos.

Ao meu orientador, Prof. Dr. Leonardo Nora, que me acompanhou nesse período, muito obrigado pelas oportunidades, confiança e todo suporte no doutorado.

Aos meus coorientadores Prof. Dr. Cesar Valmor Rombaldi, Prof. Drª Márcia Vizzotto, pelo acompanhamento, muito obrigado pelas oportunidades, confiança e todo suporte no doutorado.

Prof. Dr. Ali Ubeyitogullari, pela receção e coorientação deste projeto no exterior, bem como sua disponibilidade e auxílio com o experimento no campo.

Agradeço, também, aos demais colegas de pós-graduação, estudantes de iniciação científica e professores que enriqueceram ainda mais essa jornada.

À Universidade Federal de Pelotas e ao Programa de Pós-Graduação em Ciência e Tecnologia de Alimentos pela oportunidade e à Coordenação de Aperfeiçoamento de Pessoal de Nível Superior (CAPES) pelo apoio financeiro.

À University of Arkansas e ao Food Science Department pela oportunidade e à Programa Institucional de Internacionalização por meio da Coordenação de Aperfeiçoamento de Pessoal de Nível Superior (CAPES-Print) pelo apoio financeiro.

## Resumo

DE BARROS, Gabriel Laquete. **Integrando conhecimentos morfoanatômicos e tecnologias inovadoras para aprimorar a extração e a aplicação de antocianinas e antioxidantes da batata-doce roxa.** 2025. 159f. Tese (Doutorado em Ciência e Tecnologia de Alimentos) – Programa de Pós-graduação em Ciência e Tecnologia de Alimentos, Faculdade de Agronomia Eliseu Maciel, Universidade Federal de Pelotas, Pelotas, 2025.

A batata-doce roxa (*Ipomoea batatas* L.) tem se consolidado como uma importante fonte de antocianinas e compostos antioxidantes, despertando crescente interesse para aplicações como corantes naturais e ingredientes funcionais. Esta tese propõe uma abordagem integrada combinando conhecimentos morfo-anatômicos com tecnologias inovadoras de extração e incorporação, visando ampliar a eficiência, a estabilidade dos compostos em sistemas alimentares. Primeiramente, foi desenvolvida uma ferramenta de decisão que orienta a escolha do método de extração mais adequado com base nas características estruturais da matriz vegetal. A partir de uma revisão abrangente da literatura científica entre 2018 e 2023, foi validada experimentalmente em matrizes como amora-preta e batata-doce roxa, evidenciando a influência da estrutura vegetal sobre o rendimento e a eficiência do processo. Em seguida, investigou-se a aplicação do dióxido de carbono supercrítico (SC–$CO_2$) como alternativa sustentável aos métodos convencionais de extração. Os melhores resultados foram obtidos com 30 MPa, 35 °C e 20% de co-solvente ((mistura de etano e água 60% (v/v)), alcançando altos teores de fenólicos e antocianinas, além de expressiva atividade antioxidante. Por fim, foram desenvolvidos aerogéis bioativos a partir de pó e resíduos de batata-doce roxa combinados com amido de milho, utilizando secagem com SC–$CO_2$ para encapsular extratos das misturas do pó de batata-doce roxa e amido de milho, e resíduo de batata-doce roxa, com adição e não adição de antocianinas. A formulação com 50% de PSPP (pó de batata-doce roxa) e 50% de CS (amido de milho) carregada com antocianinas destacou-se pelo equilíbrio entre rendimento, estabilidade e atividade antioxidante, demonstrando potencial para aplicações como ingrediente funcional e corante natural. Os resultados confirmam que a integração entre conhecimento anatômico da planta, tecnologias verdes de extração e estratégias de encapsulamento permite otimizar o aproveitamento de compostos bioativos.



**Palavras-chave**: Dióxido de carbono supercrítico; técnica sustentável; Ferramenta de decisão; Aerogéis bioativos; Encapsulamento.

## Abstract

DE BARROS, Gabriel Laquete. **Integrating morpho-anatomical insights and innovative technologies to enhance the extraction and application of anthocyanins and antioxidants from purple sweet potato.** 2024. 159f. Thesis (Doctorate in Food Science and Technology) – Programa de Pós-graduação em Ciência e Tecnologia de Alimentos, Faculdade de Agronomia Eliseu Maciel, Universidade Federal de Pelotas, Pelotas, 2024.

The purple sweet potato (*Ipomoea batatas* L.) has been consolidated as an important source of anthocyanins and antioxidant compounds, attracting growing interest for applications as natural colorants and functional ingredients. This thesis proposes an integrated approach combining morpho-anatomical knowledge with innovative extraction and incorporation technologies to enhance the efficiency and stability of these compounds in food systems. First, a decision tool was developed to guide the selection of the most suitable extraction method based on the structural characteristics of the plant matrix. Built from a comprehensive review of the scientific literature between 2018 and 2023, it was experimentally validated in matrices such as blackberry and purple sweet potato, highlighting the influence of plant structure on process yield and efficiency. Next, the application of supercritical carbon dioxide (SC–$CO_2$) was investigated as a sustainable alternative to conventional extraction methods. The best results were obtained at 30 MPa, 35 °C, and 20% co-solvent (a mixture of ethanol and water, 60% v/v), achieving high levels of phenolics and anthocyanins, along with remarkable antioxidant activity. Finally, bioactive aerogels were developed from purple sweet potato powder and residues combined with corn starch, using SC–$CO_2$ drying to encapsulate extracts of the purple sweet potato powder–corn starch mixtures and purple sweet potato residues, with and without anthocyanin addition. The formulation containing 50% PSPP (purple sweet potato powder) and 50% CS (corn starch), loaded with anthocyanins, stood out for its balance between yield, stability, and antioxidant activity, demonstrating potential for applications as a functional ingredient and natural colorant. Overall, the results confirm that integrating plant anatomical knowledge, green extraction technologies, and encapsulation strategies optimizes the utilization of bioactive compounds.



**Keywords**: Supercritical carbon dioxide; Sustainable techniques; Decision tool; Bioactive aerogels; Encapsulation.

## List of Figures

Figure 1. Changes in the characteristics of anthocyanins by temperature, pH, Hydroxyl (OH) and Water (H2O), ACY-G (anthocyanin glucoside), CRB-G (Carbidol glucoside), QND-G (Khenidal glucoside), QNA-G (Anionic kenoidal glucoside), CCN-G (chalcone glucoside). ..... 27
Figure 2. A comprehensive illustrative system describing the sources of anthocyanin extraction, the solvents used for extraction, the extraction methods used, the similarity characteristics between methods, and the raw material ..... 39
Figure 3. Accumulation of anthocyanins in the main plant organs (A) and their predominant physicochemical structures (B). ..... 44
Figure 4. Decision- tree for selecting anthocyanin extraction methods based on intrinsic characteristics and response to solvents. RS – Porosity; AFNT – Affinity; STM – State of Matter; CCM – Coating Component; PS – Particle Size; ATXT – Anatomical Texture; PSCT–Polysaccharide Type; ANE – Anatomical Structure; (1) Hydrophilic; (2) Hydrophobic; (3) Water; (4) Alcohol; (5) Acid; (6)Basic; (7) Film; (8) fiber; (9) Micro; (10) Macro; (11) FLS – Fleshy; (12) JCY – Juicy; (13) DRY – Dry; (14) LGN – Lignin; (15) STC – Starch; (16) PCN – Pectin; (17) Gel; (18) CLS – Cellulose; (19) HCL – Hemicellulose; (20) MC – Mesocarp; (21) PR – Pericarp; (22) CPR – Receptacle; (23) EXP -Exocarp; (24)EC -Endocarp; (25) EP – Epidermis. ..... 45
Figure 5. Schematic diagram of SCsingle bondCO2 extraction system. (1) CO2 cylinder; (2) heating jacket; (3) needle valve; (4) compressor; (5) high-pressure pump; (6) cosolvent; (7) cosolvent pump; (8) rupture disk; (9) temperature controlling unit; (10) high-pr pressure vessel; (11) needle valve; (12) micrometering valve; (13) sample collecting vial in an ice bath; and (14) flow meter. ..... 90
Figure 6. Total phenolic contents (TPC) extracted with SCsingle bondCO2 modified with ethanol-water (50 %) at different conditions. Means ± standard deviation bars that do not share the same letter are significantly different ($p < 0.05$). ..... 95
Figure 7. Total anthocyanin contents (ANC) extracted with SC−CO2 modified with ethanol-water (50 %) at different conditions. Means ± standard deviation bars that do not share the same letter are significantly different ($p < 0.05$). ..... 95
Figure 8. Effect of cosolvent composition on the TPC and ANC yields following 20 % cosolvent modified SC single bond CO2 extraction at 30 MPa and 35 °C for 180 min. Means ± standard deviation bars that do not share the same letter are significantly different ($p < 0.05$) ..... 98
Figure 9. Effect of time on the total phenolic and anthocyanin yields following 20 % cosolvent (60 % ethanol) modified SC single bond CO2 extraction at 30 MPa and 35 °C. ..... 99
Figure 10. TPC and ANC extraction yields from different extraction methods (Table 1). Means ± standard deviation bars that do not share the same letter are significantly different ($p < 0.05$) ..... 101
Figure 11. HPLC/UV–Vis chromatograms for anthocyanins obtained through different extractions from PSP. The identification of the peaks is provided in Table 2. ..... 103
Figure 12. Reveals the impact of different treatments on structural morphology. The untreated sample (C) indicated a nearly complete coating of additional structures and obstructed the identification of clear starch morphology. Ethanolic (E1, E2) and methanolic (M1 and M2) residue after extraction showed the adhered structures comparable with SCsingle bondCO2 extraction (S16 and S18) ..... 106
Figure 13. Schematic diagram of SC-CO2 drying system. (1) CO2 cylinder; (2) heating jacket; (3) needle valve; (4) compressor; (5) high-pressure pump; (6) temperature controlling unit; (7) high-pressure vessel; (8) needle valve; (9) micrometering valve; (10) ice bath to collect ethanol; and (11) flow meter ..... 113
Figure 14. Relationship between apparent viscosity (Pa.s) and shear rate (1/s) for four

different formulations containing varying concentrations of PSPP (25%; 50%; 75%; and 100%).....119
Figure 15. Hydrogels and aerogels formed with the mixture of PSPP and CS mixture (PSPP0-CS100; PSPP25-CS75; PSPP50-CS50; PSPP75-CS25; PSPP100-CS0; and PSPR50-CS0. PSPP: purple sweet potatoes powder. CS: corn starch.....120
Figure 16. Impact of the gelatinization process on hydrogels prepared from PSPR at varying polymer concentrations (25%, 50%, and 75%) after anthocyanins extraction. PSPR: purple sweet potatoes residue (i.e., spent purple sweet potatoes after anthocyanins extraction). .....121
Figure 17. The outer and cross-section layers of aerogels infused with anthocyanins in samples from a mixture of PSPP and CS mixture at various concentrations (PSPP0-CS100-ANT; PSPP25-CS75-ANT; PSPP50-CS50-ANT; PSPP75-CS25-ANT; and PSPR50-CS0-ANT), dried using SC-CO2 at 40 ◦C and 10 MPa with a flow rate of 0.5 L/min. PSPP: purple sweet potato powder. CS: corn starch. ANT: Anthocyanins extract. PSPR: purple sweet potato residue after extraction.....123
Figure 18. SEM micrographs of empty aerogels from PSPP, PSPR, and CS mixture (PSPP0-CS100-CS100; PSPP25-CS75; PSPP50-CS50; PSPP75-CS25; PSPP100-CS0; and PSPR50-CS0. PSPP: purple sweet potatoes powder. CS: corn starch. PSPR: purple sweet potatoes residue after extraction.....124
Figure 19. The water solubility (wt.%) of aerogels from a mixture of PSP, PSPR, and CS mixtures at various concentrations (PSPP0-CS100-CS100; PSPP25-CS75; PSPP50-CS50; PSPP75-CS25; PSPP100-CS0; and PSPR50-CS0). Table 1 gives the sample descriptions. PSPP: purple sweet potato powder. CS: corn starch. ANT: Anthocyanins extract. PSPR: purple sweet potato residue after extraction.....126
Figure 20.Total phenolic compounds (TPC) and anthocyanins (ANT) in aerogels made from a mixture of PSPP and corn starch mixture at various concentrations (PSPP0-CS100, PSPP25-CS75, PSPP50-CS50, PSPP75-CS25, PSPP100-CS0, and PSPR50-CS0 (a) before and (b) after loading. .....128
Figure 21. Antioxidant properties of corn starch-based aerogels with different levels of (PSPP0-CS100, PSPP25-CS75, PSPP50-CS50, PSPP75-CS25, PSPP100-CS0, and PSPR50-CS0) using DPPH and ABTS assays before (a) and after (b) encapsulation. .....131
Figure 22. FRAP (a) and ORAC (b) assay of aerogels made from a mixture of PSPP-corn starch mixture at various concentrations (PSPP0-CS100, PSPP25-CS75, PSPP50-CS50, PSPP75-CS25, PSPP100-CS0, and PSPR50-CS0) after loading.....135
Figure 23. HPLC/UV-Vis chromatograms for aerogels obtained from a mixture PSPP and corn starch at various concentrations (PSPP0-CS100, PSPP25-CS75, PSPP50-CS50, PSPP75-CS25, and PSPR50-CS0) after anthocyanin loading.....137
Figure 24. Circular economy process applied to purple sweet potato: (1) raw material; (2) pre-treatment; (3) anthocyanin extraction; (4) post-extraction residue; (5) aerogel production; (6) anthocyanin encapsulation in aerogels .....144

## List of Tables

Table 1. Aerogel samples prepared using varying concentrations (0%-100%) of purple sweet potato powder (PSPP), purple sweet potato residue (PSPR) (25%-75%), and corn starch (CS) (0%-100%). ..... 111
Table 2.Textural properties of aerogels prepared with varying proportions of purple sweet potato powder (PSPP), corn starch (CS), and purple sweet potato residue (PSPR), determined by nitrogen adsorption using the BET method. **Error! Bookmark not defined.**
Table 3. Peak assignment, mass (M+), and ion fragmentation (MS/MS) of anthocyanins aerogels from purple sweet potato (PSP). ..... 137

## List of abbreviations and acronyms

| | |
|---|---|
| PSP | Supercritical Carbon Dioxide |
| PSPR | Purple Sweet Potato Residue |
| SC-$CO_2$ | Supercritical Carbon Dioxide |
| TPC | Total Phenolic Content |
| ANC | Anthocyanin Extract |
| CS | Corn Starch |
| BET | Brunauer–Emmett–Teller |
| BJH | Barrett–Joyner–Halenda |
| SEM | Scanning Electron Microscopy |
| HPLC | High-Performance Liquid Chromatography |
| UV-Vis | Ultraviolet-Visible Spectroscopy |
| ESI-MS | Electrospray Ionization–Mass Spectrometry |
| MRM | Multiple Reaction Monitoring |
| $p/p_0$ | Relative Pressure |
| RPM | Revolutions Per Minute |

## Table of Contents


**1 INTRODUCTION ..... 15**

**2 HYPOTHESES ..... 17**

**3 GOAL AND OBJECTIVES ..... 19**

3.1. GOAL ..... 19

3.2. **SPECIFIC OBJECTIVES ..... 19**

**4 LITERATURE REVIEW ..... 19**

4.1 Health Benefits and Functional Properties of Anthocyanins ..... 18

4.2 Anthocyanin Extraction Technologies ..... 20

4.3 Stabilization of anthocyanins using aerogels and $SCO_2$ approaches ..... 24

**5 CHAPTER 1: ANTHOCYANIN EXTRACTION METHODS: SYNTHESIS OF MORPHO-ANATOMICAL KNOWLEDGE FOR DECISION-MAKING BASED ON DECISION-TREE ..... 26**

5.1. **DISCUSSION OF RESULTS ..... 26**

5.1.1. Anthocyanin extraction methods ..... 26

5.1.1.1. Conventional extraction method (CME) ..... 27

5.1.1.2. Non-conventional extraction methods ..... 28

5.1.1.3. Conventional and non-conventional solvents for anthocyanin extraction ..... 36

5.1.1.4. Basic Decision-Tree Design Considerations ..... 38

5.1.1.5 Criteria for the decision tree in the selection of the appropriate method for extracting anthocyanins ..... 44

5.1.1.6. Decision-tree applicability criterion an example of its use ..... 46

5.2. **CONCLUSION ..... 47**

**6 CHAPTER 2 – EXTRACTION OF ANTHOCYANINS FROM PURPLE SWEET POTATO USING SUPERCRITICAL CARBON DIOXIDE AND CONVENTIONAL APPROACHES ..... 86**

**6.1 INTRODUCTION ..... 86**

**6.2. MATERIALS AND METHODS ..... 87**

6.1.2 Methods ..... 88

6.4. **RESULTS AND DISCUSSION ..... 93**

6.4.1. Sample characteristics ..... 93

6.4.2. Optimization of cosolvent-modified SC-CO2 extraction ..... 93

6.4.3. Comparison of the extraction methods ..... 100

6.4.4. Identification of anthocyanins ..... 102

6.4.5. Antioxidant activity ..... 103
6.4.6. Morphology ..... 105
6.5. **CONCLUSIONS** ..... **106**
**7 CHAPTER 3 – DEVELOPING ANTHOCYANIN-LOADED AEROGELS FROM PURPLE SWEET POTATOES USING SUPERCRITICAL CARBON DIOXIDE DRYING** ..... **108**
**7.1 INTRODUCTION** ..... **108**
7.2. **MATERIALS AND METHODS** ..... **109**
7.2.1. Materials ..... 109
7.2.2. Methods ..... 110
7.3. **RESULTS AND DISCUSSION** ..... **117**
7.3.1 Physicochemical properties of PSP ..... 117
7.3.3 Hydrogel formation ..... 119
7.3.4. Aerogel formation ..... 121
7.3.5. Aerogels Characterization ..... 123
7.3.7. Total phenolic content and total anthocyanins after loading ..... 129
7.3.8. Antioxidant activities before loading ..... 130
7.3.9. Antioxidant activities after loading ..... 132
7.4. **CONCLUSIONS** ..... **138**
7.5. Circular economy ..... 144
**8 GENERAL CONCLUSION** ..... **145**

# 1 INTRODUCTION

Anthocyanins are a group of flavonoids in fruits, vegetables, and flowers, resulting in a broad color spectrum. This group of optically intense and biologically active pigments receives substantial support for its antioxidant properties (JESUS et al., 2021). Research suggests that their antioxidant and oxidative stress-reducing properties could benefit health by providing an anti-inflammatory effect, protecting the cardiovascular system, and offering anticancer benefits (ROJAS-OCAMPO et al., 2021; SOARE et al., 2020; ZANNOU et al., 2022). These properties of anthocyanidins have also attracted the notice of researchers in nutrition, medicine, and food science because of their relationship to protective effects in the nervous system and metabolism (HENDERSON et al., 2011; MANOUSI et al., 2019; YUN et al., 2025).

Anthocyanins, a natural colorant and functional ingredient, are increasingly in demand in food and healthcare products (F. F. LI et al., 2025; LU et al., 2024; ZHAO et al., 2024). The healthful, garden-variety alternative became popular as consumers became aware of the health risks associated with artificial dyes (MAAZ et al., 2025). Anthocyanins offer a two-for-one special: the chance to make sausages and soft drinks look as good as they taste while pumping up the healthy properties of our food (MAAZ et al., 2025; WEISS et al., 2024; YUN et al., 2025). Nevertheless, some critical issues remain significant barriers to potential commercial applications (CHEN et al., 2025; GONZÁLEZ-LÁZARO et al., 2024; LAKSHMIKANTHAN et al., 2024; SHI et al., 2024).

Purple potatoes (*Ipomoea batatas),* instead, are another interesting anthocyanin material (after all, in particular regarding cyanidin and peonidin derivatives) (JESUS et al., 2021; LAILA et al., 2025; YAN et al., 2024). They are high in pigment and nutrients and are widely grown in China, Brazil, and Mozambique for traditional and popular culinary use. In addition, by-products (such as skins and processing residues) have the potential to be considered as valuable resources. Recycling these by-products fulfills the demand of a “circular economy”. It can solve environmental problems from agro-waste by converting agro-residues into biofunctional materials with high performance (JESUS et al., 2021).

One of the major problems is the chemical instability of anthocyanins, which are extremely sensitive to external factors, such as light, pH, temperature, and oxygen. Hence, these molecules are prone to rapid deterioration and poor bioactivity, which impact and restrict their functional applications in complex food systems with long-term stability (GULATI et al., 2025; RAJ et al., 2024; XUE et al., 2024). Additionally, the inefficiency of

the extraction process compounds the problem. This waste of material and labor combines to detract from the quality of the finished product while also raising the cost of manufacture. These are why novel, sustainable, and scalable methods for recovering and stabilizing anthocyanins are needed to overcome this industry's bottlenecks effectively (GUAN et al., 2025; OTTO et al., 2024; SAINI et al., 2024; XUE et al., 2024).

Current extraction techniques often rely on conventional solvent-based methods associated with several limitations (MACHADO et al., 2015; NUNES MATTOS et al., 2022; REZENDE et al., 2017). These methods frequently use organic solvents that are not environmentally friendly, require large volumes of chemicals, and involve high energy consumption. Additionally, they expose anthocyanins to harsh conditions that can degrade their bioactive properties. Supercritical carbon dioxide (SC-$CO_2$) extraction has emerged as a promising green technology that addresses these limitations. SC-$CO_2$ operates under mild conditions, reducing the risk of thermal degradation, and uses safe solvents, such as co-solvent modified approaches (ethanol-water mixtures and $CO_2$), to enhance the selectivity and efficiency of anthocyanin recovery. This technique aligns with the growing emphasis on sustainable food-processing practices while delivering high-quality bioactives for industrial applications (DE BARROS et al., 2024).

The stabilization is another critical challenge in the utilization of anthocyanins. Once extracted, these compounds are prone to degradation, which limits their shelf life and usability in functional food systems. Encapsulation, particularly in bioactive aerogels, offers an effective solution for protecting anthocyanins from environmental stressors. Aerogels are lightweight, porous structures with excellent adsorption and release properties, making them ideal carriers for bioactive compounds. Incorporating anthocyanins into aerogels enhances their stability and facilitates their controlled release and integration into diverse food matrices (MALEKI et al., 2015; MOHAMMADI et al., 2025; SOHRABI et al., 2024; K. ZHANG et al., 2024).

This research integrates three complementary approaches. The first focuses on developing a decision-tree framework to guide the selection of optimal anthocyanin extraction methods(DONG et al., 2025; SENEVIRATHNA et al., 2024). This framework incorporates morpho-anatomical characteristics of plant matrices and key extraction parameters, providing a systematic approach to improving efficiency and resource utilization. By synthesizing knowledge from diverse studies, the decision-tree tool simplifies the decision-making process for researchers and industry professionals, enabling them to

select the most suitable extraction techniques for specific plant matrices. The second approach evaluates supercritical carbon dioxide (SC-$CO_2$) extraction as a sustainable alternative to conventional methods. This study aims to optimize extraction parameters, such as pressure, temperature, co-solvent concentration, and extraction time, to maximize anthocyanin yield and preserve their antioxidant properties. SC-$CO_2$ technology significantly advances green extraction methods, combining high efficiency with minimal environmental impact. The final approach focuses on developing anthocyanin-loaded aerogels from purple sweet potatoes using SC-$CO_2$. The aerogels were developed from purple sweet potato powder and corn starch, incorporating anthocyanins into their porous structure to enhance stability and functionality. The use of purple sweet potato residues in aerogel production aligns with circular economy principles and demonstrates the feasibility of creating value-added products from agricultural by-products. These aerogels hold promise as functional ingredients and natural colorants for the food and nutraceutical industries, addressing the dual demands of sustainability and consumer health.

In summary, the research aimed to contribute to the sustainable utilization of anthocyanins while advancing the principles of circular economy. This work holds significant implications for the food and nutraceutical industries, offering scalable solutions that align with environmental and economic sustainability goals.

## 2 HYPOTHESES

2.1. Due to the influence of morpho-anatomical characteristics on the efficiency of anthocyanin extraction, a decision-tree framework can systematically optimize the selection of extraction methods, improving yield and resource utilization compared to conventional approaches.

2.2. Supercritical carbon dioxide (SC-CO,ÇÇ) extraction, by operating under mild conditions and using selective co-solvents, is expected to minimize anthocyanin degradation caused by heat and oxidative stress, enabling higher recovery and preservation of bioactive properties compared to traditional solvent-based methods.

2.3 Bioactive aerogels derived from purple sweet potato residues, through their ability to protect anthocyanins from environmental stressors such as light and pH fluctuations, are anticipated to enhance stability and functionality while aligning with circular economy principles by utilizing agricultural by-products in a sustainable food system.

# 3 GOAL AND OBJECTIVES

## 3.1. Goal

To develop and implement sustainable strategies for extracting and stabilizing anthocyanins from purple sweet potato, utilizing decision-making tools and methods based on supercritical carbon dioxide and bioactive aerogels, in accordance with circular economy principles.

## 3.2. Specific objectives

3.2.1. To develop a decision-making tool based on morpho-anatomical characteristics to optimize the selection of anthocyanin extraction methods in different plant matrices.

3.1.2. To investigate the influence of morpho-anatomical parameters of plant matrices on the yield and quality of extracted anthocyanins.

3.1.3. To evaluate and optimize the use of supercritical carbon dioxide (SC-$CO_2$) as a sustainable alternative for anthocyanin extraction, comparing it with conventional methods.

3.3.4. To develop bioactive aerogels using purple sweet potato residues and corn starch to encapsulate and stabilize extracted anthocyanins, enhancing their antioxidant functionality.

3.3.5. To demonstrate the feasibility of integrating circular economy principles in the extraction and application of anthocyanins by utilizing agricultural by-products (purple sweet potatoes residue) as base materials for functional systems.

# 4 LITERATURE REVIEW

## 4.1 Health Benefits and Functional Properties of Anthocyanins

Anthocyanins are natural pigments widely distributed in the plant kingdom, belonging to the flavonoid family of phenolic compounds (ZOU et al., 2024). These water-soluble pigments are synthesized in the cytosol and stored in vacuoles, contributing to various plant tissues' red, purple, and blue colors, including fruits, vegetables, and flowers (CAO et al., 2024). Their functionality includes: enhancing the visual appeal of foods and offering potent health benefits due to their strong antioxidant properties (LIDIKOVÁ et al., 2025). Chemically, anthocyanins are glycosides of anthocyanidins, composed of an aglycone base (anthocyanidin), sugar moieties, and occasionally acyl groups, which enhance their water solubility and molecular stability (MENGIST et al., 2025; NGUYEN et al., 2016). The most common anthocyanins found in nature cyanidin, delphinidin, pelargonidin, peonidin, petunidin, and malvidin are differentiated by their unique patterns of hydroxylation and methylation on the B-ring, influencing their color manifestation, antioxidant capacity, and molecular interactions within food matrices (G. L. DE BARROS et al., 2024; EVANS et al., 2009; QIU et al., 2025).

In food systems, anthocyanins are used as natural colorants. They are considered safer and more appealing alternatives to synthetic dyes like FD&C Red No. 40 and Yellow No. 5. Their pH-sensitive nature enables a broad color spectrum, ranging from red in acidic environments to purple and blue in neutral or alkaline media, making them suitable for beverages, confectionery, dairy, and baked goods. (PATNI, 2024; ZHANG et al., 2016). Beyond coloration, anthocyanins offer notable bioactive properties, including antioxidant, anti-inflammatory, anti-obesity, and cardioprotective effects (BORDA et al., 2025; DONG et al., 2022; ZHANG et al., 2017). They neutralize reactive oxygen species (ROS), protecting cells from oxidative damage a key factor in aging and chronic disease development. Several studies have confirmed that regular intake of anthocyanin-rich foods can help reduce the risk of cardiovascular diseases and diabetes by improving lipid profiles and regulating glucose metabolism (KLINGER et al., 2024; OLIVEIRA et al., 2020; YANG et al., 2024).

Despite their recognized benefits, anthocyanins face challenges regarding stability and functional performance, being susceptible to environmental conditions such as pH, temperature, light, and oxygen (ZHU et al., 2024). These pigments exhibit red coloration in acidic environments (pH < 3) but shift to purple or blue as pH increases, often degrading into colorless chalcones or hemiketals under neutral or alkaline conditions (H. W. CHEN et al., 2024; PEI et al., 2024). Prolonged heat exposure can lead to thermal degradation, diminishing their effectiveness as natural colorants and antioxidants. At the same time, light

and oxygen can accelerate oxidative degradation, shortening the shelf life of anthocyanin-enriched food product (KUMKUM et al., 2024; LAKSHMIKANTHAN et al., 2024; STANCA et al., 2024). These limitations necessitate advanced stabilization and encapsulation techniques to preserve anthocyanin bioactivity and allow effective incorporation into industrial applications.

### 4.2. Purple sweet potatoes as anthocyanins sources

The purple sweet potato (*Ipomoea batatas*) emerges as a promising source of anthocyanins, particularly cyanidin and peonidin glycosides, due to its high pigment concentration, nutritional value, and agricultural adaptability (JESUS et al., 2021). Its by-products, such as peels and processing residues, are also rich in anthocyanins and represent an untapped resource for circular economy models aimed at waste reduction and sustainable material development. These residues can serve as valuable raw materials for producing high-value ingredients, especially when modern green extraction and stabilization strategies are applied. Addressing extraction inefficiencies and improving pigment stability can significantly enhance purple sweet potato anthocyanins for industrial-scale applications (HAYES et al., 2008; SENDRI et al., 2024).

However, challenges persist in scaling up cost-effective and eco-friendly extraction and stabilization techniques especially considering the sensitivity of anthocyanins to pH, light, and oxygen and in raising consumer awareness to foster broader market acceptance (NURDJANAH et al., 2022). In the case of purple sweet potato, future efforts should also address factors such as yield optimization, production costs, and the socio-economic relevance of cultivation in major producing countries. Globally, the average yield is around 14 t/ha, but under optimal conditions in countries such as the United States and parts of Asia, yields can reach 20–26 t/ha. In many African regions, yields remain significantly lower at about 4.7 t/ha, although South Africa has achieved over 40–50 t/ha under advanced management practices. Sweet potato is grown in 114 countries worldwide, with Asia contributing about 61–66% of total production and Africa 29–34%. In Africa alone, production reached approximately 29.5 million tons in 2022, with Malawi, Tanzania, Nigeria, and Angola among the leading producers (KAUR et al., 2024). In Mozambique, production was estimated at around 625,000 tons in 2018. These figures highlight the importance of optimizing value chains, from cultivation to functional food applications. Advancing technologies such as SC-$CO_2$ extraction and aerogel-based stabilization, while valorizing agricultural by-products, will be crucial to drive innovation and ensure long-term sustainability in functional food development (FORGHANI et al., 2025).

### 4.1 Anthocyanin Extraction Technologies

Conventional extraction methods for anthocyanins predominantly utilize solvent-based techniques, employing organic or aqueous solvents such as ethanol, methanol, acetone, or water, often acidified with hydrochloric or citric acid, to enhance pigment solubility and stability. While these methods are straightforward, cost-effective, and supported by well-established protocols validated across various plant matrices, they present environmental and health challenges (ARRUDA et al., 2021; JIN et al., 2017; MAITY, 2015). The toxicity of organic solvents, the necessity for recovery systems, and the high energy consumption associated with solvent evaporation are significant drawbacks. Additionally, prolonged exposure to heat and oxygen during extraction can lead to the degradation of anthocyanins, thereby diminishing their functional properties (ALIBADE et al., 2021; MANOUSI et al., 2019).

To address these limitations, emerging technologies such as supercritical carbon dioxide (SC-$CO_2$) extraction, ultrasound-assisted extraction (UAE), and microwave-assisted extraction (MAE) have been developed to enhance extraction efficiency while preserving bioactivity (FARIAS et al., 2022; S. S. ZHANG et al., 2024; ZHENG et al., 2016). SC-$CO_2$ extraction, recognized as a green technology, operates above the critical temperature and pressure of $CO_2$, allowing it to function as both a gas and a liquid. This unique characteristic enables effective penetration of plant matrices when combined with co-solvents like ethanol or water. This method minimizes thermal and oxidative degradation, utilizes a non-toxic and recoverable solvent system, and eliminates the need for harmful organic solvents(JIANG et al., 2024; SURESH et al., 2024). However, it requires substantial equipment investment and the use of co-solvents due to the polarity of anthocyanins (DE BARROS et al., 2024). Its application in purple sweet potato has demonstrated effectiveness, yielding high anthocyanin content with retained antioxidant activity, particularly from processing residues, thereby aligning with circular economy practices (ZUIN, 2016).

Conversely, ultrasound-assisted extraction (UAE) employs high-frequency sound waves to create cavitation, disrupting plant cell walls and facilitating the release of anthocyanins into the solvent. This technique enhances mass transfer and extraction efficiency through localized pressure and temperature spikes. UAE offers several advantages over conventional methods, including faster extraction times, reduced solvent and energy requirements, and better preservation of thermosensitive anthocyanins due to shorter processing durations (KIM et al., 2024; LEONARSKI et al., 2025). However, it also presents limitations, particularly the risk of anthocyanin degradation if parameters such as ultrasonic power and duration are not optimized, along with limited scalability for industrial applications.
Microwave-assisted extraction (MAE) utilizes microwave energy to heat plant tissues, leading

to the rupture of cell walls and the release of anthocyanins into the solvent. This method provides high efficiency with minimal solvent use, offering advantages such as uniform heating, shorter processing times, enhanced extraction efficiency, high reproducibility, and compatibility with green solvent systems like ethanol-water mixtures. However, excessive microwave intensity or duration can lead to degradation, and initial investments for large-scale deployment can be high (FARIAS et al., 2022).

When comparing extraction methods, each presents distinct advantages and trade- offs, depending on specific goals and industrial contexts. While conventional solvent-based methods remain widely adopted for their simplicity, emerging technologies like SC-$CO_2$, UAE, and MAE offer improved extraction yields, environmental benefits, and enhanced compound stability. Notably, SC-$CO_2$ aligns well with green chemistry and circular economy principles, supporting the sustainable valorization of agricultural residues, such as purple sweet potato by-products.

Looking ahead, further research should focus on optimizing these advanced methods for industrial scalability, particularly for underutilized crops, and integrating decision-support tools to enhance efficiency and sustainability in anthocyanin recovery. Despite advancements in extraction technologies, anthocyanins remain highly sensitive to environmental conditions. Their degradation compromises pigment stability, visual appeal, and antioxidant capacity, limiting their practical application in food systems. Therefore, addressing stability challenges is crucial for extending the shelf life and functional performance of anthocyanin-rich products. Anthocyanins: sensitive and advanced stabilization technique. (CUI et al., 2025; FEITOSA et al., 2025).

Thermal degradation presents another major challenge, as anthocyanins are highly susceptible to heat during common food processing operations such as pasteurization, sterilization, and cooking. Exposure to temperatures above 50–80°C significantly decreases anthocyanin content and can lead to the formation of polymeric pigments with diminished color intensity and bioactivity. Preventing such thermal damage involves the use of milder processing techniques or encapsulation technologies that shield anthocyanins from direct heat. In addition, anthocyanins are vulnerable to oxidative degradation triggered by ultraviolet and visible light exposure, which can cleave molecular bonds and reduce stability. Oxygen further accelerates oxidative reactions, promoting pigment bleaching and the formation of undesirable by-products, especially through interactions with other phenolics that diminish antioxidant performance. To preserve anthocyanin integrity, advanced packaging approaches such as opaque or UV-blocking materials, along with modified atmosphere packaging (MAP) to reduce oxygen availability, are essential interventions during storage and distribution (HUANG et al., 2024; SONG et al., 2025; ZHANG et al.,

2025).

## 2.2. Aerogels as Stabilization Platforms

In complex food systems, anthocyanins interact with proteins, lipids, and other polyphenols, which affects their stability and bioavailability; for instance, interactions with proteins may cause pigment precipitation, oxidized lipids can accelerate degradation through secondary oxidation products, and co-pigmentation with polyphenols may intensify color but also destabilize the compounds under certain conditions. (TANG et al., 2024). To address these challenges, various stabilization techniques have been developed, including encapsulation technologies such as spray drying, freeze drying, and aerogel formation, which protect anthocyanins from environmental stressors; aerogels, in particular, offer porous, lightweight structures that ensure controlled release and superior protection. Stabilizers like acids, sugars, or polysaccharides help maintain an optimal microenvironment for example, citric acid preserves an acidic pH to prevent degradation (FORGHANI et al., 2025; MALEKI et al., 2015; MOHAMMADI et al., 2025). Low-temperature processes further minimize thermal damage, while innovative packaging solutions, including UV-blocking materials and oxygen scavengers, enhance shelf life by limiting exposure to harmful conditions. These stability strategies are especially relevant for purple sweet potato (PSP) anthocyanins, which face similar degradation risks during processing and storage.

Encapsulation in bioactive aerogel matrices derived from PSP residues mitigates the impacts of pH, heat, and oxidation while supporting sustainable food applications. Technologies like supercritical carbon dioxide (SC-$CO_2$) extraction also align with green chemistry principles, preserving anthocyanin bioactivity with reduced environmental impact. Ultimately, the stabilization of anthocyanins remains a critical research area aimed at overcoming their sensitivity to environmental conditions and ensuring their viability in food, pharmaceutical, and nutraceutical industries (NOMAN et al., 2025). Among encapsulation techniques, spray drying stands out for its speed and affordability, although high temperatures may partially degrade anthocyanins. Freeze drying offers better retention of color and bioactivity due to its gentle processing, albeit with higher energy demands and slower throughput. Bioactive aerogels, produced via freeze-drying or SC-$CO_2$ drying, offer exceptional protection and encapsulation efficiency, particularly when sourced from natural biopolymers like PSP residues, contributing both to product performance and sustainable processing solutions.

### 4.3. Stabilization of anthocyanins using aerogels and $SCO_2$ approaches

Aerogels offer significant advantages for anthocyanin stabilization due to their high surface area and porosity. They provide excellent protection against environmental stressors and enable controlled release properties, making them ideal for functional food and nutraceutical applications (MALEKI et al., 2015). Their incorporation of agricultural residues, such as purple sweet potato peel or residual fibers, enhances sustainability and supports circular economy principles. Additionally, a mixture of different non-valued crops can help to improve the high value of processed foods. For example, aerogels derived from purple sweet potato residues and corn starch have shown notable promise in stabilizing anthocyanins while creating value-added materials (L. LI et al., 2025).

Furthermore, co-pigmentation of natural processes involving non-covalent interactions between anthocyanins and molecules like polyphenols, flavonoids, or metal ions serves to enhance both stability and color intensity, particularly in beverages and food products (K. ZHANG et al., 2024). However, its effects can be limited under extreme environmental conditions and are often complemented by encapsulation. The incorporation of stabilizing agents such as polysaccharides (e.g., pectin, xanthan gum, chitosan) forms protective matrices that minimize anthocyanin exposure to oxygen and light, while sugars and organic acids like glucose, sucrose, and citric acid help maintain acidic conditions favorable to the flavylium cation form, enhancing color stability (DARABI et al., 2016; LIU et al., 2017).

Other than that, advances in material science have further improved stabilization strategies through nanostructured systems like nanoparticles and nanofibers, which improve both protection and bioavailability, and through hybrid gels that combine natural and synthetic polymers to provide superior chemical and mechanical stability. Among these, aerogels remain a standout option due to their structural advantages and biocompatibility, with their development from agricultural by-products such as purple sweet potato residues representing a promising convergence of innovation and sustainability in anthocyanin stabilization. (KUANG et al., 2015; ZHENG et al., 2016).

Recent studies demonstrate that supercritical $CO_2$ drying effectively produces aerogels with high structural integrity and efficient anthocyanin retention, thus offering a robust solution to the challenges of industrial-scale stabilization. In parallel, agricultural by-products such as peels, stems, and other processing residues are often rich in bioactive compounds, yet remain underutilized. Purple sweet potato residues, in particular, offer significant potential due to their high anthocyanin, phenolic, and dietary fiber content. These residues can be repurposed into functional ingredients through the extraction of bioactives, developed into sustainable materials such as aerogels or edible films, or even applied in

secondary uses like animal feed or organic fertilizers post-extraction.

This approach minimizes waste and enhances the economic and environmental value of the entire production chain. Moreover, supercritical carbon dioxide (SC-$CO_2$) extraction exemplifies a green, solvent-free technology that aligns with these sustainability goals, offering a cleaner and more efficient alternative for recovering anthocyanins from underutilized biomass. As a result, combining SC-$CO_2$ extraction with bio-based material development supports both innovation and circularity in anthocyanin applications (KAUR et al., 2023).

The application of circular economy principles in anthocyanin production, particularly through the use of supercritical carbon dioxide (SC-$CO_2$) extraction and agricultural residue valorization, offers substantial environmental and economic advantages. SC-$CO_2$ extraction reduces the reliance on harmful solvents by employing $CO_2$ and minimal amounts of co-solvents like ethanol, both of which are environmentally safe and recyclable, contributing to a cleaner, energy-efficient process.

The integration of this green technology with the reuse of purple sweet potato residues establishes a closed-loop system that enhances sustainability across the value chain. Agricultural by-products, such as peels and processing waste, are transformed into high-performance aerogels, biodegradable, lightweight carriers that stabilize anthocyanins and enable their controlled release in functional food and nutraceutical applications. These aerogels not only reduce environmental impact but also add value to what would otherwise be waste, reinforcing resource efficiency.

# 5 CHAPTER 1: ANTHOCYANIN EXTRACTION METHODS: SYNTHESIS OF MORPHO-ANATOMICAL KNOWLEDGE FOR DECISION-MAKING BASED ON DECISION-TREE

This review's primary objective was to investigate the fundamental principles underlying the efficacy of anthocyanin extraction methods, particularly their interaction with diverse cellular anatomical structures found in plant matrices. A comprehensive combination of systematic and non-systematic literature searches was used to conduct this review. Initially, a systematic review was performed to investigate methods for extracting anthocyanins (PAGE et al., 2021). Simultaneously, a non-systematic review was conducted to explore the anatomy and physiology of plant structures containing anthocyanins. Subsequently, the literature was organized based on citation frequency and its relevance in constructing a decision-tree.

For the systematic review, comprehensive searches were conducted covering the years 2018 to 2023. At first, many publications were identified, totaling 994, 970, 810, and 10 records: Web of Science, Scopus, Medline (via PubMed), and SciELO, respectively. In addition, duplicate publications, primary sources not relevant to the central object of study, review articles, and books were excluded, resulting in a total of 1053 publications. The most cited publications on anthocyanin extraction methods (those with more than ten citations) were highlighted for inclusion in this study. Additionally, recent and relevant literature was used as a criterion for the search method to include articles that may have yet to achieve a high citation rate due to their recent publication date. The selection process resulted in 36 publications to be analyzed in this review (PAGE et al., 2021).

For a non-systematic review, we examined the literature on the botanical anatomy and physiological mechanisms involved in anthocyanin accumulation within plant structures. This literature provided valuable insights into how anthocyanins are stored within cellular structures and their metabolic pathways. Finally, synthesized information from systematic and non-systematic reviews was used to construct the decision-tree.

## 5.1. Discussion of results

### 5.1.1. Anthocyanin extraction methods

Anthocyanin extraction methods can be classified into conventional and innovative (Fig. 3). Among the 36 articles selected for the systematic review, five reviews used conventional methods, 29 publications referred to innovative extraction, and two used a combination of both (De Barros et al., 2024). The following description details the categorization and operating principles of these methods.

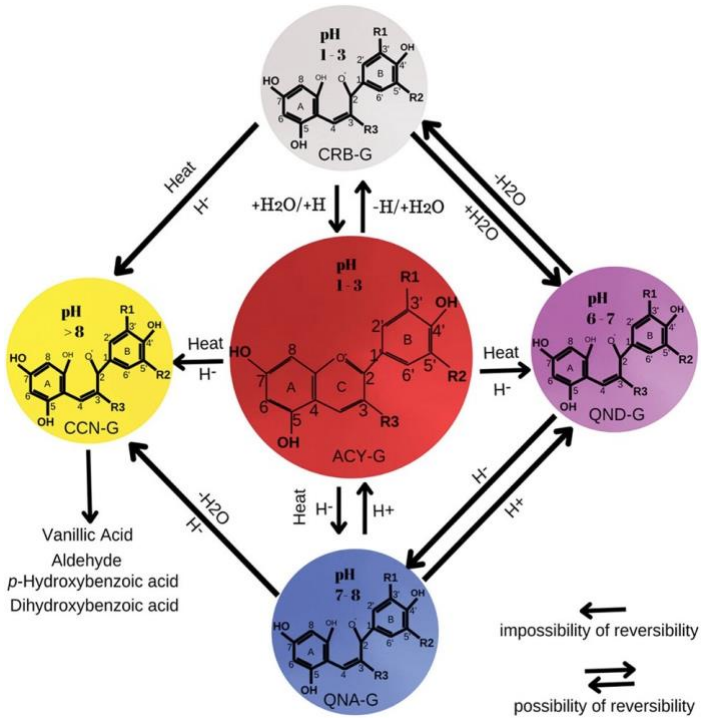


**Figure 1.** Changes in the characteristics of anthocyanins by temperature, pH, Hydroxyl (OH) and Water (H2O), ACY-G (anthocyanin glucoside), CRB-G (Carbidol glucoside), QND-G (Khenidal glucoside), QNA-G (Anionic kenoidal glucoside), CCN-G (chalcone glucoside). Source: designed by the Author, 2025

#### 5.1.1.1. Conventional extraction method (CME)

The CME used conventionally follows procedures commonly employed for anthocyanin extraction (Fig. 1). It can be categorized based on the process, techniques, and type of solvent employed. The most widely recognized conventional methods are: Maceration: mixing the raw sample, whether fresh or dry, directly with a solvent after disrupting the cell processes using tools such as a crusher and pestle (LÓPEZ et al., 2018). Infusion: Like maceration, water is used as a solvent instead of other liquids (YONG et al., 2018).

##### 5.1.1.1.1 Digestion

The sample undergoes maceration, and the temperature is also increased, typically above the environmental condition (25 °C) (LÓPEZ et al., 2018).

Decoction: This method involves preparing an infusion with water heated above its boiling point (YIN et al., 2022).

##### 5.1.1.1.2 Percolation and Filtration

The sample is mixed continuously in a solvent-dried state. Thus, the renewal processes occur in a percolator and then filtration (TAN et al., 2020).

#### 5.1.1.1.3 Soxhlet

This method involves cyclic and continuous mixing of a solid-state sample with a solvent within a Soxhlet system over a controlled period (WANG et al., 2023).

The solvent selection for anthocyanin extraction follows the 'like dissolves like' principle. Anthocyanins, inherently polar compounds, tend to dissolve in solvents of similar polarity. Water, ethanol, methanol, acetone, or other solvents can also be used. However, methanol and ethanol, both polar solventes (ZHANG et al., 2020), are commonly used for anthocyanin extraction due to their practical ability to dissolve anthocyanins from the extracts (Yi et al., 2021; Grillo et al., 2020).

Water, a polar solvent, is frequently used instead of organic solvents due to environmental and health concerns. Although less polar than methanol and ethanol, acetone is still effective for anthocyanin extraction. Therefore, the solvent mixtures are often used to improve extraction efficiency by taking advantage of the complementary solubility properties of different solventes (LIU et al., 2019). These mixtures can enhance the efficiency in anthocyanin extraction by providing a more comprehensive range of solubility, maximizing yield and specificity in anthocyanin isolation from vegetal sources (KUMAR et al., 2019).

### 5.1.1.2. Non-conventional extraction methods

These techniques involve the green process and use of safe solvents to improve the yield of anthocyanins extraction.

#### 5.1.1.2.1 Enzyme-Assisted Aqueous Extraction (EAE)

The enzymatic method is a structural biological manipulation approach used in plants to expose anthocyanins by employing individual or combined enzymes (FERNANDEZ-AULIS et al., 2019). This method is widely used in various scientific fields, particularly for extracting bioactive compounds. Anthocyanin extraction involves breaking down cell walls and facilitating the release using enzymes. EAE procedures can also be simple to complex (FERNANDEZ-AULIS et al., 2019). Depending on the desired objectives, enzymatic extraction can be combined with other extraction techniques (LEICHTWEIS et al., 2019). This strategy allows access to anthocyanin compounds retained within cell organelles by using the basic principle of cellular degradation in the extracellular and intracellular walls. Thus, the method enables the extraction of anthocyanins trapped in cellular structures (WANG et al., 2023).

Enzymes can be classified into two main groups: carbohydrases (1A) and polysaccharides (1B) or proteases (2A) and proteinases (2B). Therefore, group 1 breaks

down complex carbohydrates like cellulose, hemicellulose, and pectin. This group includes cellulases, hemicellulases, and pectinases. Group 2 can break down proteins into amino acids. Cellulases, hemicellulases, and pectinases can be used individually or in combination (FERNANDEZ-AULIS et al., 2019). However, group 2 should be utilized separately to avoid hydrolysis of the enzymatic proteins (MEREGALLI et al., 2020).

Enzymatic efficiency depends on several factors, including cell structure (WANG et al., 2023), enzymatic structure (FERNANDEZ-AULIS et al., 2019), enzymatic composition (MUANGRAT et al., 2018), and pH. Generally, the pH range for enzymatic hydrolysis in anthocyanin extraction is between 3.0 and 5.0, as enzymes involved in anthocyanin extraction often exhibit optimal activity in this acidic pH range (RODRIGUES et al., 2020). However, the temperature range for extracting anthocyanins varies depending on the enzyme and source material, typically between 25°C and 50°C. Thus, removing the anthocyanins at moderate temperatures is preferable to prevent degradation.

Additionally, the ratio between the enzyme and treated sample can also vary. Still, it is often expressed as a percentage or ratio of enzyme weight to the weight of the treated sample, with a typical range of 1-5% (w/w). The solid-liquid ratio for anthocyanin extraction typically ranges from 1:5 to 1:20 (w/v) (RODRIGUES et al., 2020). Contact time, which indicates the duration of enzyme treatment, can vary widely, ranging from 30 minutes to 24 hours for anthocyanin extraction, depending on the enzyme and other extraction conditions (FERNANDEZ-AULIS et al., 2019).

#### 5.1.1.2.2 Microwave-Assisted Extraction

Microwave extraction is a process that can extract anthocyanins by introducing electromagnetic waves into the polar molecules. Then, the energy can be absorbed and cause ions to migrate, then start to move around (HASHEMI GAHRUIE et al., 2020). The process can create vibrations in the molecules and polarize the water present, possibly increasing pressure and temperature (KUTLU et al., 2021).

The Microwave extraction method can break down plant cell structures sensitive to heat, allowing anthocyanins to move out of the cells (FERREIRA et al., 2019). The effectiveness of this method depends on various factors, such as the strength of the microwaves, the duration of exposure, the type of solvent used, and the characteristics of the plant material (Kutlu et al., 2021; Pereira et al., 2020).

Furthermore, due to the heightened thermal effects caused by microwave operation, several adjustments have been made to reduce temperature elevation during extraction procedures. These modifications include microwave extraction under atmospheric pressure (Loncaric et al., 2020), oxygen flow-assisted microwave extraction (He et al. 2016), and

nitrogen-protected microwave-assisted extraction (NPMAE) (KUMAR et al., 2019). Nevertheless, various methods of extraction have been explored, including vacuum microwave-assisted extraction (VMAE) (Rocha et al., 2023), Soxhlet extraction combined with microwave-assisted extraction (FMASE) (Ardestani et al., 2016), ultrasonic-assisted microwave extraction (UMAE) (Sabino et al., 2021), microwave hydro-distillation (MWHD or MAHD) and microwave steam distillation (MSD) (WANG et al., 2023), solvent-free microwave extraction (SFME) (Sabino et al., 2014), and microwave vacuum hydrodistillation (VMHD) (AKOGOU et al., 2018). Furthermore, in 2022, methods for optimizing extraction efficiency while minimizing the impact of heat on sample integrity were proposed, including microwave-assisted extraction techniques such as microwave gravity hydro-diffusion (MHG) (Rohilla et al., 2022), solvent-free pressurized microwave extraction (PSFME) (WANG et al., 2023), and microwave-assisted two-phase aqueous extraction (MA-ATPE) (Saldaña et al., 2021). These techniques have been developed to ensure the extracted samples remain intact and undamaged.

#### 5.1.1.2.3 Ultrasound-assisted extraction (UAE)

UAE method uses compression and expansion generated by acoustic cavitation to induce shear forces, resulting in cell rupture and anthocyanin extraction (TEIXEIRA et al., 2021). The ultrasound can be divided into ultrasonic and ultrasound processes. The ultrasonic waves are at either low frequency (100-1000 kHz) at low power and amplitude or high frequency (20-100 kHz) with high power and amplitude, the latter being commonly used for anthocyanin extraction (GALVÃO et al., 2020).

Extraction can be performed directly through sonication. The device, connected to a transducer, is immersed in the extraction vessel and directly contacts the sample (ZHANG et al., 2020). Ultrasounds are generally more cost-effective and accessible but may lead to uneven energy distribution and lower extraction efficiency than the direct method (JIANG et al., 2020). Ultrasound techniques can be adapted to optimize extraction outcomes across various technologies (PAPPAS et al., 2021). In general, the efficiency in ultrasonic and ultrasound extraction is influenced by power, temperature, solid-liquid ratio, and extraction and pre-processing time (MOURTZINOS et al., 2018).

#### 5.1.1.2.4 Ohmic heating-assisted extraction (electroconductive heating)

Ohmic heating extraction (OH) is a method that involves the transfer of electricity through a system consisting of a power supply, isolation transformer, treatment chamber, frequency generator, and microprocessor board (ANDRADE et al., 2021).

This method works based on the ionic components present in plant tissues, such as

salts and acids, that conduct electricity (Panic et al., 2019). The electricity passing through the components of a glass ohmic heating cell is converted into heat energy. An increase in temperatre can damage cell structures, which can lead to the exposure of anthocyanins due to increased diffusion (PANIC et al., 2019).

In addition, the extraction efficiency of anthocyanins through electric conductivity heating is influenced by various factors, such as the sample's moisture content, the electric field's intensity, the presence of electrons and salts in the raw material, the duration of exposure in the extraction system, and how the system is combined or adapted with other extraction methods (HEINONEN et al., 2016).

#### 5.1.1.2.5 High voltage electric field assisted extraction

The method of the high-voltage electric field involves applying loads, sometimes with pulses predominating, using variable time and intensity, either in continuous or static mode (DIA et al., 2015; TUHANIOGLU et al 2022). However, the extraction technique described in this study relies on external electrical forces to permeate cell membranes in plant tissues (SUPANIVATIN et al., 2023).

These forces cause the formation of hydrophilic pores in the cell membranes, which opens them and causes them to lose their protective function. This exposes anthocyanins to the surrounding environment (LIU et al., 2019). The protective membrane is typically lost when the transmembrane potential exceeds a critical value of about 1 V (DIA et al 2015). This reduces the thickness of charge-carrying molecules and the permeabilization of smaller molecules) High-voltage electric field extraction can be classified into two primary categories. Jafari and Saien (SUPANIVATIN et al., 2023). discuss High Electrostatic Field (HEF) and High Voltage Electrical Discharges (HVED).

The High Electrostatic Field (HEF) system maintains a constant current or voltage throughout the experiment. This technique utilizes parallel plate electrodes to ensure uniform electric field distribution during operation. In contrast, High Voltage Electrical Discharges (HVED) involve chemical reactions and physical processes. This method injects energy directly into an aqueous solution through a plasma channel created by a high-current electrical discharge (>40 kV; >10 kA) between two submerged electrodes (RIZWAN et al., 2021). The process of HVED operates in two phases: the pre-break phase and the break phase. In the pre-break phase, relatively weak shock waves are generated, forming tiny bubbles that disrupt cell structures and accelerate the extraction of intracellular compounds (TUHANIOGLU et al., 2022).

During the intensified electrohydraulic phase, which occurs during the transition from pre-breaking to the breaking phase, various effects take place. These include strong shock waves, intense UV radiation (200–400 nm), production of highly concentrated free radicals, bubbles containing plasma, and vigorous liquid turbulence. These phenomena lead to the mechanical destruction of cellular tissues and oxidation, which may impact the antioxidant activity of bioactive compounds (LIU et al., 2019). Overall, this extraction method provides a more effective mechanical disintegration of cell walls, leading to a more efficient extraction. Therefore, this technique has been utilized for extracting bioactive compounds from various raw materials (LIU et al., 2019).

The efficiency of anthocyanin extraction via pulsed electric fields (PEF) depends on several factors, including the strength of the applied electric field (ranging from 0.1 to 20 kV/cm), type of raw material, exposure time, electric field intensity, specific energy input pulse, chamber size, initial temperature, and combination with other extraction methods (LIU et al., 2019; TUHANIOGLU et al., 2022). Pulsed electric fields (PEF) are an innovative technique for enhancing anthocyanin extraction efficiency by disrupting plant cell structures. This involves applying short pulses of high electric field strength to a sample. The principle behind anthocyanin extraction using PEF is to induce permeabilization of cell membranes, thereby facilitating the release of intracellular compounds, including anthocyanins (LIU et al., 2019).

However, PEF has not been used to extract anthocyanins from plant cells. The process starts with membrane permeabilization, which leads to electroporation or electropermeabilization. This procedure results in rearranging the lipid bilayer in the cell membrane and forming nanopores. These nanopores facilitate the passage of ions, water, and other small molecules across the membrane, ultimately increasing diffusion and leaching, thus improving the extraction efficiency of anthocyanins (SUPANIVATIN et al., 2023).

#### 5.1.1.2.6 Irradiation Extraction

Anthocyanins can be extracted through irradiation, a physical and non-thermal process. This process exposes cell structure to high-energy ions that chemically break down protective substances surrounding the anthocyanins into vacuoles (LOTFI et al., 2015).

Nonetheless, the degree of modification depends on factors such as the type of raw materials, amount of radiation, and radiation source (Lotfi et al., 2021). Food irradiation treatment involves exposing food to either ionizing or non-ionizing radiation. Ionizing radiation sources include gamma rays, X-rays, and high-energy electrons, while non-

ionizing radiation sources include electromagnetic radiation, such as UV rays, visible light, and infrared radiation (TAGAMI et al., 2024).

Gamma radiation extraction is a continuous process involving the flow of high-energy photons capable of energizing electrons within atoms in the food matrix. This energization process causes the transition of atoms to higher energy levels (TAGAMI et al., 2019). Atoms with unpaired electrons in their outer shell can react with the outer shell electrons of atoms that comprise cell components, producing free radicals in hydrogen and hydroxyl bonds from water molecules (TAN et al., 2020).

This process triggers the hydrolysis of pectins after depolymerizing carbohydrate polymers, which softens the cell components and exposes anthocyanins (MORAES et al., 2020).

#### 5.1.1.2.7 Pulsed Light Extraction

The extraction of anthocyanins using pulsed light is an emerging method that can be described according to different procedures (MORAES et al., 2018). This method includes intense pulsed light, high-intensity pulsed UV light, pulsed white light, or pulsed UV light. The technique involves applying very short pulses of light (ranging from 1 μs to 0.1 s) using a xenon lamp to supply the high-intensity pulse generation device on the extraction matrix. The process can be conducted with contact or non-contact, using a range of wavelengths from 100 nm to 1100 nm (CASSOL et al., 2018).

Additionally, the extraction of anthocyanins through pulsed light involves two fundamental mechanisms: the photochemical effect and the photothermal effect (YANG et al., 2024). The photochemical effect is associated with the UV portion of the pulsed light spectrum, depending on the direct interaction between photon energy and matrix molecules. During the pulsed light process, chemical compounds absorb optical energy, causing photoionization, decomposition of chemical bonds, and changes in the structural conformation of the applied matrix (ARAUJO et al., 2021).

Additionally, some photons can transfer their energy to the material thermally, increasing the temperature of the applied matrix. This mechanism primarily affects the infrared and visible portions of the pulsed light spectrum, resulting in physical changes to cells and cellular structures. These changes include loss of cell membrane permeability, expanded vacuoles, shape alteration, and lack of cell walls (BAGADE and PATIL, 2021). The effectiveness of pulsed light technology depends on the pulses emitted, lamp types used and their combinations, emission time, optical properties, and matrix species used (BAGADE et al., 2020).

#### 5.1.1.2.8 Supercritical Fluids Extraction

The transfer of mass from plant cells can be achieved using pressurized fluid techniques through three main methods: supercritical fluid extraction (SFE), pressurized liquid extraction, and high-pressure liquid extraction (ZHANG et al., 2020 and LIU et al et al 2019). SFE involves carbon dioxide and co-solvents (YI et al., 2021). This process occurs at temperatures and pressures well above the critical points (7.4 MPa and 31.1 °C) and carbon dioxide, which modifies its properties to improve mass transfer during anthocyanin extraction (OUALCADI et al., 2020). The selectivity in SFE is a current research focus, and parameters can be optimized to suit specific compounds and matrix characteristics. SFE is a valuable technique in various fields, including food, pharmaceuticals, and natural products (ZHANG et al., 2020). The extraction process typically involves a static period during which the solvent remains in contact with the sample and a dynamic period during which the solvent continuously passes through the sample (CHAMUTPONG et al., 2021). The extraction efficiency relies on various factors, including temperature, pressure, particle size, type and quantity of co-solvent, sample moisture content, extraction duration, CO2 flow rate, and liquid-to-solid ratio (OTHMAN et al., I., 2021).

#### 5.1.1.2.9 Pressurized and High-pressure liquids extraction

Pressurized Liquid Extraction (PLE) and High-Pressure Liquid Extraction (HPLP) are analytical chemistry techniques that isolate anthocyanin compounds from specific matrices. Although they share similar operating principles, they differ only in the methods employed (LÓPEZ et al., 2018 and TENA et 2021). PLE, also known as accelerated solvent extraction (ASE), involves using liquid solvents at temperatures above their boiling points (around 200°C) from medium to high extraction pressures (3.5 to 20 MPa). The PLE anthocyanins extraction kept the solvent liquid at temperatures above its boiling point to enhance the solubility of the analytes (TENA et al., 2022). The extraction yield depends on various factors (i.e., temperature, pressure, static time, and the number of cycles to which the matrices are subjected). Efficient extraction of analytes from a sample into a solvent can be achieved by increasing pressure and temperature.

High-pressure liquid extraction is a technique for extracting anthocyanins. The term 'high pressure' can refer to different methods, but extraction typically involves using elevated pressure in liquid systems to enhance extraction efficiency. One subgroup comprises discontinuous high hydrostatic pressure (HHP). In contrast, the other subset comprises continuous techniques such as high-pressure homogenization (HPH), microfluidization (MF), and ultra-high-pressure homogenization (UHPH) (MORAES et al., 2022).

The critical difference from other pressurized liquid extraction techniques is that high

pressure keeps the solvent above its boiling point (MOKGEHLE et al., 2022). This method simplifies extraction, reducing the amount of solvent used and the time required. High-pressure methods, such as those using pressures exceeding 100 MPa (HP), 300 MPa (UHP), or 400 MPa (UHPH), provide better solvent penetration into cell membranes and improve bioaccessibility (TEIXEIRA et al., 2024).

The efficiency of compound extraction depends on factors including solvent composition, pressure, temperature, particle size, moisture content of the material, extraction time, and solvent-to-solid ratio (GRILLO et al., 2020). In brief, pressurized liquid extraction (PLE) is a technique that utilizes pressure. In contrast, high-pressure liquid extraction (HPLP) can encompass a broader range of strategies for compound extraction.

Radiofrequency heating-assisted extraction: Radio frequency-assisted anthocyanin extraction is a technology that uses radio electromagnetic waves (3 kHz-300 MHz) to interact with target matrix molecules. This interaction induces heating within the plant tissue, causing protective structures to break down (IVANE et al., 2024). As a result, anthocyanins become more accessible, facilitating their extraction during the process (IVANE et al., 2024).

The principle of the system consists of a densified bed of conductive particles positioned between two electrodes that are cyclically charged by a radio frequency transducer. This setup causes the ions of the matrix components or the solvents used to migrate toward the oppositely charged electrodes. In addition, polar molecules align with the established electric field's polarity, resulting in molecular and ionic friction. Friction during the extraction process generates heat within the matrix, as described by Izadifar and Baik (CHAKRABORTY and UPPALURI., 2020). This process can be conducted at room temperature, with less amount of solvent. The process works well with plant structures that contain high pectin content (MAZZA et al., 2019).

Stirred-Tank Extraction: By improving the kinetic conditions within the target matrix, extraction of anthocyanins using stirred tanks enhances mass transfer (PEREDO et al., 2019). This method relies on a mechanical apparatus that includes a containment tank for matrices, inert stirring, mechanical agitators, a thermometer, a heating system, a rotor, and other essential components (PEREDO et al., 2019). In addition, the element in this system has a crucial role in facilitating anthocyanin extraction by adjusting and functioning according to predefined parameters. This optimization improves operational efficiency by breaking down protective elements surrounding anthocyanins, thereby exposing them for extraction (ARRUDA et al 2021).

The performance of agitated bath extraction includes temperature, solvent ratio, stirring speed, extraction time, and integration with other extraction techniques or sample processing (PEREDO et al., 2019 and and ARRUDA et al., 2021). These parameters

contribute to the efficiency and yield of the extraction process. Optimization and control are essential to achieve desired outcomes.

Combined extraction method: Technological advancements have led to proposals that combine two or more extraction methods to enhance the extraction of anthocyanins from natural sources (WAN et al., 2009). The extraction of anthocyanin is influenced by both kinetic and thermodynamic factors, which significantly impact extraction yield (LOYPIMAI et al., 2015). Although the efficacy of an anthocyanin extraction procedure can be observed, it is essential to understand the extent of extraction to prevent excessive degradation during the process (Buniowska et al., 2017).

Combining two or more methods aims to improve extraction efficiency and speed (PEREIRA et al., 2020; WAN et al., 2009; JAFARI et al., 2022). These combinations may involve conventional or innovative extraction systems depending on the desired objectives (PEIRO et al., 2019). The efficiency of combined extractions relies on synergies between the coupled systems, which may vary depending on the raw material being extracted (WAN et al., 2009).

#### 5.1.1.3. Conventional and non-conventional solvents for anthocyanin extraction

Solvents are the main component that directly interacts with the method. The specific names are based on the principles used to obtain them and their method during anthocyanin extraction (NALIYADHARA et al., 2022). In comparison, many solvents are considered conventional (DALVI-ISFAHAN et al., 2016). Therefore, the growing trend of non-conventional solvents is towards using natural, environmentally friendly solvents with sustainable operating principles, often called green solvents as depicted in Fig.1.

##### 5.1.1.3.1 Conventional solvents

A suitable extraction solvent must have access to plant tissues and be able to dissolve anthocyanins and other bioactive compounds in their cell organelles (BIAN et al., 2021). However, conventional solvents that are commonly used include water ($H_2O$), ethanol ($C_2H_5OH$), acetone ($CH_3COCH_3$), methanol ($CH_3OH$), diethyl ether $(C_2H_5)_2O$, chloroform ($CHCl_3$), hexane ($C_6H_{14}$), petroleum ether, toluene ($C_6H_5CH_3$), xylene ($C_6H_4(CH_3)2$), dichloromethane ($CH_2C_{l2}$), acetonitrile ($CH_3CN$), ethyl acetate ($CH_3COOC_2H_5$), butanol ($C_4H_9OH$), cyclohexane ($C_6H_{12}$) and others (PEREIRA et al., 2020; IVANE et al., 2025; DALVI-ISFAHAN et al., 2016; BEDNARIK et al., 2024).

When selecting an extraction solvent, the following factors should be considered: Selectivity: The solvent must target the specific compound in the plant, whether it's polar or non-polar (ZHANG et al., 2020 and LIU et al., 2024). Boiling point: Choose a solvent with a

low boiling point to facilitate removal after anthocyanin extraction and purification. Reactivity: The solvent should not chemically react with the compounds in the extract to avoid degrading the compounds of interest. Viscosity: Generally, a low viscosity is preferred, but it shouldn't be too low to interfere with the diffusion and solubility of the compounds. Safety: Choose a non-flammable, non-toxic, and non-corrosive solvent to prevent environmental and health hazards. Cost: The solvent should be cost-effective to make the extraction method viable. Vapor pressure: Low vapor pressure helps avoid solvent loss during extraction, allowing for easy evaporation and solvent recovery afterward. Recovery: The solvent should be easily separated from the extract using simple methods. Considering these factors will help select the most appropriate solvent for anthocyanin extraction to ensure efficiency, safety, and cost-effectiveness.

#### 5.1.1.3.2 Non-conventional solvents

##### 5.1.1.3.2.1 Ionic liquids (ILs)

The class of solvents used for "green extraction" that can aid in the separation of polar and nonpolar compounds (ZIN et al., 2020). Furthermore, ILs are organic salts in a liquid state and consist of an organic cation paired with an organic or inorganic anion. These solvents exhibit several unique properties: they have low electrical conductivity, are nonionic (nonpolar), have high viscosity, low vapor pressure, low flammability, good thermal stability, and a wide liquid phase range, making them ideal for dissolving a wide range of polar and nonpolar compounds (NARESH et al., 2015).

Due to their distinctive chemical functional groups, ILs facilitate matrix-solvent interactions when used for anthocyanin extraction. Many ILs are readily available commercially or can be synthesized by reaction of appropriate cationic and anionic components (SALTA et al., 2024). Although ILs have received increasing attention for their excellent extraction properties, they also have drawbacks. These include the toxicity of

specific components, their stimulating properties, and their high cost, which limits their widespread use despite their considerable utility (KALAISELVAN et al., 2018).

#### 5.1.1.3.2.2 Natural Deep Eutectic Extraction Solvent (NADEES)

Extraction using deep eutectic natural solvents is a technique that maximizes the physicochemical affinity between the solvent and the cellular organelles that protect anthocyanins (MANDAL et al., 2020). These solvents are typically made by mixing two or more components, each containing at least one hydrogen bond donor and one hydrogen bond acceptor, forming liquid salts (SANTAMERA et al., 2020). The resulting green solvent is often composed of naturally occurring sugars and acids, following the principles of green chemistry (PEIRO et al., 2019). After preparation, these solvents exhibit lower melting points than their components, which is attributed to the formation of intermolecular hydrogen bonds (MANDAL et al., 2020). The efficiency of extraction using deep eutectic solvents depends on various factors, including the solvent composition, the extraction technique used, the contact time with the raw material ALHENDI et al. (2017), the solvent concentration, and the solid/liquid ratio (SANTAMERA et al., 2020; MANDAL et al., 2021).

### 5.1.1.4. Basic Decision-Tree Design Considerations

Several approaches were emphasized in establishing criteria for understanding how anthocyanin extraction methods work for different vegetal matrices (JIANG et al., 2020; BEDNARIK et al., 2024; NOWACKA et al., 2021). These include the relationship between anthocyanin storage organs and extraction methods, common research on anthocyanin extraction, the difficulty of comparing extraction methods in raw materials with different structures, and anatomical structures and physical-chemical composition in anthocyanin Extraction.

#### 5.1.1.4.1 Relationship between anthocyanin storage organs and extraction methods

Anthocyanins are pigments in plant cells found in vacuoles (AKOGOU et al., 2018 and LOARCE et al., 2020). Anthocyanins are mainly present in different plant organs, including flowers or inflorescences, leaves, roots or underground organs, fruits, and seeds are shown in Fig. 2 (AKOGOU et al., 2024). Therefore, to get high-yield anthocyanin extraction on this matrix source, specific procedures are necessary due to the complex and diverse compositions of their structure composition. Additionally, techniques that enhance mass transfer are necessary (DALVI-ISFAHAN et al., 2016). The process involves selecting the appropriate method, which guarantees the adequate rupture of structural barriers and preserving compound stability at the same time (PEREIRA et al., 2020). The

procedures reduce particle size, break down interfering structures such as pectin, cellulose, hemicellulose, lignin, or other cell wall components, and separate compounds that can limit anthocyanin extraction, such as lipids and proteins. Additionally, solubilizing certain materials like starch and utilizing appropriate solvents such as ethanol, methanol, water, and soluble sugars play crucial roles (PEREIRA et al., 2020 and LOARCE et al., 2020). During material preparation, it is essential to understand the specifics of the tissue fraction where anthocyanins are protected. For example, in fruits such as jabuticaba and grapes (most cultivars), over 90% of anthocyanins are in the skin, protected by pectin and fibers. Therefore, using a unit operation to separate this composition from anthocyanins can greatly help to improve the best anthocyanins extraction from the skins (JIANG et al., 2020 and BEDNARIK et al., 2024).

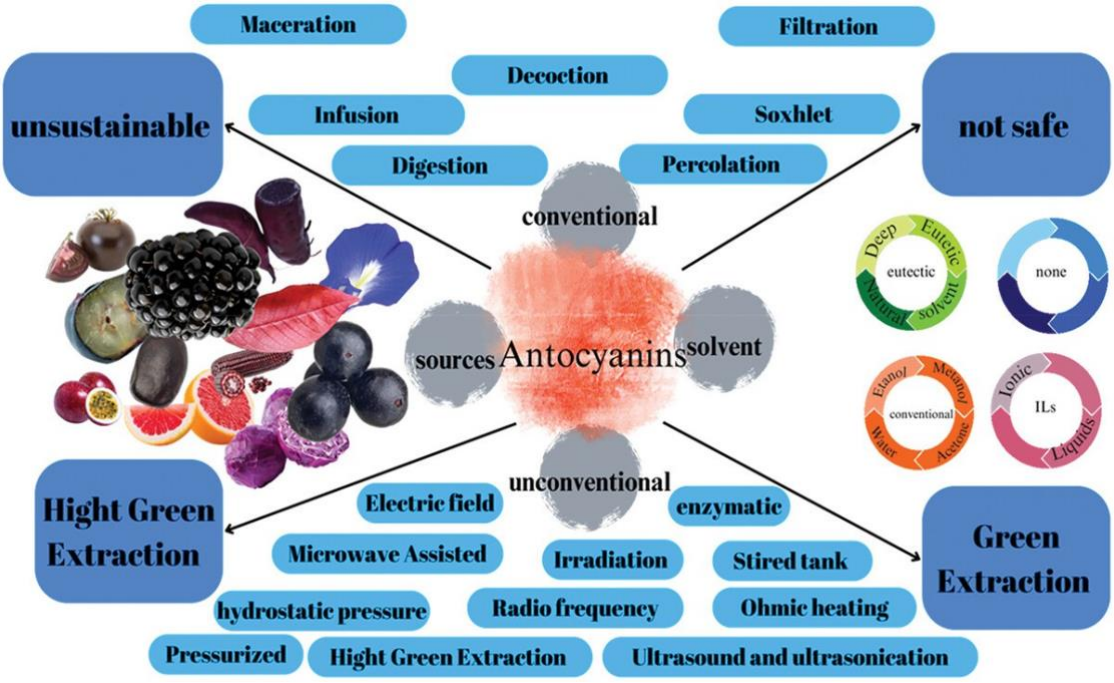


**Figure 2.** A comprehensive illustrative system describing the sources of anthocyanin extraction, the solvents used for extraction, the extraction methods used, the similarity characteristics between methods, and the raw material. Source: designed by the Author, 2025

**5.1.1.4.2 Common research for anthocyanin on extraction**

The analyzed set of studies shares several common experimental characteristics:

(1) Comparison of conventional and unconventional extraction methods (WANG et al 2023 and LOARCE et al 2020).

(2) Designs applied to optimize factors and achieve optimal points (KUASNEI et al., 2022

and BABOVA et al., 2016).

(3) Simulation of extraction methods for large-scale application (HASHEMI-GAHRUIE et al., 2020; MANDAL et al., 2020; BRIONES-LABARCA et al., 2015).

(4) Evaluation of the performance of extraction methods based on pre-treatment to modify the physical state of raw materials, including dry and fresh matter. The studies referenced for this section are (ZHANG et al., 2019 and YANAGISAWA et al., 2024).

(5) Comparison of combined extraction methods, with references to studies by JIANG et al. (2020) and GONZÁLEZ et al. (2022).

(6) This section compares raw materials processed in organic and conventional solvents, with references to studies by FERNÁNDEZ et al. (2024) and MURTHY et al. (2024).

(7) This section compares modified extraction methods from WATHON et al. (2019) and WU et al. (2019).

(8) In the studies conducted by Porto and NATOLINO (2018) and PARRA-CAMPOS and ORDONEZ-SANTOS (2023), modeling systems combined with multivariate optimization were utilized to determine optimal points.

The works significantly contribute to the extraction of anthocyanins from the specific raw materials studied. Additionally, the authors describe the food matrices and preparation procedures used. This information enables the construction of a deductive strategy to propose methods for untested materials.

#### 5.1.1.4.3 Difficulty of comparing extraction methods in raw materials with different structures

MATOS, MOTA, and CARMO (2022) compared conventional extraction methods, high hydrostatic pressure, and ultrasound-assisted extraction. The results showed that ultrasound extraction was the most effective method, producing 407.15 mg of cyanidin-3-glucoside per 100 g of fresh sample. However, scalability concerns led to the recognition of the resilience of conventional methods. Similarly, SYRPAS et al. (2021) found that enzyme-assisted extraction yielded the highest anthocyanin and antioxidant capacity from blueberry pomace. In contrast, RYU and KOH'S (2018) optimization studies for anthocyanin extraction in black soybeans favored conventional extraction. The studies examined factors such as HCl concentration (0.3-0.5%), solid-liquid ratio (1/30g/mL-1/50g/mL), and extraction temperature (30-50°C). Similarly, LIU et al. (2018) emphasized using conventional purple passion fruit peel extraction. The optimal conditions for achieving the best results were determined to be a solution-solid ratio of 20:30 mL/g, power ranging from 500-900 W, delay time of 1:3 s, extraction time of 20-60 min, and cavitation time of 1:3. These conditions resulted in a yield of 0.826 mg/g of cyanidin-3-glucoside. In a comparable study on jambolan

(*Syzygium cumini* L.) extracts, dos SANTOS et al. (2022) found conventional extraction optimal, emphasizing the importance of optimizing temperature and extraction time. These findings highlight the variability of extraction factors affected by the physiological structures in plant matrices.

Although each study identified at least one optimal extraction method or factor, as described in the previous paragraph, discrepancies arise when comparing the yields obtained, such as 407.15 mg of cyanidin-3-glucoside per 100 g of fresh sample in jabuticaba peel (MATOS et al., 2022) and 136.68 mg/100 g of fresh sample in black soybean (RYU and KOH, 2018). The difference in anthocyanin extraction can be attributed to variations in raw materials and pretreatment methods that alter the material's physical state. According to ÁVILA-HERNÁNDEZ et al. (2022), who evaluated anthocyanin extraction from strawberries pre-treated by lyophilization, the yield of total anthocyanins was approximately 0.428 g / 100 g, which was higher than the yield from non-lyophilized treatment. Studies on extraction from two blackberry cultivars have found higher amounts of monomeric anthocyanins in lyophilized raw materials. They explicitly yielded approximately 436.48 mg/100g of dry matter of cyanidin-3-o-glucoside (CUESTA-RIAÑO et al., 2022). However, outcomes may vary in some cases (MIGLIORINI et al., 2019). Conducted research comparing Red Chicory (*Cichorium intybus*) extracts and concluded that the best conditions for extracting bioactive compounds were obtained using a fresh sample.

The difference in results can be attributed to the variation in the simple and combined extraction methods. This causes one matrix to be extracted extensively at the expense of another. JIANG et al. (2020) studied the extraction of anthocyanins in Akebia trifoliata (Thunb.) Koidz flowers. They compared a combined system (radio-frequency-assisted enzymatic extraction) with conventional and enzymatic extraction. The results showed that radiofrequency-assisted enzymatic extraction had the highest crude yields (26.55%) and anthocyanin content (50.87 mg cyanidin-3-O-glycoside equivalents/100 g). FERNÁNDEZ et al. (2024) demonstrate the functionality of kinetics and mathematical modeling in the ultrasound-assisted extraction of anthocyanins from jaboticaba bark (Myrciaria cauliflora). Experimental designs based on multivariate analysis models are increasingly common, and the obtained results are primarily from laboratory-scale studies (LIN, SHI and WANG (2023). However, a question always arises as to whether extraction methods can be applied on a large scale using only residual biomass from the industry. According to WATHON et al. (2019) who extracted anthocyanins from bark residues of Aronia melanocarpa (Michx.) after juice extraction, the system can be replicated on a large scale. However, WU et al. (2019) found that it is possible to extract 281.56 ± 3.02 mg/100 g of cyanidin-3-glucoside from the residues of Euryale ferox Salisb. MORAES et al. (2020), investigated the extraction of

anthocyanins from blackberries using microwave hydrodiffusion. They concluded that while the methodology can be operationalized on an industrial scale, the application costs are too high.

YIN et al. (2022) demonstrated that solvent extraction of black rice resulted in an anthocyanin content of 266 mg/100 g of fresh sample. In contrast, PEDRO, GRANATO, and ROSSO (2015) reported a yield of 117 mg/100 g, 79% lower than the result of YIN et al. (2022) using enzymes. Furthermore, JHA et al. (2017) reported even lower yields of 3.36 mg/100 g when extracting anthocyanins from black rice husks using ultrasound and microwave-assisted methods. JU, GREGO, and ZHANG (2013) highlighted the significance of comprehending the composition of plant structures before compound extraction, as cells have inherent resistance to various degradation mechanisms. In general, the approach for anthocyanin extraction methods presented in the work above makes it very difficult to select the best method when intending to apply to different matrix sources.

#### 5.1.1.4.4 Main anthocyanin storage structures plant organs

Anthocyanins are widely distributed in various plant parts, including fruits, roots, tubers, leaves, flowers, and seeds Fig. 3-A (PEREIRA et al., 2020). A thorough understanding of the anatomy of plant organs is critical for selecting appropriate extraction methods (ALBUQUERQUE et al., 2020).

ROOTS: Roots are classified as primary or secondary based on structural characteristics. The piliferous zone marks the beginning of adventitious root development and typically consists of a single layer of thin-walled cells. The innermost layer, called the endodermis, is specialized, while the vascular cylinder or stele can take the form of a radial protostele or a medullary protostele (EVANS and EVANS, 2009). Anthocyanins are typically found in the cortical region, which is the outermost layer of the root. However, the concentration of anthocyanins can vary among different species and cultivars of tuber roots and in other parts of the root.

TUBERS: Tubers originate from root systems, and specific cultivars exhibit a reddish or purple coloration due to the accumulation of anthocyanins in plant tissues. Examples of such tubers include purple sweet potato and purple yam (MATOS et al., 2022).

LEAFS: The leaf is a fundamental plant organ consisting primarily of a protective epidermis, parenchymal mesophyll, and vascular system. Variations in epidermal cell structure, stomatal distribution, and epidermal trichomes are commonly observed among different leaf types. The mesophyll, which serves as the main site of reserve storage in plants, can also store anthocyanins, with concentrations often higher in the mesophyll than in other leaf tissues (EVANS and EVANS, 2009).

FLOWERS: The floral stem or pedicel exhibits distinct structures, such as bracts with a reduced calyx and a corolla that often resembles leaf-like structures. Various elements such as epidermal cells, epithelial and covering hairs, mesophyll cells, sebaceous glands, and crystals contribute to the intricate composition of flower parts. Anthocyanins are commonly found in flower petals and impart red, purple, or blue colors (CASER et al., 2020).

FRUITS: Fruits are diverse and can be categorized as dry or fleshy, each corresponding to a specific fruit type. These include berries, drupes, legumes, capsules, and achenes, each with unique characteristics such as seed dispersal mechanisms and pericarp composition. Anthocyanins are often concentrated in fleshy fruits' skin or outer layers, contributing to their coloration and antioxidant properties (LIMA et al., 2017; Pal and JADEJA, 2019).

Seeds possess a sclerenchymatous layer and exhibit characteristic variations in the number of cell layers, structure, arrangement, color, and content. The seed epidermis typically consists of thick-walled cells, often lignified, associated with storage tissues known as perisperm and endosperm. While anthocyanins are less abundant in seeds than other plant organs, they may still be in trace amounts in the seed coat or outer layers (BI et al., 2010 and ZANNOU & KOCA, 2022).

#### 5.1.1.4.5 Anatomical structures and physical-chemical Composition in Anthocyanin Extraction

Since plant structures are primarily composed of various polysaccharides, understanding their composition is crucial for selecting appropriate extraction methods for anthocyanins, as illustrated in Fig. 3. Cellulose, which forms the main structure of plant cell walls, provides strength and rigidity and influences the efficiency of extraction techniques by affecting tissue permeability (KUMAR et al., 2019). Hemicellulose Fig. 3 B. Another component of cell walls contributes to tissue flexibility and elasticity, potentially affecting the permeability of extraction solvents into plant tissues (CHACHAR et al., 2024). Lignin, while providing stiffness and resistance to degradation, can hinder the extraction process due to its dense structure, requiring specialized methods to overcome its barrier effects (LIMA et al., 2017). Starch, an energy reserve stored in plastids, can affect extraction efficiency depending on its distribution in plant tissues and accessibility to extraction solvents (KUMAR et al., 2019). Pectens in the middle lamella and cell walls can influence extraction by affecting tissue consistency and adhesion, potentially altering the release of anthocyanins during the extraction process (CHACHAR et al., 2024). Therefore, consideration of the composition and distribution of these polysaccharides is essential to optimize anthocyanin extraction from plant matrices.

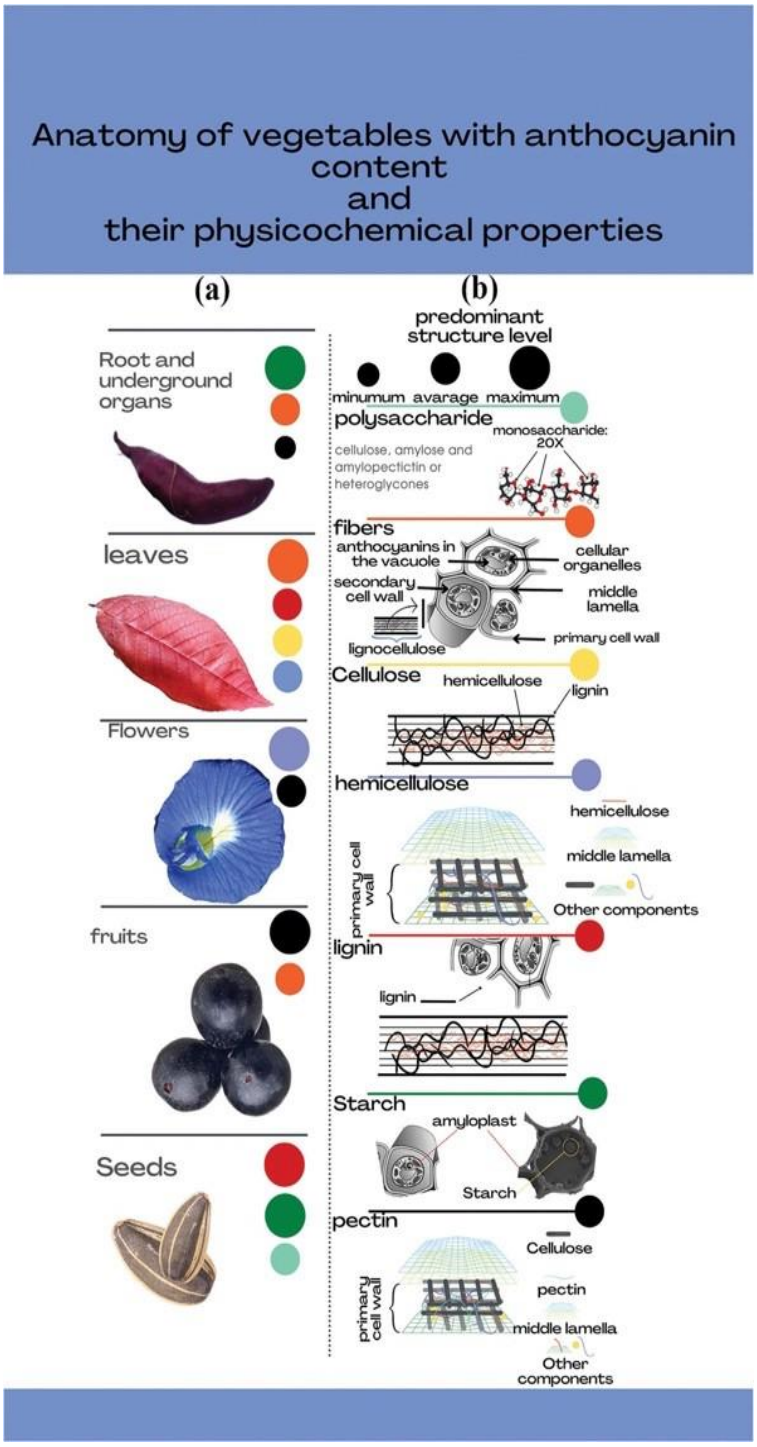


**Figure 3.** Accumulation of anthocyanins in the main plant organs (A) and their predominant physicochemical structures (B). Source: designed by the Author, 2025

### 5.1.1.5 Criteria for the decision tree in the selection of the appropriate method for extracting anthocyanins

Despite the extensive evaluation of several innovative methods for anthocyanin extraction, selecting an appropriate method remains a significant challenge due predominantly to the specific properties of the raw material (RYU & KOH, 2018). This challenge is compounded by a fundamental understanding of the plant matrix's morpho-anatomical charactics and the operational principles underlying these methods (ZIN et al.,

2020; LOARCE et al., 2020; ÁVILA-HERNÁNDEZ et al., 2022).

#### 5.1.1.5.1 Description of the decision-tree for selecting Anthocyanin Extraction Methods

The decision tree in Fig. 4 is useful for selecting anthocyanin extraction methods that promote accurate, streamlined, and sustainable approaches (LI et al., 2021; ALIFAKI et al., 2022; MIGLIORINI et al., 2019). Our proposed decision tree design facilitates selecting the most suitable method based on the specific characteristics of the chosen plant material.

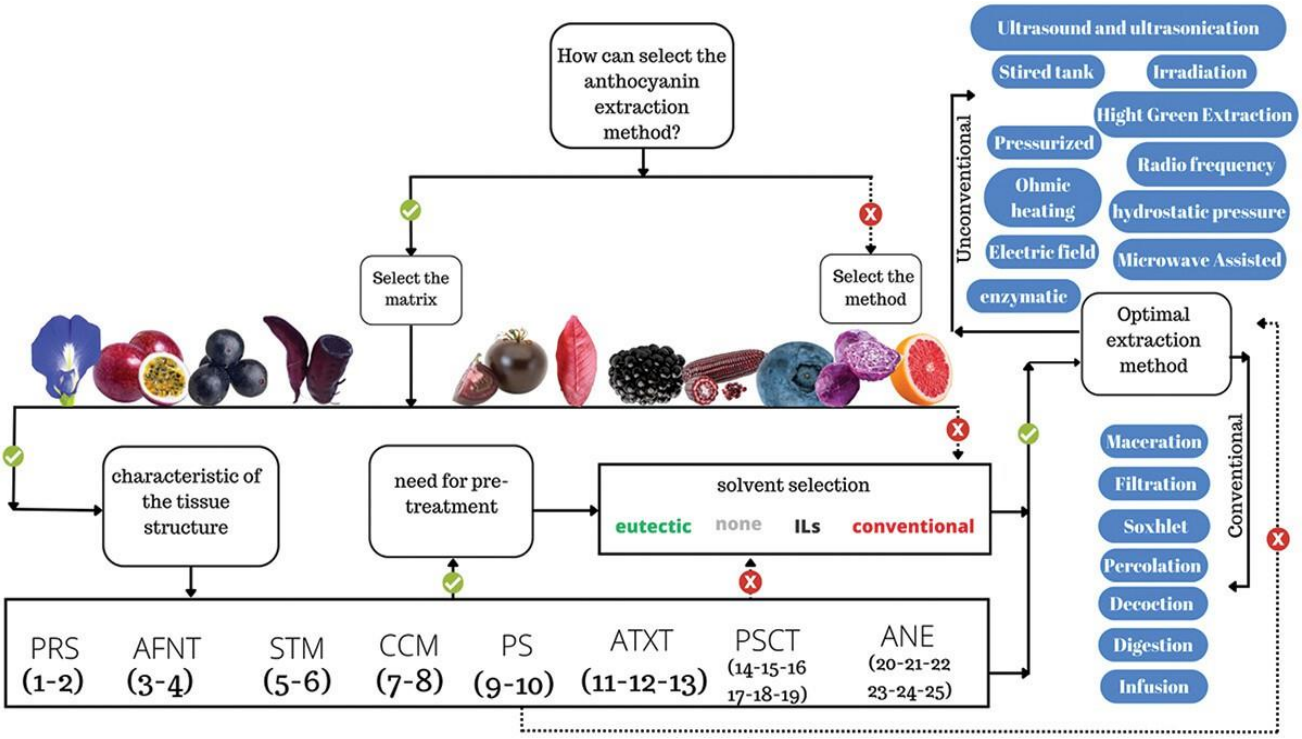


**Figure 4**. Decision- tree for selecting anthocyanin extraction methods based on intrinsic characteristics and response to solvents. PRS – Porosity; AFNT – Affinity; STM – State of Matter; CCM – Coating Component; PS – Particle Size; ATXT – Anatomical Texture; PSCT– Polysaccharide Type; ANE – Anatomical Structure; (1) Hydrophilic; (2) Hydrophobic; (3) Water; (4) Alcohol; (5) Acid; (6)Basic; (7) Film; (8) fiber; (9) Micro; (10) Macro; (11) FLS – Fleshy; (12) JCY – Juicy; (13) DRY – Dry; (14) LGN – Lignin; (15) STC – Starch; (16) PCN – Pectin; (17) Gel; (18) CLS – Cellulose; (19) HCL – Hemicellulose; (20) MC – Mesocarp; (21) PR – Pericarp; (22) CPR – Receptacle; (23) EXP -Exocarp; (24)EC -Endocarp; (25) EP – Epidermis. Source: designed by the Author, 2025

The decision-tree, as shown in Fig. 4 assists in selecting an anthocyanin extraction method based on the predominant plant matrix and its structural characteristics (FERNANDEZ-AULIS et al., 2019; GONZÁLEZ et al., 2022; CASER et al., 2020). These

characteristics include porosity (PRS), which indicates whether the structure allows easy passage of water (hydrophilic) or not (hydrophobic), and polarity affinity (AFNT) in water (polar) or alcohols (nonpolar) (CASER et al., 2020; Liu et al., 2020; NARESH et al., 2015; HIRANRANGSEE et al., 2016). However, plant extract anthocyanins are sensitive to harsh conditions and may exhibit acidic or basic properties depending on their affinity in water (AFNT) (GONZÁLEZ et al., 2022; BARROS et al., 2023). Acidic conditions are present when the pH value is below 4.5, while primary conditions occur above pH 4.5. Furthermore, plant structures may have protective components such as coatings (MCC) in films or fibers (SANG et al., 2017; LOTFI et al., 2015; LIU et al., 2019). Films and fibers can be disrupted through heat or high pressures that exceed their elastic limit (ADEEL et al., 2023; BAE et al., 2006).

Vegetables possess diverse anatomical textures, which vary from species to species. These textures may be juicy, fleshy, or dry, sometimes featuring mixed structures (PAGE et al., 2020; Grillo et al., 2020; MOKGEHLE et al., 2022; ALHENDI et al., 2017; ZAVALA-LOPEZ et al., 2017). These structures are composed of different polysaccharides, which determine the suitable disruption mechanism. Polysaccharides may be stored in different structural sections depending on the plant organ (ENE) (FERNANDEZ-AULIS et al., 2019).

After selecting a matrix for anthocyanin extraction, researchers must conduct fundamental analyses. Firstly, they must identify the type of plant structure they are working with, such as leaves, floral organs, roots or tubers, root system developments, or fruits (FERNANDEZ-AULIS et al., 2029; ZHANG et al., 2021; BEDNARIK et al., 2024; SANG et al., 2018; GONZÁLEZ et al., 2022; HE et al., 2017). Secondly, they should determine the characteristics of the plant structure, identifying the fraction or tissue where anthocyanins are concentrated. Researchers should analyze the components that make up the structure, particularly those that contribute to anthocyanin coloration, and understand their physical and chemical properties (ARAUJO et al., 2021). This information can be used to identify appropriate mechanisms for extraction, including pre-treatments, extraction techniques, and solvent selection. Finally, researchers can select one or more extraction methods that align with the principles established through their analysis (ZANNOU & KOCA, 2022).

#### 5.1.1.6. Decision-tree applicability criterion an example of its use

Our laboratory research focused on developing natural dyes from two distinct matrices: blackberry and purple sweet potato. We optimized the extraction conditions for

these matrices, which typically take about six months. However, questions about the optimal extraction method for less-studied matrices are common in the research environment. This underscores the importance of a decision-tree. For instance, consider the decision logic applied to Blackberry. Blackberries are a type of drupe fruit with specific attributes, including porosity (PRS)-1, affinity (AFNT)-4, state of matter (STM)-5, coating component (CCM)-7, PS-10, anatomical texture (ATXT)-12, polysaccharide type (PSCT)-16, 18, and 19, and anatomical structure (ANE)-20, 23. To ensure the preservation of mesocarp anthocyanins while breaking down macro surface structures, a suitable method must be selected based on Fig. 4 and the principles of anthocyanin extraction methods. Conventional methods, such as maceration, may be appropriate, but prolonged exposure could lead to degradation. Alternatively, traditional percolation could be used if blackberry is lyophilized. However, methods such as decoction, Soxhlet extraction, infusion, and digestion could be more practical due to the need for continuous heating.

Regarding emerging methods, microwave, ohmic heating, and high-voltage electric fields are considered unsuitable due to the heat they generate during operation. On the other hand, pressurized fluid, high hydrostatic pressure, and ultrasonication methods can be used without difficulty. The Purple Sweet Potato is a tuberous root-type matrix with specific attributes (PRS-1; AFNT-4; STM-6; CCM-8; PS-10; ATXT-13; PSCT-15; ANE-22). Conventional methods such as maceration, infusion, and digestion can be applied. Percolation is viable with pre-treatment like freeze-drying, although it may reduce the yield.

Conversely, methods like Soxhlet and decoction are considered unsuitable. Among the emerging techniques, microwave, enzymatic, ohmic heating, and high voltage electric fields (HVEF) are considered the most suitable. Conversely, high hydrostatic pressure and pressurized fluids can be used with matrix pre-treatment. However, tank agitation, radio frequency, irradiation, ultrasonic bath, and ultrasonication methods may need to be more efficient due to the relationship between their operating principle and the need to induce mass diffusion in the matrix.

Laboratory tests confirmed the effectiveness of these recommendations (data not shown). For blackberries, the best results were obtained using conventional extraction with 50% ethanol, regardless of the acidification level, at room temperature. In the case of purple sweet potatoes, the best results were obtained using 50% ethanol acidified to pH 2, especially when subjected to agitation in a shaking bath for one hour at 40°C (data not shown). The anthocyanin extraction behavior was similar across three different cultivars of both raw materials.

## 5.2. Conclusion

In conclusion, this study provides a comprehensive evaluation of various methodologies used for anthocyanin extraction, ranging from conventional techniques to more innovative, non-conventional methods. Each technique leverages fundamental chemical and physical principles, with their efficacy largely dependent on key variables such as solvent selection, temperature control, solvent-to-matrix ratio, contact time, and the pre-treatment of plant matrices. These factors significantly optimize the yield and purity of anthocyanins, influencing both laboratory research and industrial applications.

The morpho-anatomical structures of plant tissues whether roots, tubers, leaves, flowers, fruits, or seeds present unique challenges and opportunities for anthocyanin extraction. Each plant organ contains specialized cells and varying distributions of key substances like cellulose, hemicellulose, lignin, amylose, amylopectin, and pectin, which must be carefully considered when selecting an extraction method. The presence of these structural components can significantly impact the interaction between the extraction solvent and the matrix, as well as the efficiency of cell wall disruption, which is a critical step in the extraction process.

By implementing a decision-tree approach, this study offers a practical tool to help researchers and industry professionals systematically select the most appropriate extraction method based on the specific characteristics of the plant matrix. This framework considers the morpho-anatomical structure, extraction parameters, and solvent systems to streamline the decision-making process. As a result, this approach can optimize resource use, reduce experimental trial and error, and enhance the overall efficiency of anthocyanin extraction.

The decision-tree model was validated using blackberry and purple sweet potato matrices, demonstrating its applicability across different plant structures. The results show that this tool can not only improve the selection process but also significantly contribute to reducing time and resource investment. This methodology provides a valuable contribution to anthocyanin research by facilitating more targeted and efficient extraction methods, which are critical for both scientific inquiry and commercial applications in the food and nutraceutical industries. In the broader context, this study underscores the importance of considering plant matrix variability and extraction method characteristics in anthocyanin research. It also opens avenues for further development of decision-support tools that can be adapted to other bioactive compound extractions, enhancing productivity in natural product research. Ultimately, this decision-tree framework represents a significant step forward in optimizing extraction protocols and contributing to more sustainable and efficient food science and technology practices.

# 6 CHAPTER 2 – EXTRACTION OF ANTHOCYANINS FROM PURPLE SWEET POTATO USING SUPERCRITICAL CARBON DIOXIDE AND CONVENTIONAL APPROACHES

## 6.1 Introduction

Sweet potato (*Ipomoea batatas* L.) is a tuberous root that has a wide range of soil and climatic adaptability conditions and an extended shelf life (LAO; CHENG; WANG et al., 2020). Purple sweet potato (PSP) contains valuable attributes, ranging from nutritional richness to nutraceutical potential (PALUPI et al., 2024). Anthocyanins are the most notable health-boosting compounds found in PSP, among many other compounds (LI et al., 2019). These compounds offer compelling bioactive benefits and promise to become a sustainable and promising source of natural colorings (SETYAWATY, 2020). This prospect can be a game-changer in the food industry, particularly in colorants for food, that can help to replace synthetic colorings within the Red 30 to 40 spectrums (XU et al., 2023; VEGA et al., 2023).

Anthocyanins constitute the largest group of polar and reversible antioxidant compounds, allowing their coloration to be applied in various sectors (TENA et al., 2022). However, properly extracting these compounds is essential for their utilization in food matrices (AKOGOU et al., 2018). In the extraction of bioactive compounds, solvent extraction has been widely accepted as the conventional method (MATTOS et al., 2022; KOZICKA & HALLMANN, 2023; VEGA et al., 2023). Despite the existence of several conventional anthocyanin extraction methods, for samples with high starch content, maceration or blinder crushing associated with a temperature above the environmental condition (25 °C) are typically used to facilitate the release of anthocyanins surrounding the cellular structure (HEINONEN et al., 2016; AKOGOU et al., 2018).

However, the type of solvent is critical to get a high yield during the extraction (VEGA et al., 2023; MATTOS et al., 2022). Despite the importance of yield during the extraction to produce ingredients intended for consumption, solvents such as methanol, acetone, and their mixtures are not recommended for extraction when the destination use is in food ingredients due to their high toxicity (TENA et al., 2022 HALLMANN, 2023).

Nevertheless, combining ethanol and water (50% v/v) is common in anthocyanin extraction because of satisfactory results in several cases (AKOGOU et al., 2018 & NUNES et al., 2022). Recent studies utilizing SC-CO2 have highlighted the significance of integrating sustainable and eco-friendly methods in extracting compounds while ensuring optimal performance and efficiency (NAJAFABADI et al., 2023). These methods aim to reduce the amount of organic solvents, preserve the sample during extraction by minimizing exposure to light, oxygen, and temperature, and ensure safety

by using minimal solvent volumes (TENA et al., 2022). Thus, SC-CO2 has emerged as a promising approach for the extraction of various bioactive compounds from several food matrices (TUHANIOGLU & UBEYITOGULLARI, 2022; ZHU & CUI, 2019; ROCCHETTI et al., 2022; MONROY et al., 2016).

SC-CO2 extraction systems significantly reduce the solvent volumes compared to conventional techniques (YAVUZ-DÜZGÜN & ÖZÇELIK, 2023). Additionally, SC-CO2 can enhance profitability by reducing energy costs (TENA et al., 2022). Compared to other green extraction methods, such as ultrasound-assisted, microwave-assisted, and enzyme-assisted extractions, SC-CO2 offers a unique system that operates at relatively low temperatures (~50 °C) in a dark, oxygen-free environment (CHEMAT et al., 2023; BAGADE and PATIL, 2021; VARDAKAS et al., 2024).

SC-CO2 extraction represents a state of CO2 maintained at a temperature and pressure above its critical point (7.4 MPa and 31.1 °C) (Idham et al., 2022). CO2 is a green solvent, offering advantages like low toxicity, non-flammability, and environmental sustainability (KANG et al., 2024). To selectively extract polar compounds (i.e., anthocyanin) while minimizing degradation, SC-CO2 is typically paired with a polar cosolvent (TUHANIOGLU & UBEYITOGULLARI, 2022). Although numerous studies have been conducted on extracting anthocyanins from plants using SC-CO2, research on the factors that enhance anthocyanin and antioxidant extractions from PSP is still in its early stages (MONROY et al., 2016; LAO et al., 2020; and PAZIR et al., 2021).

Replacing conventional methods with SC-CO2 requires a comprehensive screening of factors synergistically contributing to increased yield. It is crucial to study the influence of pressure, temperature, cosolvent, and sample ratio in a single study to achieve more precise results for potential industrial applications.

Therefore, this study aimed to extract anthocyanins from PSP using cosolvent-modified SC-CO2. The specific objectives were to ( i ) examine the influence of SC-CO2 extraction conditions, including pressure, temperature, cosolvent, and solvent: sample ratio, on anthocyanin content and ( ii ) characterize the extracts for their TPC (total phenolic content), AC (anthocyanins content), AA (antioxidant activity), and composition. The optimized SC-CO2 extraction conditions were compared with the conventional methanolic and ethanolic extractions. Furthermore, the impact of various extraction methods on PSP morphology was analyzed.

## 6.2. Materials and Methods

### 6.1.1 Materials

Purple sweet potatoes (PSP) were purchased from a local grocery store (AR, USA). Ethanol, methanol, potassium persulfate, acetic acid, sodium acetate trihydrate, and cyanidin-3-glucoside were purchased from Fisher Scientific (PA, USA). Formic acid, gallic acid, and ferric chloride were purchased from MP Biomedicals (OH, USA). DPPH (2,2-Diphenyl-1-picryl-hydrazyl) was purchased from TCI (OH, USA), and Trolox (6-hydroxy-2,5,7,8-tetramethylchroman-2-carboxylic acid) was obtained from Millipore Sigma (MO, USA). Liquid CO2 (99.99% purity) was supplied by Airgas, Inc. (AR, USA).

### 6.1.2 Methods

#### 6.1.2.1 Sample preparation

PSP tubers (500 g) were sliced into 50 mm thick pieces and freeze-dried (LABCONCO, MO, USA) at -45 °C for 48 h with a vacuum pressure of 0.048 mbar. The moisture content of the lyophilized PSP was 4.1 ± 0.7% (w/w, wet basis). Then, the dried samples were powdered using a Blixer food processor (Robot Coupe USA, Inc., MS, USA) and sieved through (200 mesh). The samples were stored at room temperature (23 ℃) in an airtight polypropylene bag until further assays.

#### 6.1.2.2 Color analysis

The color of PSP samples was determined using a colorimeter (Minolta CR-300, Konica Minolta, NJ, USA). The device was calibrated using a white calibration plate before use. The results were expressed as L* (lightness/darkness), a* (redness/greenness), and b* (yellowness/blueness) values (DUTT and NATH, 2024).

#### 6.1.2.3 Brix analysis

The soluble solid content was determined at constant room temperature (23 ºC) using a portable digital refractometer (Instrutherm, RTDS-28, São Paulo, Brazil). The results were expressed as degrees Brix (°Brix) (BARROS et al. 2023).

#### 6.1.2.3 Lipid content

According to LIJUN et al. (2023), lipid content was determined using a Soxhlet apparatus in triplicates. Dried PSP samples (3 g) were placed into a cellulose extraction thimble and topped with a cotton ball. Subsequently, the thimble was inserted in the Soxhlet apparatus attached to an Erlenmeyer flask containing 120 mL of petroleum ether to start the extraction process. After 8 h of extraction, the residual solvent was fully evaporated in an oven until a constant weight was achieved. The resulting lipids were weighed, and

the lipid content was calculated using the following equation:

Lipid content (%,dry basis) = (lipid weight (g))/(sample weight (g)) x 100 (Eq. 1)

**6.1.2.4 Extraction of phenolic compounds**

Conventional solvent extraction methods were compared with cosolvent-modified SC-CO2 extraction, as detailed in Table 1.

**6.1.2.4.1 Conventional extraction**

The conventional extraction was conducted according to AKOGOU et al. (2018), with some modifications. Briefly, the extractions were carried out with different solvents, solvent-solute ratios, and extraction times (Table 1). After each extraction, the suspensions were centrifuged for 20 min at 3100g and 0 °C. Finally, the extracts were collected in 40 mL brown glass vials, flushed with nitrogen, and stored at -20 °C until further analyses.

**6.1.2.4.2 SC-CO2 extraction**

The modified SC-CO2 extraction was conducted using the method of TUHANIOGLU and UBEYITOGULLARI (2022). Additionally, modified SC-CO2 was carried out using a lab-scale SC−CO2 extractor (SFT-120, Supercritical Fluid Technologies, Inc., DE, USA) coupled with a cosolvent pump (LL-Class, Supercritical Fluid Technologies, Inc., DE, USA) (Fig. 5). The high-pressure CO2 pump had an internal thermoelectric cooling module; hence, no additional cooling bath was necessary.

The samples were mixed with 60% (w/w) glass beads (3 mm diameter) to prevent caking and ensure a uniform solvent distribution. The vessel was filled with glass wool to prevent clogging. CO2 was flushed through the system for 5 s to remove any trapped air, and then the needle and micrometering valves' temperatures were set to 80 °C to prevent freezing due to the Joule-Thompson effect. The vessel was then set to specific temperatures (35-55 °C) and pressures (30-40 MPa). After the static extraction (20 min), the CO2 flow was started and kept constant throughout the process (120-180 min) at 2 L/min (measured at ambient conditions). Extracted fractions were continuously collected in a 40 mL brown glass vial submerged in an ice bath. After the extraction was terminated, the samples were centrifuged for 20 min at 3100g and 0 °C, flushed with nitrogen, and stored in a freezer at -20 °C until further analyses.

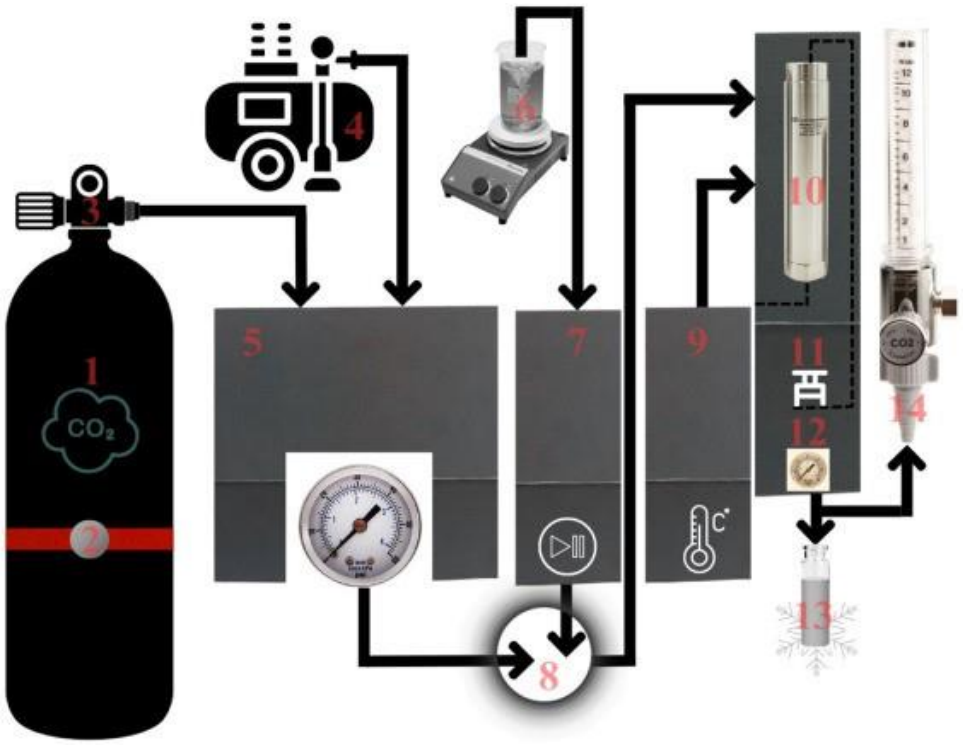


**Figure 5.** Schematic diagram of SCsingle bondCO2 extraction system. (1) CO2 cylinder; (2) heating jacket; (3) needle valve; (4) compressor; (5) high-pressure pump; (6) cosolvent; (7) cosolvent pump; (8) rupture disk; (9) temperature controlling unit; (10) high-pr pressure vessel; (11) needle valve; (12) micrometering valve; (13) sample collecting vial in an ice bath; and (14) flow meter. Source: designed by the Author, 2025

Additionally, the selection of specific temperatures (35-55 °C), pressures (30-40 MPa), and cosolvent concentrations (10-30%) in the SC-CO2 extraction process was guided by both theoretical considerations and findings from previous studies. Temperatures within this range were chosen based on the need to maintain the integrity of heat-sensitive anthocyanins while optimizing the solubility and diffusion rates of bioactive compounds. Previous research has shown that temperatures above 55 °C may lead to the degradation of anthocyanins, while lower temperatures could result in insufficient solubility and extraction efficiency (CHEMAT et al., 2023). The pressure range of 30-40 MPa was selected to improve the extraction of phenolic compounds (KANG et al., 2022). For cosolvent concentrations, ethanol-water mixtures were used at varying ratios (10-30%) based on their ability to modulate the polarity of the SC-CO2 system. This is crucial for extracting polar compounds such as anthocyanins. Ethanol is a preferred cosolvent due to its safety and effectiveness. Lower concentrations (10%) were tested to assess the baseline extraction capacity, while higher concentrations (up to 30%) were used to explore the maximum enhancement of anthocyanin yield (TENA

et al., 2020).

#### 6.1.2.5 Determination of total phenolic content

Total phenolic content (TPC) was quantified in PSP extracts using the Folin-Ciocalteu method, as detailed by KAUR and UBEYITOGULLARI (2023). In brief, 100 µL of the extract was combined with 500 µL of 0.2 N Folin-Ciocalteu's phenol reagent using deionized,initiating a 5 min reaction period at room temperature (23 °C). Subsequently, 400 µL of 0.7 M sodium carbonate solution was introduced, and the mixture underwent a 2 h incubation time at room temperature (23 °C). TPC was determined colorimetrically (Milton Roy Spectronic 1201 UV/Vis spectrophotometer, PA, USA) based on a gallic acid (0–200 ppm) standard curve at 760 nm (R2 = 0.99). The analyses were conducted in triplicates. The TPC was expressed as mg of gallic acid equivalent (GAE) per g of dry PSP.

#### 6.1.2.6 Determination of total anthocyanins and their identification

The total monomeric anthocyanins content (ANC) was determined according to GONÇALVES et al. (2024), with slight modifications. The centrifuged extracts were analyzed using a spectrophotometer (Milton Roy Spectronic 1201, PA, USA) at 535 nm for anthocyanins. The standard curve (R2 = 0.99) was prepared using cyanidin-3-glucoside (0 to 1000 ppm) for total anthocyanins, and the results were expressed in mg of cyanidin-3-glucoside (C3G) per 100g of dry PSP. Additionally, the identification of anthocyanins was carried out with HPLC/UV-Vis (SPD-20AV UV/VIS detector, Shimadzu Corp., Japan) and HPLC-ESI-MS using an HP 1000 series HPLC and a Bruker Esquire 2000 quadrupole ion trap mass spectrometer equipped with a binary pump, vacuum degasser, auto-sampler, and thermostatic column compartment. The analyses were executed following the protocol summarized by Brownmiller and Prior (2008) with slight modifications. A 250 × 4.6 mm Symmetry C18 column (Waters Corp., MA, USA) was employed for the chromatographic separation. The mobile phase comprised of a gradient of 5% formic acid (A) and 100% methanol (B). The flow rate was maintained at 1.0 mL/min, and the linear gradient started from 2% B to 60% B over 60 min. Anthocyanin peaks were optimized by UV-Vis and identified with mass spectrometry (MS) at 510 nm. The following conditions of capillary voltage at -4.1 kV, nebulizer gas pressure at 32 psi, and dry gas flow at 12 L/min were used to condition the system. The tandem mass spectrometry (MS/MS) system was carried out in positive ion mode, and multiple reaction monitoring (MRM) mode was used for acquisition.

### 6.1.2.7 Determination of antioxidant activities

#### 6.1.2.7.1 Determination of DPPH radical scavenging activity

The DPPH radical scavenging activity was conducted according to Im, KIM and LEE (2021). In brief, 150 µL of sample extracts were reacted with 200 µL of 0.15 mM DPPH in ethanol, maintained at 25 °C for 30 min. Then, the absorbance was measured at 517 nm. The calibration curve (R2=0.99) was prepared using different Trolox concentrations (0-150 ppm). The results were expressed in mg of Trolox equivalents (TEV) per g of dry sample.

#### 6.1.2.7.2 ABTS radical scavenging activity assay

The ABTS assay was conducted following the procedures by SARI et al. (2019) with some modifications. The ABTS radical cation (ABTS+) solution was prepared by combining a 7 mM ABTS+ stock solution in ethanol with 2.45 mM potassium persulfate in a 1:2 volume ratio in water, allowing the reaction to proceed for 8 h before use. Subsequently, the solution was diluted with ethanol to achieve an initial absorbance of 0.700±0.02 at 734 nm. Then, 2 mL of the ABTS+ solution was carefully mixed with 100 µL of the sample extracts and incubated for 10 min in the dark at room temperature (23 ℃). The absorbance was measured at 734 nm, and the results were expressed as mg of Trolox equivalent antioxidant capacity (TEAC) per g of dry sample.

#### 6.1.2.7.3 Ferric reducing antioxidant power (FRAP) assay

The FRAP assay of PSP extracts was carried out according to AHMADZADEH et al. (2023). FRAP solution was prepared by mixing acetate buffer, TPTZ (2,4,6-Tris(2-pyridyl)-s-triazine)) solution, and FeCl3 solution in the ratio of 10:1:1 (v/v/v), respectively. The acetate buffer was prepared by mixing sodium acetate trihydrate and acetic acid in deionized water until the pH reached 3.6. The TPTZ solution was obtained by dissolving TPTZ in a 40 mM hydrochloric acid solution. The 20 mM FeCl3 was prepared by dissolving FeCl3 powder in deionized water (TUNNISA et al., 2022). The FRAP solution was incubated in a water bath for 30 min at 37 °C and 100 rpm. A volume of 150 µL of PSP extract was added to 2,850 µL of FRAP solution and vortexed. Then, the solution was incubated in a dark environment at room temperature (23 °C) for 30 min. Finally, the absorbance was measured at 593 nm. Gallic acid solutions (0 to 50 ppm; R2 = 0.99) in water, were used to obtain a standard curve, and the results were expressed as mg of gallic acid equivalent (GAE) per gram of dry sample.

#### 6.1.2.8 Scanning electron microscopy (SEM)

The surface morphology was analyzed using an SEM (FEI NovaNanolab200 Dual-Beam system). Before the analysis, the samples were coated with a gold layer using EMITECH SC7620 Sputter Coater (MA, USA). The coated samples were then subjected to SEM analysis under a low vacuum mode at a working distance of 5 mm at 15 mA and 15 k (KAUR and UBEYITOGULLARI, 2023).

### 6.3 Statistical Analysis

Statistical analysis was performed using R Studio (Version R version 4.2.1). After confirming that the assumptions of parametric analysis (such as normality and homogeneity of variances) were met, ANOVA ($\alpha = 0.05$) was performed to understand the statistically significant differences between the means of multiple groups or conditions according to our experimental design to compare the effects of different extraction parameters on multiple response variables. Subsequently, multiple comparisons of the means were conducted using the Tukey test at $\alpha = 0.05$. The experiments were conducted in triplicates and presented as mean ± standard deviation.

### 6.4. Results and discussion

#### 6.4.1. Sample characteristics

To ensure consistent results in planned experiments, we first analyzed the PSP color parameters (L*, a*, b*), pH, Brix, and lipid content. The brightness (39.65 ± 0.17), greenness/redness (20.47 ± 0.11), and blueness/yellowness (1.23 ± 0.09) values indicated that the PSP is a distinctly purple cultivar with a tendency towards darker shades. Additionally, the °Brix and lipid contents were 18.26 ± 0.01 °Brix, and 1.46 ± 0.02% (dry basis), respectively. The observed color profile, characterized by a relatively dark hue with red and yellow tones, confirms the cultivar's identity and suggests that the PSP used in this study was at an optimal ripeness stage. Recent studies, such as those by FERREIRA et al. (2023), have highlighted the importance of cultivar selection and maturity stage in determining anthocyanin-rich crops' antioxidant capacity and pigment concentration. This supports the observation that this study's dark color and moderate PSP acidity indicate high bioactive compound content, essential for industrial applications in natural food colorants. The pH of the PSP was measured to be 5.7 ± 0.12, showing a moderate predominance of acidic conditions in the samples. According to CHEIN et al. (2019), the acidic environment of the sample is crucial to preserve the purple color and prevent anthocyanin degradation.

### 6.4.2. Optimization of cosolvent-modified SC-CO2 extraction

Figs. 6 and 7 show the extraction process to optimize TPC and ANC on PSP utilizing ethanol-water (50% v/v) as cosolvent-modified by SC-CO2. Effects of pressure (30 MPa and 40 MPa), temperature (35 and 55 °C), and cosolvent rate (10%, 20%, and 30%) were evaluated. The positive impact of the high cosolvent rate (i.e., 30%) was evident in both the TPC and ANC, which was due to the increased polarity of the SC-CO2 mixture at higher rates of ethanol. It was found that using 10% cosolvent rates (Table 1, S1-4) resulted in poor extractions under any conditions. The simultaneous increase of pressure and temperature significantly reduced the yields ($p<0.05$). Therefore, the TPC and ANC were significantly lower at 55 °C and 40 MPa (TPC: 100±0.54 mg/g, ANC: 28±0.12 mg/100g) than at 35 °C and 30 MPa (TPC: 133±0.34 mg/g, ANC: 38±0.17 mg/100g) at 30% cosolvent ($p<0.05$) (Figs. 6 and 7). On the other hand, the temperature did not significantly affect the yields at cosolvent rates of 20% or above and a pressure of 40 MPa ($p>0.05$). The only exception was observed in ANC at 30% cosolvent, where SC-CO2 extraction at 35 °C (36±2.01 mg/g) resulted in a higher extraction than 55 °C (28±0.32 mg/g) ($p<0.05$), which could be due to the higher density of the solvent mixture.

Furthermore, at 55 °C and 30% cosolvent ratio, changing the pressure (30-40 MPa) did not demonstrate any significant impact on the ANC and TPC yields ($p>0.05$). Instead, at 35 °C and 30% cosolvent ratio, TPC was higher at the lower pressure (30 MPa), even though ANC was not different as the pressure changed from 30 to 40 MPa. The highest TPC and ANC were achieved using 30 MPa, 30% cosolvent, and 35 °C. The findings demonstrate a significant influence of the cosolvent rate (10%, 20%, and 30 %) on the TPC and ANC yields ($p<0.05$), indicating that it is imperative to operate at a rate exceeding 20% to achieve maximum TPC and ANC extraction. The efficiency of SC-CO2 in disrupting PSP cell walls likely stems from the combined mechanical and chemical effects of SC-CO2, which penetrates into cell membranes more effectively than liquid solvents. This mechanism is supported by findings from Zhu and Cui (2019) & Yavuz-Düzgün & Özçelik (2023), who observed similar effects in other plant matrices.

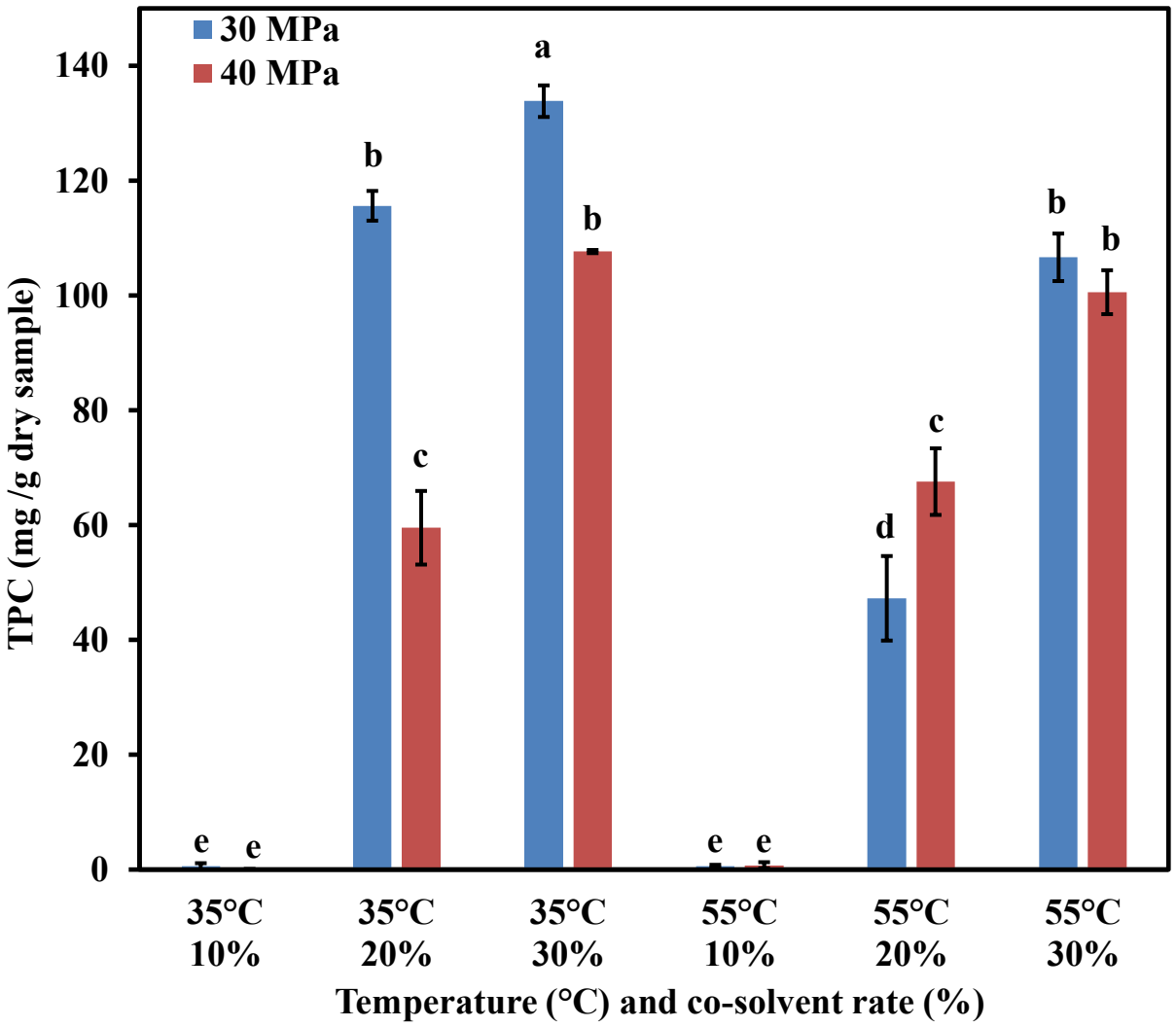


**Figure 6.** Total phenolic contents (TPC) extracted with SCsingle bondCO2 modified with ethanol-water (50 %) at different conditions. Means ± standard deviation bars that do not share the same letter are significantly different ($p < 0.05$).

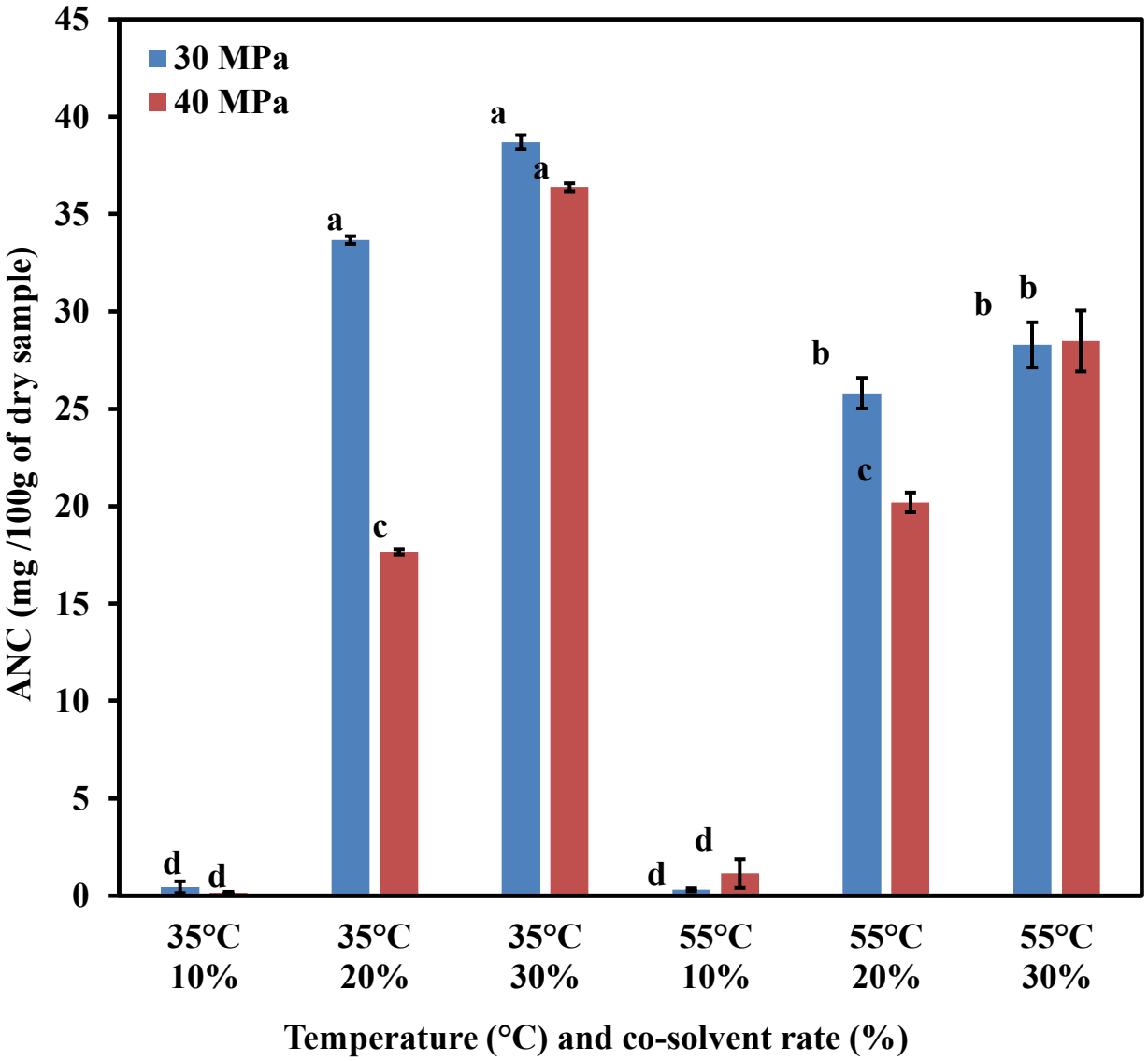


**Figure 7.** Total anthocyanin contents (ANC) extracted with SC−CO2 modified with ethanol-water (50 %) at different conditions. Means ± standard deviation bars that do not share the same letter are significantly different ($p < 0.05$).

In general, the negative correlation between pressure or temperature and extraction yields is related to competition between conditions (density and volatility). Increasing temperature can increase the solubility of compounds by enhancing their volatility. However, beyond a certain point, further temperature increases can reduce the density of SC-CO2, thereby reducing its solvating power (YOUN et al., 2023). Additionally, higher temperatures may increase the volatility of anthocyanins, causing degradation before they can be extracted, a challenge noted in previous studies involving the extraction of thermolabile compounds (CHEMAT et al., 2023). Generally speaking, the solvent ratio in SC-CO2 (10%<20%<30%) can effectively influence the extraction yield. SC-CO2, with its gas-like diffusivity and liquid-like dissolving power, dissolves the wax layer and phospholipid layers of cell membranes, disrupting cell structures and

releasing anthocyanins (MACIEL-SILVA et al., 2022). An acidic environment created by CO2 enhances anthocyanin solubility. The decompression effect further destroys cell structures, driving mass transfer. This effect is influenced by the mass ratio of CO2 to the solid-liquid mixture. A higher solid-liquid mixture (30%) intensifies this effect, improving extraction efficiency (PAUDEL et al., 2015).

The solvent ratio is a vital parameter, with lower ratios leading to more effective extraction due to a stronger explosive effect and improved mass transfer (YANG et al., 2017). A similar effect was reported by XU et al. (2010), where the maximum result was 58.29±0.56mg/100g (ANC), and the minimum was 55.60±0.34 mg/100g (ANC) when used at 60 °C and high (410/440, w/v) and low (140/710, w/v) volume ratio of solvent (solvent/sample), respectively. The results by XU et al. (2010) showed that using a higher volume ratio resulted in a slightly higher yield of the target compound (ANC), which aligns with the general understanding that a higher volume of CO2 can enhance extraction efficiency (ROCCHETTI et al., 2022).

Similarly, a lower volume ratio resulted in a slightly lower yield, indicating that the reduced amount of solvent could have been more effective in fully extracting the compounds from the sample. Furthermore, the outcome can vary based on the solvent type, specific anthocyanins present, extraction time, and other factors (MORATA et al., 2023). Considering the sensitivity of the phenolic compounds, the elevated temperatures may cause structural changes in the phenolic compounds, resulting in reduced yields. Our findings align with the study conducted by DARAEE et al. (2019), which tested the impact of SC-CO2 on extracting TPC and chlorogenic acid (CGA) from sunflowers. The study reported that the increased cosolvent rate improved CGA extraction (DARAEE et al., 2019). Despite several factors affecting the yield of TPC and ANC through cosolvent flow, two factors (i.e., the high selectivity of the SC-CO2 extraction system and diffusion from the cell matrix) can be explained correctly. Solute diffusion from the cell matrix can substantially improve the contact time between the PSP sample, solvent, and cosolvent; consequently, a higher extraction yield can be achieved.

The impact of cosolvent composition was further examined for TPC and ANC (Fig. 8) at the fixed conditions (20% cosolvent rate, 30 MPa, and 35 °C for 180 min). In a water mixture, ethanol concentrations of 30, 40, 50, 60, and 70% (v/v) were tested as cosolvents in the SC-CO2 system (Fig. 8). The yield of TPC and ANC increased when the ethanol and water mixture reached 40% (v/v). The highest levels of TPC (143.66±3.5 mg/g dry basis) and ANC (41.67±2.0 mg/100g dry basis) were achieved at a 60% ethanol concentration. When 60% ethanol was utilized as a cosolvent in SC-CO2 extraction, the TPC increased by 53% compared to using 30% ethanol. In addition, when 70% (v/v)

ethanol was utilized as a cosolvent, the TPC exhibited a reduction of 47% compared to 60% (v/v). This could be partially attributed to the combination of higher polarity and density in both solvents (ethanol and water) during extraction, combined with SC-CO2 (PHAN et al., 2022). Consequently, this promoted more excellent hydrogen bonding and dipole-dipole interaction, thereby intensifying the solubility of phenolic compounds in the resultant extract. In addition, water may enhance the surface area due to the swelling of the solid matrix and facilitate the solid–solvent interactions (de SOUZA et al., 2018). According to a study by Monroy et al. (2016), a lower amount of ethanol during SC-CO2 extraction can reduce the water solubility in SC-CO2, so it is possible to create two phases. This condition was also confirmed by the image taken when 30% ethanol (v/v) was used (not shown in this work); some samples inside the vessel remained dry after 180 min of extraction. These results are consistent with the findings of PHAN et al. (2022).

They discovered that the TPC in custard apple peel was significantly higher at 109.38 mg/g when using 12% (v/v) ethanol, compared to only 4.58 mg/g with 15% (v/v) ethanol (PHAN et al., 2022). However, an excessive elevation in the ethanol cosolvent ratio could diminish the interaction between solvent and solutes. As a result, this can decrease the extraction efficiency (YOUN et al., 2023). Similarly, TUHANIOGLU and UBEYITOGULLARI (2022) reported that 50% (v/v) of ethanol as a cosolvent was superior to pure ethanol in extracting total phenolics and flavonoids from black sorghum bran. This analysis can help understand the extraction progression, offering critical insights into potential trends or saturation stages (PETERSSON et al., 2010).

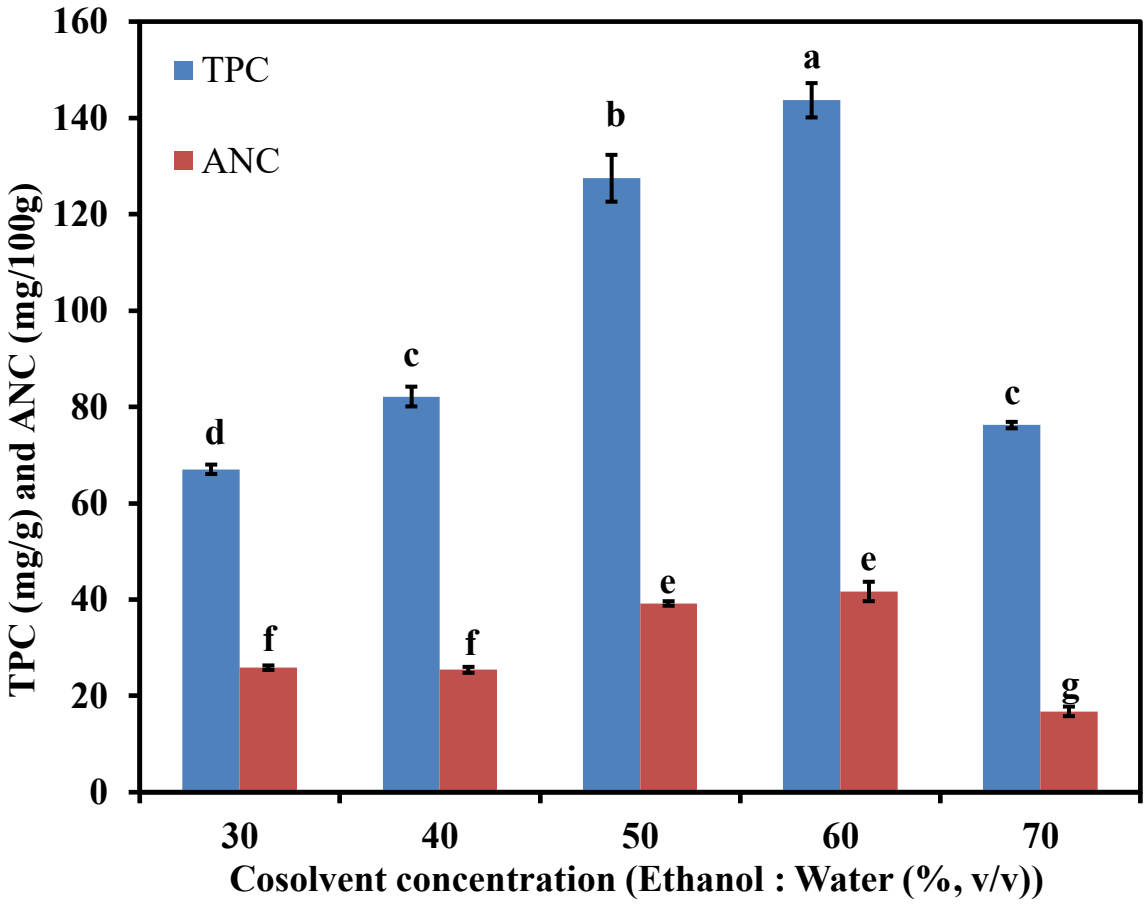


**Figure 8.** Effect of cosolvent composition on the TPC and ANC yields following 20 % cosolvent modified SC single bond CO2 extraction at 30 MPa and 35 °C for 180 min. Means ± standard deviation bars that do not share the same letter are significantly different ($p < 0.05$).

The impact of extraction time (up to 12 h) at 30 MPa, 35 °C, and 20% cosolvent (60% ethanol) on TPC and ANC is illustrated in Fig. 9. The TPC gradually rises throughout the 12 h run. This can be attributed to the sample matrix's complexity and the considerable phenolic content in various layers of PSP starch (ZHU & CUI, 2019). Moreover, TPC showed a sudden increase between the 2nd and 4th h (from 28±043 to 468±1.2 mg/g), followed by a gradual decline in the rate of increase until the 12th h. It is likely that phenolic compounds linked to the surface and other external layers of starch were released during the initial stages of extraction (YAVUZ-DÜZGÜN & ÖZÇELIK, 2023). However, as extraction time is extended, the starch matrix undergoes a structural transformation, potentially forming a more robust barrier that hinders TPC release, which resulted in a gradual decline in extraction efficiency, as ROCCHETTI et al. (2022) reported.

Furthermore, ANC increased sharply after the 2nd h (25±0.93 mg/100g), reaching a plateau at the 4th h (107±1.76 mg/100g). In other words, ANC did not improve after the 4th h. To the best of our knowledge, there is currently no literature available on the

extraction of TPC and ANC from PSP for 12h. However, similar trends were observed by PAZIR et al. (2021) when they compared the extraction of ANC from grape pomace at different times (30th to 180th min). They found that the total ANC yield was the lowest at 30 min (579.2±108.8 mg/kg dry matter) and highest at 180 min (1,216.7±279.7 mg/kg dry matter). The study by IDHAM et al. (2020) discovered that using a 75% ethanol (v/v) cosolvent-modified SC-CO2 resulted in a greater yield of TPC and total ANC after 120 min compared to 15 min of extraction time. It was also noted that the levels of TPC and ANC remained stable from the 120th min to the 150th min.

The extraction time proves to be a crucial parameter for achieving an efficient SC-CO2 extraction. Enhancing the efficiency of the SC-CO2 process entails prolonging the contact time between SC-CO2 and the sample material (IDHAM et al., 2020). However, due to the structural characteristics of the sample, the infiltration of solvent and diffusion of targeted compounds within particles still need to be improved. Consequently, as the extraction yield recovered during the slower extraction phase is negligible, emphasis is placed on the swift extraction phase (YAVUZ-DÜZGÜN & ÖZÇELIK, 2023). Additionally, in Fig. 9, the trend of low increment of TPC and ANC within the initial 3rd h in the initial phase (IF) was clear. Then, from the 3rd to 4th h, there was an increasing extraction rate (IER) until it tended towards saturation. Beyond this point, equilibrium was achieved between the 4th and 12th h as diffusion was dominant.

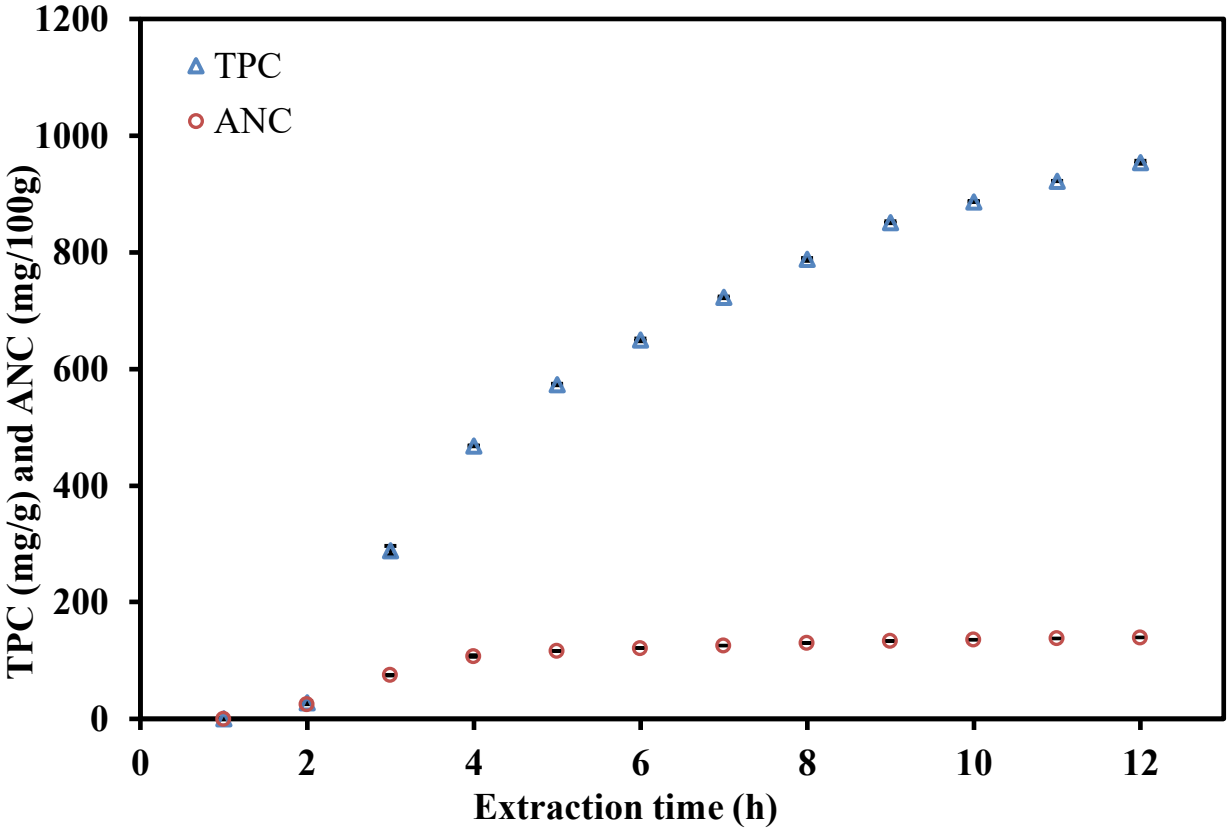

**Figure 9.** Effect of time on the total phenolic and anthocyanin yields following 20 % cosolvent (60 % ethanol) modified SC single bond CO2 extraction at 30 MPa and 35 °C.
Fonte: Elaborado pelo autor, 2024

As TAYLOR (2009) explained, extraction occurs rapidly during the IF, primarily influenced by the solute's solubility in SC-CO2. However, during the IER phase, the best interaction between solute and matrix resulted in a high extraction rate and a transition to a diffusion-controlled process. The phenomenon observed in the IF region can also be attributed to restricted access of SC-CO2 mixtures to the target solute or limited cosolvent to mobility within the PSP. Additionally, the complexity of the PSP sample can also impact the extraction rate in this region. Furthermore, after 4 h, an equilibrium state was observed. In this case, the trend indicated a complete extraction, and the solute extraction ceased to increase with prolonged extraction time (IDHAM et al., 2020). Hence, a 2 to 4 h extraction period was necessary to achieve an acceptable yield of TPC and ANC from PSP, considering the cost and time of extraction.

### 6.4.1. Comparison of the extraction methods

The first part of this study optimized the SC-CO2 extraction conditions to maximize the TPC and ANC yields from PSP. Condition S16 (35 °C, 20% cosolvent, 30 MPa for 3 h) was selected as the optimized condition among different temperatures at 35 °C and 55 °C, cosolvent concentrations of 10, 20, 30 % (v/v), and pressures of 30 MPa and 40 MPa. Then, we compared the best SC-CO2 extraction condition with all conventional extraction methods (E1, E2, M1, and M2). These parameters were selected based on prior literature by Tuhanioglu and Ubeyitogullari (2022). Then, the best condition of the initial experiment (S16) was compared with S18 in terms of solvent:sample ratios (25:1-45:1v/w), keeping the other factors constant (35 °C, cosolvent concentrations of 20% (v/v), and 30 MPa). The increased solvent:sample ratio was investigated for comparison with the conventional methods at the same solvent:sample ratio (45:1). As expected, increasing the solvent:sample ratio significantly increased the TPC and ANC yields ($p < 0.05$), where S18 resulted in the highest yield of TPC (339.81±6.07 mg/g), and ANC (135.99±4.97/100g). Thus, the S18 results were 62.48% and 73.01% higher than S16 in TPC and ANC, respectively.

Therefore, the optimized SC-CO2 conditions (S18) were chosen to make a comparison with conventional extraction methods, as presented in Fig. 10 (E1, E2, M1, and M2). In M1 extraction, the solvent ratio was lower (15:1) compared to M2 (45:1), resulting in lower TPC and ANC. The highest TPC and ANC values among the

conventional methods were observed in M2 as 541±4.64 mg/g and 147±4.22 mg/100g, respectively ($p<0.05$). The optimized SC-CO2 extraction using a 60% ethanol (v/v) mixture, temperature of 35 °C, pressure of 30 MPa, sample ratio of 45:1(v/w), and extraction time of 180 min (S18) resulted in a TPC of 339±6.07 mg/g, matching those of E1 (281±11.16 mg/g) and E2 (260±8.69 mg/g) ($p>0.05$). However, the solvent:sample ratio was higher in the S18 compared to E1 and E2. This conclusion is supported by Chen et al. (2023), who demonstrated that optimized SC-CO2 extraction with ethanol as a cosolvent offers similar or better yields than conventional methods.

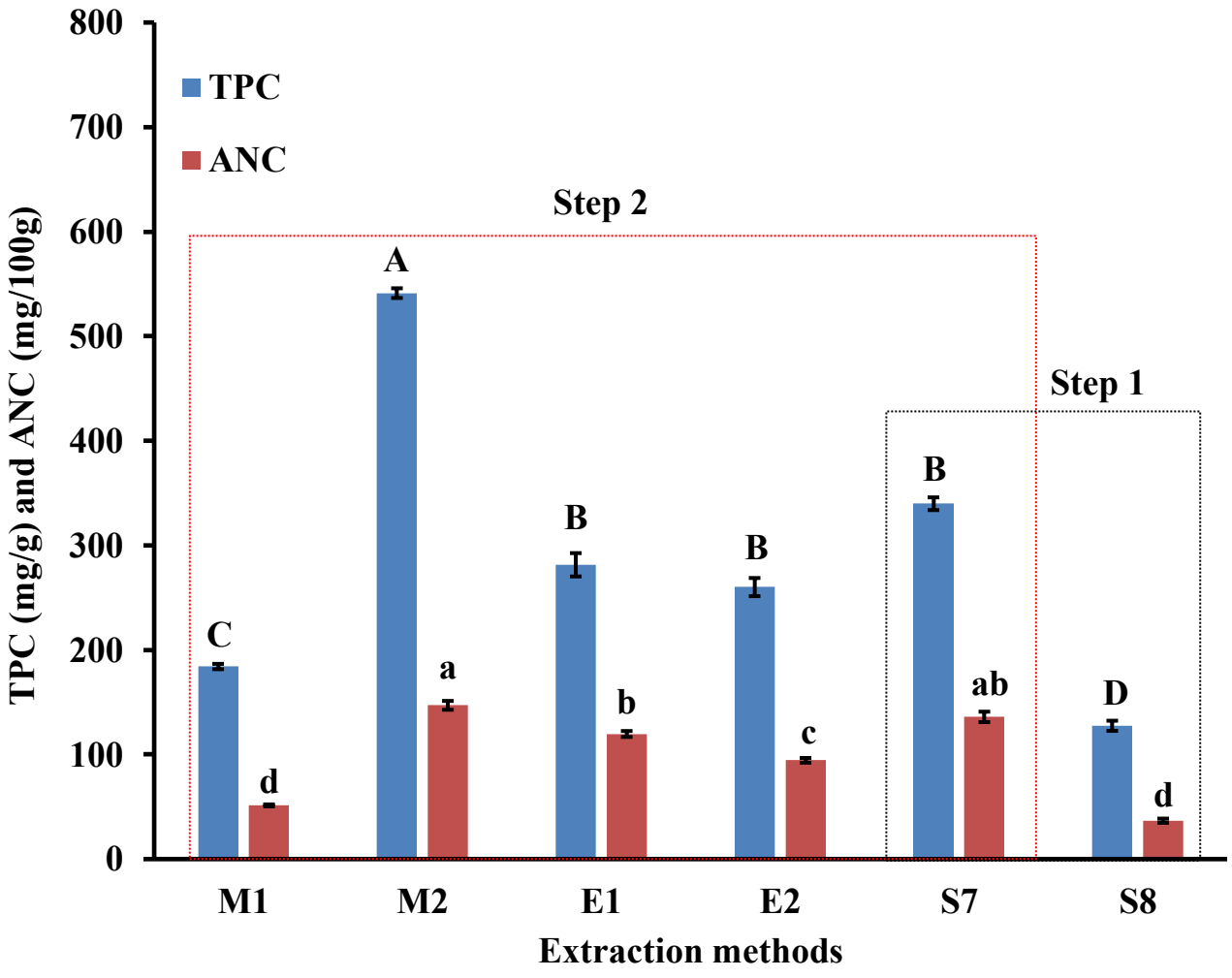


**Figure 10.** TPC and ANC extraction yields from different extraction methods (Table 1). Means ± standard deviation bars that do not share the same letter are significantly different ($p < 0.05$).

Sample mixing rate directly correlates with efficiency during the extraction process; this can be explained by the principles of solvent penetration and solute solubility described by ALARA et al. (2021). In conventional extraction methods, a higher solvent:sample ratio increases the solvating capacity due to the increased dissolution

and diffusion of phenolic compounds and anthocyanins (ACHARYA et al., 2015). With a lower solvent ratio in M1, the solvent becomes saturated more quickly, reducing its ability to dissolve additional phenolic compounds and anthocyanins. Additionally, the mass transfer rates are lower due to the limited solvent volume, leading to less efficient extraction (ALARA et al., 2021; TAKACS-NOVAK et al., 2017). The M1 was 62.48% lower than SC-CO2 (S18) and 30.77% higher than S16. Coherently, the highest TPC and ANC were found using methanolic extraction (M2), as reported by VEGA et al. (2017). Despite the high yields of methanol, it is important to explore eco-friendly alternatives due to its potential hazards. Emerging solvents like SC-CO2 are favored for their sustainable and green extraction processes. The mixture of water (polarity = 9.0) and ethanol (polarity = 5.2) improved the chemical and physical properties in terms of polarity, diffusibility, and affinity with phenolics and antioxidants in PSP samples. Additionally, SC-CO2 extraction decreased the pH in the extraction vessel, helping to extract and preserve phenolics in PSP extract.

While SC-CO2 extraction has demonstrated effectiveness comparable to traditional methods in lab-scale systems, future research should focus on large-scale operations and cost analysis to make SC-CO2 more accessible for commercial use.

### 6.4.2. Identification of anthocyanins

The MS/MS analysis of the anthocyanins from PSP samples across five treatments is represented in Fig. 11, where 22 peaks were identified (Table 2). Among the conventional extractions, the ethanolic extractions (Fig. 11- E1 and E2) yielded different major anthocyanin types compared to methanolic extractions (Fig. 11 - M1 and M2). Both E1 and E2 showed peaks 6, 9, 12, 17, and 20 as the predominant anthocyanins with different intensities, where cyanidin-3-p-hydroxybenzoylsophoroside-5-glucoside (6) was the dominant compound in both extractions with E1 showing consistently higher peak intensities for all significant anthocyanins. In contrast, the methanolic extractions (M1 and M2) displayed peaks 6, 12, 17, 18, 19, and 20 as the predominant species, with peak 17 (peonidin-3-caffeoyl-feruloyl sophoroside-5-glucoside) being the most abundant in both cases. Notably, peak intensities were significantly higher in M2 compared to M1 (Fig. 11), which aligns with the approximately threefold increase in ANC observed for M2 compared to M1. Notably, the anthocyanin profile of S18 closely resembled that of the methanolic extractions (Frod et al., 2019), with significantly higher peak intensities than E1 and E2.

The anthocyanin profile extracted by SC-CO2 was dominated by cyanidin derivatives, highlighting the selectivity of this method for specific bioactive compounds.

Recent research by ZHAO et al. (2023) using HPLC-MS/MS techniques confirmed that cyanidin-based anthocyanins are predominant in PSP, mainly when extracted under mild conditions that prevent degradation. Additionally, the ethanolic extract from S18 can be valued in the food industry as a natural colorant and functional ingredient due to its stability under processing conditions and ability to enhance antioxidant capacity in food products (YANG et al. 2023; WU et al., 2005).

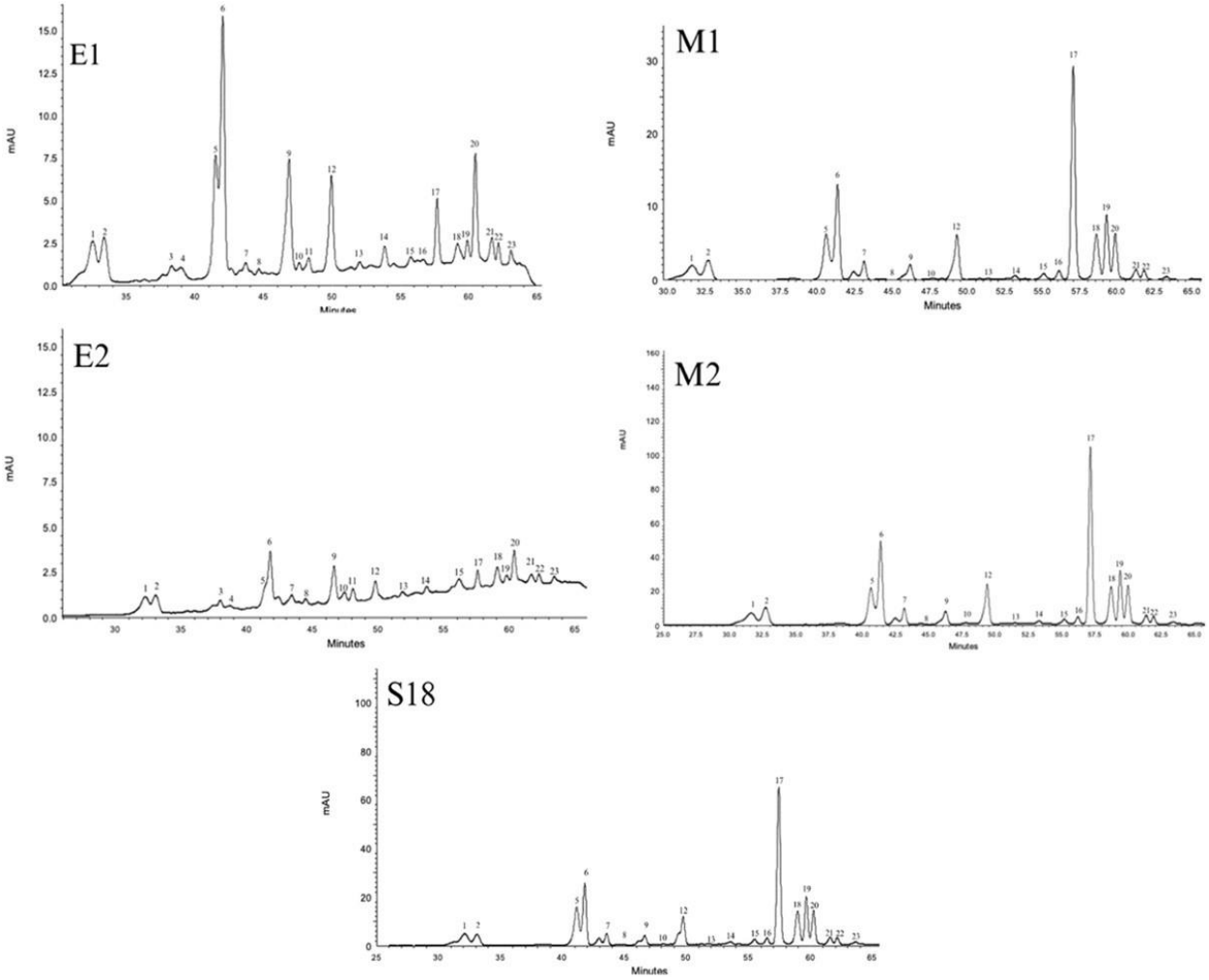


**Figure 11.** HPLC/UV–Vis MS chromatograms for anthocyanins obtained through different extractions from PSP. The identification of the peaks is provided in Table 2.

The anthocyanins identified in our work are consistent with those reported in other studies on purple sweet potatoes. The similar molecular weights (m/z) and fragmentation patterns (MS/MS m/z) across different works underscore the reliability of our findings (FROD et al., 2019; JESUS et al., 2021, LI et al., 2019; MAKOTO et al. 2001, SENEVIRATHNA et al., 2021; XU et al., 2015). The peonidin derivative (M+ (m/z) 1067.4)) found in peak 13 with the exact fragmentation pattern was not identified. Similar

derivatives are noted in the study described by CHEN et al. (2019), and SENEVIRATHNA et al. (2021).

### 6.4.3. Antioxidant activity

The antioxidant activities of S18, E1, E2, M1, and M2 methods were compared using DPPH, ABTS, and FRAP assays (Table 3). The lowest DPPH value was observed in E1 at 4.95±0.71 mg TEV/g, while the highest values were obtained with M2 (19.12±0.15 mg TEV/g) and S18 (18.17±0.41 mg TEV/g). It is important to note that the difference in DPPH yields of M2 and S18 is not significant, which means a cosolvent-modified SC-CO2 can equalize methanolic extracts in DPPH yields ($p<0.05$). S18 showed higher percentages of DPPH (73 and 54%), ABTS (78 and 59%), and FRAP (89 and 34%) values compared to E1 and E2, respectively. The superior antioxidant activity observed in the S18 extract, as indicated by DPPH, ABTS, and FRAP assays, underscores the efficacy of SC-CO2 in preserving the functional properties of anthocyanins and other phenolic compounds. A recent study by Nguyen et al. (2023) found that SC-CO2 extraction could retain higher antioxidant activity than conventional methods, particularly in fruit matrices rich in anthocyanins.

The ABTS radical scavenging effects in the S18 and M2 were determined as 7.3±0.2 mg/g and 7.6±0.1 mg/g, respectively, which are statistically similar ($p>0.05$). Furthermore, the ABTS radical scavenging activity in E2, M1, and E1 were 2.2, 2.8, and 3.7 times less than S18, respectively. For FRAP among the extractions, M2 (2134.7±2.6 mg/100g) showed the highest yield, followed by S18 (1398.6±3.5 mg/100g) ($p < 0.05$). Consistently, E1 yielded the lowest FRAP value at 153.7±2.0 mg/100g.

In general, the antioxidant activities studied in our experiment provided considerable improvements on those obtained by de SOUSA et al. (2022) in SC-CO2 with cosolvent extraction of blackberry (*Rubus* spp. Xavante cultivar) seeds studied, where the values obtained were 12,996 µmol TEV/100 g for DPPH, 12,948 µmol TEV/100 g for ABTS, and 14,243 µmol TEV/100 g for FRAP. The DPPH antioxidant activity in sample S18 matched the range reported by Im, Kim, and Lee (2021) for PSP, which was 6.10 to 7.66 mg TEV/g dry matter. All results from this study were within the range described by ZHU et al. (2010), except for two treatments. One treatment used 50 °C for 60 min with an 80% methanol-water mixture and a 15:1 solvent/sample ratio, and the other used 35 °C for 50 min with a 50% ethanol-water mixture and the same ratio. These treatments had a lower solvent/sample ratio compared to the others, impacting their efficiency. The DPPH method can be limited for hydrophilic compounds because of their interaction with water. The water-soluble ABTS method is additionally used to

achieve a more comprehensive understanding of antioxidant activity (CHEN et al., 2019).

The ABTS radical scavenging method can be assessed across a broad pH range, which is beneficial for examining the impact of pH on antioxidant mechanisms in food components. The results in the present study were similar to the range found by LEE et al. (2019) when comparing the effects of intracellular reactive oxygen species (ROS) in sweet potato colors. Their results were from 13 mg TEV/g dry sample to 57 mg TEV/g dry sample ($p<0.05$). Even though ABTS is an antioxidant radical cation not found in food or biological systems (SCHAICH et al., 2015), our result showed a significant performance in the SC-CO2 extraction method compared with other conventional extraction methods. FRAP, based on the single electron transfer technique, assesses antioxidant capacity by measuring the reduction of the ferric ion complex (Fe3+) to the blue ferrous ion complex (Fe2+), especially in acidic environments (MUNTEANU & APETREI, 2021). In comparison with the study by CAI et al. (2016), the treatment at 50 °C, 60 min of extraction time, 80% methanol + water mixture, ratio 45:1 (v/w) stands out (Table 1). On the other hand, there was a notable increase in FRAP (approximately 34.5%) by SC-CO2 extraction (S18) compared with conventional extraction (E2). Furthermore, the comparison between the optimal methanol-based treatment in conventional extraction and the ethanol-based treatment highlights the superior efficiency of methanol, demonstrating a 56.8% higher extraction efficiency. Surprisingly, the performance of ethanol in conventional extraction falls short by 22.3% compared to SC-CO2 extraction. These results compellingly reinforce the positive impact of SC-CO2 extraction, emphasizing its superior antioxidant efficacy. In addition, the SC-CO2 extraction approach is distinguished by environmentally friendly and sustainable aspects.

### 6.4.4. Morphology

Fig. 12 reveals the impact of different treatments on structural morphology. The untreated sample (C) indicated a nearly complete coating of additional structures and obstructed the identification of clear starch morphology. Ethanolic (E1, E2) and methanolic (M1 and M2) residue after extraction showed the adhered structures comparable with SC-CO2 extraction (S16 and S18).

According to NURDJANAH et al. (2020), the cellular structures surrounding the starch in PSP are cell wall material. Almost similar structures were revealed in E1 and E2. Despite treatment M2 being previously identified as the most efficient (Table 2), it retained adhered starch structures on the surfaces, and M1 and M2 showed similar structures.

A study from OCHOA and OSORIO-TOBÓN (2023) in PSP associates these

layers with fibers or proteins that remain post-extraction due to the lack of crucial conditions to remove them. The SC-CO2 treatment, S16, effectively removed adhered materials from the starch surface. Gonzalez et al. (2022) observed similar morphological changes in plant tissues subjected to SC-CO2 extraction, where the disruption of cellular structures facilitated the release of intracellular contents. Despite the lack of comprehensive studies in the scientific literature evaluating microscopic behaviors of structures post-exposure to SC-CO2 extraction, S18 (SC-CO2 + 20% cosolvent at 30 MPa and 35 °C for 180 min using 45:1 solvent:sample (v/w), suggests a simultaneous extraction of anthocyanins and potentially other polymers in PSP samples.

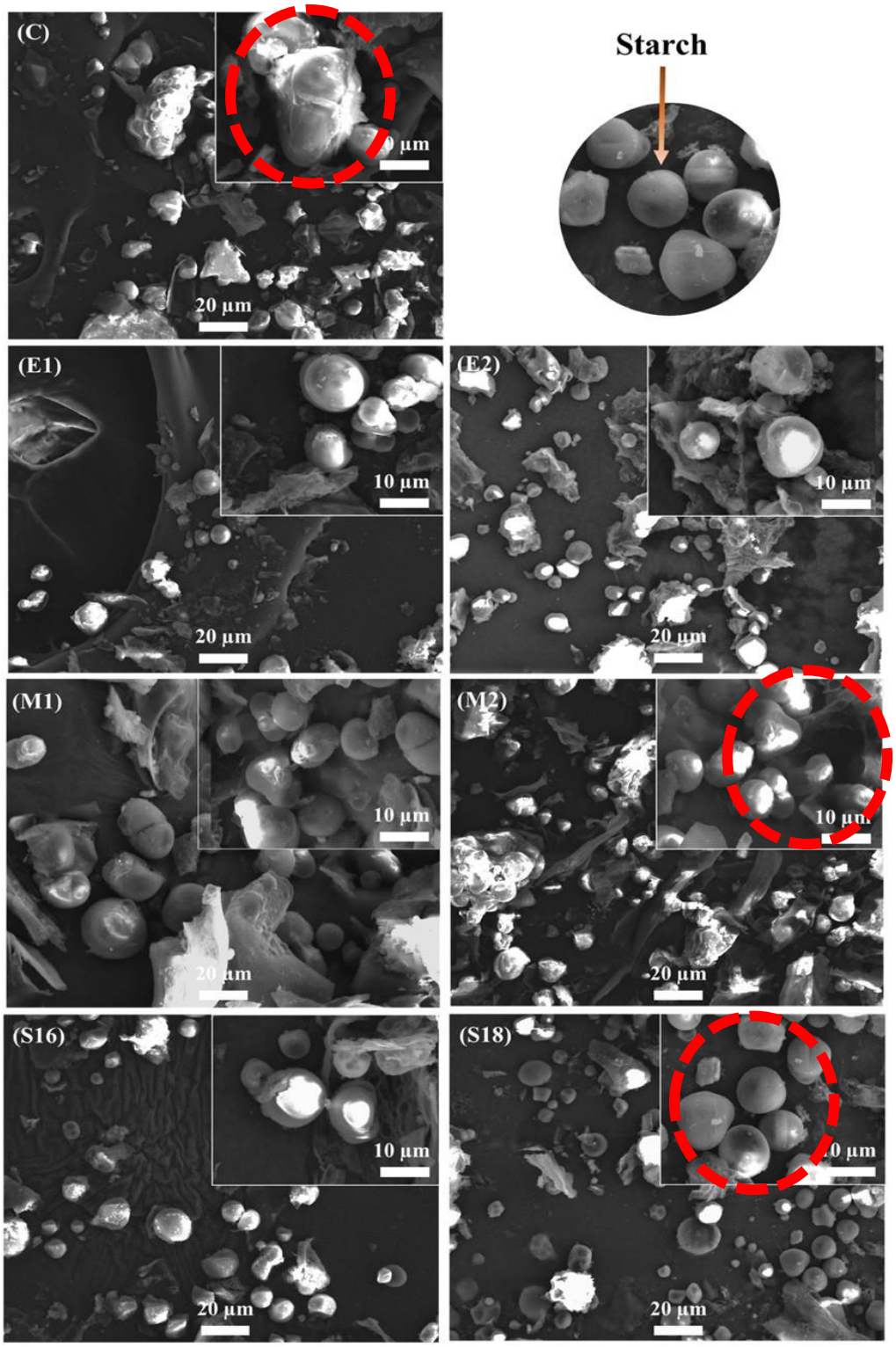


**Figure 12.** Reveals the impact of different treatments on structural morphology. The untreated sample (C) indicated a nearly complete coating of additional structures and obstructed the identification of clear starch morphology. Ethanolic (E1, E2) and methanolic (M1 and M2) residue after extraction showed the adhered structures comparable with SCsingle bondCO2 extraction (S16 and S18).

## 6.5. Conclusions

The findings demonstrated that cosolvent-modified SC-CO2 extraction offers a promising and environmentally friendly alternative for extracting phenolic compounds from purple sweet potato (PSP). The optimized conditions for ethanol-water-modified SC-CO2 extraction included a 20% cosolvent ratio, 30 MPa pressure, 35 °C temperature, and 180 min of extraction time with a 45:1 (v/w) solvent-to-sample ratio. Under these conditions, compared to the conventional extraction method with a high methanol-water ratio (M2), the total phenolic content (TPC) was 339.8 ± 6.1 mg gallic acid equivalents (GAE)/g, similar to the 340 mg GAE/g achieved by the M2 method. Similarly, the anthocyanin content (ANC) achieved by the optimized SC-CO2 method was 136.0 mg cyanidin-3-glucoside (C3G)/100 g, comparable to 136 mg C3G/100 g achieved by the M2 method. At the optimized SC-CO2 extraction condition, the antioxidant activities were 18.2 mg TEV/g, 7.3 mg TEV/g, and 1398.6 mg GAE/100 g, for DPPH, ABTS, and FRAP, respectively. On the other hand, the M2 method resulted in 19.1 mg TEV/g, 7.6 mg TEV/g, and 2134.7 mg GAE/100 g for DPPH, ABTS, and FRAP, respectively. The HPLC analyses indicated that the dominant anthocyanins extracted using M2 and cosolvent-modified SC-CO2 were peonidin derivatives. Also, ethanol-water-modified SC-CO2 extraction showed a high removal of cell wall material from the starch surface.

In conclusion, this study demonstrated that ethanol-water-modified SC-CO2 can be a viable and environmentally friendly alternative to traditional methanolic extraction methods for bioactive compound recovery from PSP. The TPC, ANC, and antioxidant activity assays underscore the potential of SC-CO2 methods for broader application in extracting natural food components while minimizing environmental impact. Specifically, the anthocyanins and phenolic compounds extracted using this method could be utilized as natural colorants and antioxidants in the food and nutraceutical industries. Future research is needed to confirm these results in large-scale SC-CO2 extraction systems.

# 7 CHAPTER 3 – DEVELOPING ANTHOCYANIN-LOADED AEROGELS FROM PURPLE SWEET POTATOES USING SUPERCRITICAL CARBON DIOXIDE DRYING

## 7.1 Introduction

The growing consumer preference for healthier and environmentally sustainable food products has driven the food industry to seek natural alternatives to synthetic additives (ALIOTTA et al., 2019; CORTEZ et al., 2017; SIGURDSON et al., 2017). Among these additives, synthetic colorants have been a focus of concern due to their potential health risks, including allergic reactions and links to chronic diseases (DE OLIVEIRA et al., 2024; SUDHAKARAN, 2024). These health concerns, regulatory pressures, and environmental sustainability demands have accelerated research into natural colorants derived from plant sources (AMAROWICZ et al., 2019; BENUCCI et al., 2022; OLADZADABBASABADI et al., 2022; SIGURDSON et al., 2017). Natural pigments, such as anthocyanins, enhance the aesthetic appeal of food products and provide additional health benefits due to their antioxidant, anti-inflammatory, and antimicrobial properties (CEVALLOS-CASALS et al., 2003; DOWNHAM et al., 2000; ROSELL et al., 2024). However, transitioning from synthetic to natural colorants presents significant challenges, particularly their stability, consistency, and compatibility within diverse food matrices (SIGURDSON et al., 2017). In this context, biopolymer-based aerogels emerge as a dual-solution platform: (i) in intelligent packaging, they act as moisture scavengers managing headspace humidity to slow spoilage and as colorimetric freshness indicators when loaded with anthocyanins, enabling visual detection of pH and amine increases typical of meat and fish deterioration; (ii) in foods, they serve as protective carriers that stabilize and deliver anthocyanin colorants, improving color retention and controlled release under processing and storage conditions, thereby facilitating the replacement of synthetic dyes (JIANG et al., 2024). Evidence shows cellulose and nanocellulose aerogels function as high-capacity hygroscopic desiccants in packaging (MIRMOEINI et al., 2023), while anthocyanin-loaded aerogel labels and aerogel-based sensors reliably report freshness of fish and chicken via TVB-N/pH-responsive color shifts, supporting real-time quality monitoring (ZHANG et al 2024). Additionally, numerous studies confirm anthocyanins' strong pH sensitivity for freshness indication in meat and seafood films and their effective integration into biopolymer/aerogel matrices (LI et al., 2023; ZHAO et al., 2022). As food ingredients, anthocyanin-enriched systems structured with aerogels have demonstrated improved stability and functionality, supporting their use as clean-label natural colorants in confectionery and other matrices (BENUCCI, 2022).

Purple sweet potato (PSP) is a rich source of anthocyanins and natural pigments

responsible for its vital color and numerous health benefits, including antioxidant and anti-inflammatory effects (CEVALLOS-CASALS et al., 2003; NURDJANAH et al., 2022). These pigments are appreciated for their color and starch content, which can contribute to addressing the synergistic potential of promising colorant ingredients (CHEN et al., 2019; FROND et al., 2019). Encapsulating anthocyanins into an aerogel matrix can address the stability issues by reducing molecular mobility and protecting them from adverse conditions (BENUCCI et al., 2022; COSTA et al., 2019).

Aerogels are highly porous, lightweight materials known for their low density, large surface area, and high porosity. They are produced using supercritical carbon dioxide (SC-$CO_2$) drying, which removes solvents from gels while preserving their structure (KAUR, CHEN, et al., 2024). This method avoids the issues of surface tension and capillary forces that can occur during air or freeze-drying, which often lead to shrinkage and a decrease in surface area (SADAF et al., 2024). SC-$CO_2$ drying maintains the nanoporous structure of aerogels, making them suitable for various applications. This environmentally friendly technique also operates under mild conditions, protecting sensitive components (HATAMI et al., 2024). It also encourages using renewable, low-cost biopolymers, contributing to sustainability in industries like food and pharmaceuticals (HASSOUN et al., 2022).

The aerogel's porous structure can enhance anthocyanins' stability, ensuring consistent performance and prolonged shelf life in food systems. The integration of PSPP into corn starch (CS) aerogels offers additional advantages beyond color stability. The aerogel matrix's high surface area and uniform dispersion ensure even color distribution in food products, mimicking the uniformity of synthetic dyes (AHMADZADEH et al., 2022). Moreover, the retention of antioxidant properties in anthocyanins contributes to the functional value of the final product, aligning with consumer demands for natural, health-promoting additives (CEVALLOS-CASALS et al., 2003). To the best of our knowledge, no published studies have specifically investigated the development of aerogels using PSPP as the primary raw material while preserving its original composition.

CS, another natural polymer, is often combined with other starches to enhance aerogels' mechanical properties and biodegradability (MONTES et al., 2022; ZHAO et al., 2022). Its film-forming and stabilizing properties contribute to the structural integrity of the aerogel, ensuring compatibility with various food applications (COSTA et al., 2019). Previous studies have produced CS aerogels with outstanding properties (AHMADZADEH, & UBEYITOGULLARI, 2023; UBEYITOGULLARI et al., 2019). The synergistic combination of starch from CS with PSPP to make aerogels can provide a

novel approach to creating sustainable, multifunctional food colorants.

The objective of this study aimed to develop a starch-based aerogel using PSPP and CS mixtures via an SC-CO2 drying system for potential food applications. Specifically, (i) to study different concentrations of PSPP and CS to create aerogels, (ii) evaluate the physical properties (surface area, porosity, morphology, and water solubility) of the developed aerogels, and (iii) assess the antioxidant activities (ABTS, DPPH, FRAP, ORAC) of the aerogels after anthocyanin loading. This research reports the development of anthocyanins-loaded aerogels from PSP that can be potentially used as natural, sustainable, and bioactive colorants, contributing to developing functional, eco-friendly materials for diverse applications in the food industry and beyond.

## 7.2. Materials and methods

### 7.2.1. Materials

Purple sweet potatoes (PSP) were purchased from a local grocery store (AR, USA), and the corn starch with 55% amylose content was kindly provided by Ingredion Incorporated (IL, USA). Ethanol, methanol, potassium persulfate, acetic acid, sodium acetate trihydrate, and cyanidin-3-glucoside were purchased from Fisher Scientific (PA, USA). Formic acid, gallic acid, and ferric chloride were purchased from MP Biomedicals (OH, USA). DPPH (2,2-Diphenyl-1-picryl-hydrazyl) was purchased from TCI (OH, USA), and Trolox (6-hydroxy-2,5,7,8-tetramethylchroman-2-carboxylic acid) was purchased from Millipore Sigma (MO, USA). Liquid $CO_2$ (99.99% purity) was supplied by Airgas, Inc. (AR, USA).

### 7.2.2. Methods

#### 7.2.2.1 Sample preparation

PSP tubers (500 g) were cut into pieces 50 mm thick and subjected to freeze-drying (LABCONCO, MO, USA) at -45 °C for 48 h under a vacuum pressure of 5.6 Pa. The freeze-dried PSP had a moisture content of 11.3 ± 0.7% (w/w, wet basis). The dried samples were ground into a powder using a Blixer food processor (Robot Coupe USA, Inc.) and then passed through a sieve with a mesh size of 200.

#### 7.2.2.2 Color analysis

The color of PSP samples was determined using a colorimeter (Minolta CR-300, Konica Minolta, NJ, USA). The device was calibrated using a white calibration plate before use. The results were expressed as *L** (lightness/darkness), *a** (redness/greenness), and *b** (yellowness/blueness) values.

#### 7.2.2.3 Brix analysis

The soluble solid content was accurately measured at a constant temperature of 20 ºC using a portable digital refractometer (Instrutherm, RTDS-28, São Paulo, Brazil). The results were expressed in degrees Brix (°Brix), quantifying the soluble solids in the sample (BARROS et al., 2023).

#### 7.2.2.4 Extraction and concentration of anthocyanins

The extraction was conducted using a cosolvent-modified SC-$CO_2$ extraction method adapted from De Barros et al. (2024) and stored at -47 °C until further use.

Anthocyanin extract was freeze-dried using the same system and conditions described above. Once the freeze-drying process was completed, the anthocyanins were gathered and stored in opaque vials at -47 °C.

#### 7.2.2.5 Viscosity measurements

The viscosity analysis was performed as an initial step to understand the capacity of paste formation in hydrogels made from PSPP and CS mixtures. This process aimed to select the optimal formulation of ingredients to create a consistent and solid hydrogel with a high anthocyanin content. Thus, the measurements were determined using the method described AHMADZADEH, HETTIARACHCHY, et al. (2023). A controlled-stress rheometer (model MCR 302e, Anton Paar, Graz, Austria) was used under specific temperature and shear rate conditions. Four different formulations were prepared with varying concentrations of PSPP and CS mixtures (PSPP25-CS75, PSPP50-CS50, PSPP75-CS25, and PSPP100-CS0), as detailed in Table 1. The samples were heated to 95 °C for 30 min to induce gelatinization, allowing the starch granules to swell, hydrate, and release amylose using a Thermomix (Vorwerk, CA, USA) at a shear rate of 4260 rpm. After heating, the viscosity of the samples was measured at 95 °C without cooling for 5 min. Viscosity measurements were conducted using a Peltier plate system for precise temperature control, with a parallel-plate geometry (40 mm diameter) and a 1 mm gap between the plates. The shear rate ranged from 0.1 to 100 $s^{-1}$.

#### 7.2.2.6. Aerogel preparation

#### 7.2.2.6.1 Hydrogel formation

The hydrogels were formed according to the method of AHMADZADEH and UBEYITOGULLARI (2023). The formulations are provided in Table 1. Briefly, a Thermomix (Vorwerk, CA, USA) was utilized to prepare the dispersions, mixing at 95 °C and a shear rate of 4260 rpm for 30 min. Once gelatinization was achieved, the resulting gel was poured into cylindrical polypropylene molds measuring 1.5 cm in diameter and 9 cm in length. These molds were sealed with parafilm to minimize water loss and then stored at 4 ℃ for 48 h to facilitate retrogradation.

**Table 1.** Aerogel samples prepared using varying concentrations (0%-100%) of purple sweet potato powder (PSPP), purple sweet potato residue (PSPR**) (25%-75%), and corn starch (CS) (0%-100%).

| Treatment Name (%, w/w in water) | Abbreviation |
|---|---|
| PSPP:CS (0:20) | PSPP0-CS100 |
| PSPP:CS (5:15) | PSPP25-CS75 |
| PSPP:CS (5:15) + anthocyanin extract* | PSPP25-CS75-ANT |
| PSPP:CS (10:10) | PSPP50-CS50 |
| PSPP:CS (10:10) + anthocyanin extract* | PSPP50-CS50-ANT |
| PSPP:CS (15:5) | PSPP75-CS25 |
| PSPP:CS (15:5) + anthocyanin extract* | PSPP75-CS25-ANT |
| PSPP:CS (20:0) | PSPP100-CS0 |
| PSPR:CS (5:0) | PSPR25-CS0 |
| PSPR:CS (10:0) | PSPR50-CS0 |
| PSPR:CS (10:0) + anthocyanin extract* | PSPR50-CS0-ANT |
| PSPR:CS (15:0) | PSPR75-CS0 |

*Extract from purple sweet potato after concentration (2209.65 ± 9.12 mg/100 g of cyanidin-3-glucoside) were loaded at 8.5 mL per alcogel unit (*v/unit*) during the solvent exchange step. **PSPR was obtained after anthocyanins extraction.

#### 7.2.2.6.2 Alcogel formation

After retrogradation, the hydrogels were removed from the molds and cut into monoliths (2 cm in length). A systematic solvent exchange process created alcogels by gradually substituting water with ethanol. The hydrogel monoliths were immersed in 30%, 50%, 70%, and 100% (*v/v*) ethanol for one hour in each concentration. Finally, the monoliths were soaked in 100% ethanol for 24 h to ensure complete solvent exchange. This gradual process prevented rapid dehydration, which could cause shrinkage or damage the gel structure. After solvent exchange, the alcogels were prepared for the subsequent drying process as described KAUR, CHEN, et al. (2024)

#### 7.2.2.6.3 SC-$CO_2$ drying

The formed alcogels were dried using a supercritical carbon dioxide system (SFT-120, Supercritical Fluid Technologies, Inc., DE, USA), as shown in Fig. 13, following the method of KAUR, CHEN, et al. (2024). The alcogel samples were placed in the stainless

steel vessel and covered with glass wool from the top and bottom of the vessel (Fig. 13). The vessel temperature was maintained at 40 °C while the pressure was set at 10 MPa. The CO2 flow rate was 0.5 L/min (measured under ambient conditions of 23 °C and 0.1 MPa), and the drying process continued for 4 h. The dried samples (Table 1) were stored in airtight containers, shielded from light using aluminum foil, and placed in a desiccator to avoid moisture absorption.

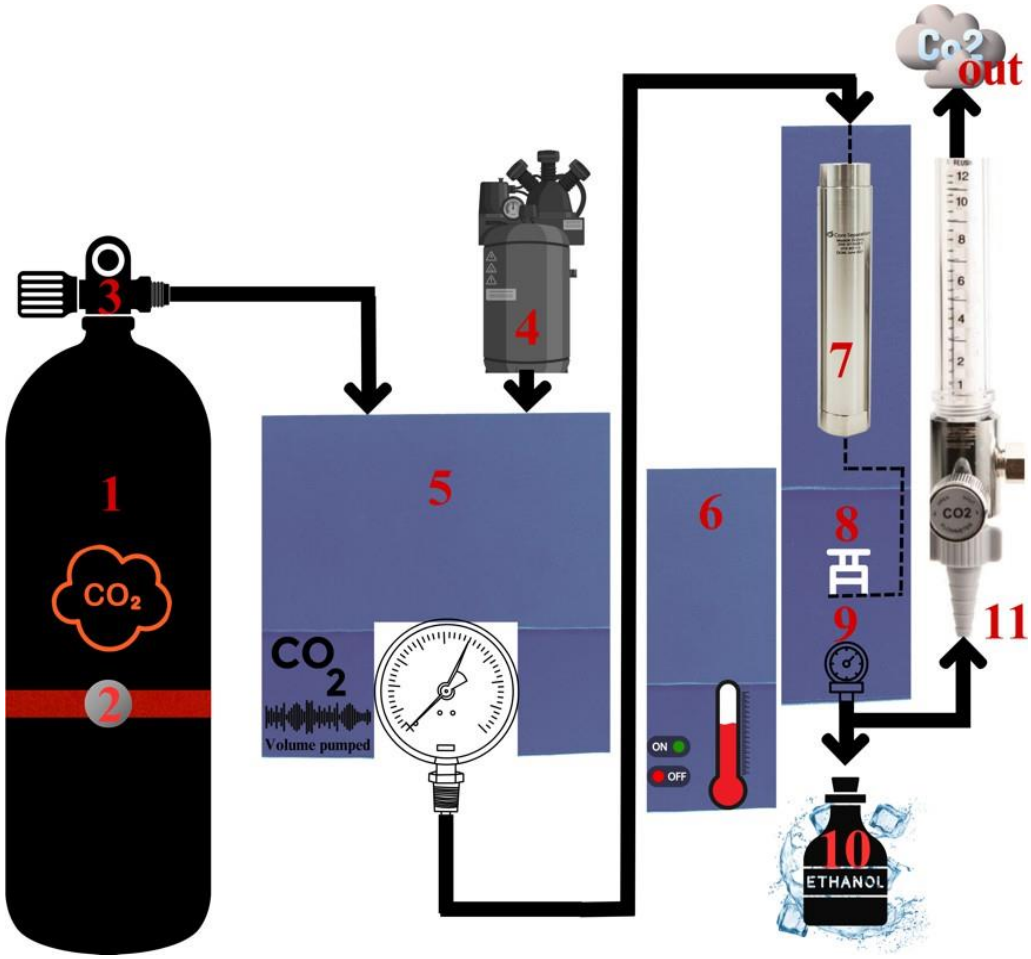


**Figure 13.** Schematic diagram of SC-CO2 drying system. (1) CO2 cylinder; (2) heating jacket; (3) needle valve; (4) compressor; (5) high-pressure pump; (6) temperature controlling unit; (7) high-pressure vessel; (8) needle valve; (9) micrometering valve; (10) ice bath to collect ethanol; and (11) flow meter. Source: designed by the Author, 2025

### 7.2.2.7. Anthocyanin impregnation into the aerogel

The procedure for anthocyanin impregnation into the alcogels was adapted from the method outlined by MIRMOEINI et al. (2023), with slight modifications to optimize the process for effective loading and uniform distribution of anthocyanins within the alcogel

matrix. In brief, a concentrated anthocyanin solution was prepared by dissolving the anthocyanin extract in 95% ethanol. Only the treatments identified with “ANT” (Table 1) were subjected to impregnation: the respective alcogels were submerged in the anthocyanin-rich solution and soaked for 48 h at room temperature (23 °C), allowing thorough diffusion of anthocyanins into their porous structure.

#### 7.2.2.8. *Aerogel characterization*

##### 7.2.2.8.1 Morphology

The morphology of the aerogels was examined using a scanning electron microscope (SEM, FEI NovaNanoLab200 Dual-Beam system, FEI company, OR, USA). Samples were prepared by slicing cross-sections and applying a thin gold coating (EMITECH SC7620 Sputter Coater, MA, USA) to improve conductivity. SEM operates at 15 kV and 15 mA, at 5mm working distance under vacuum (BARROS et al., 2023; DE BARROS et al., 2024).

##### 7.2.2.8.2 Surface area, pore size, and pore volume

Nitrogen adsorption-desorption at low-temperature analysis was employed to assess the surface area and pore characteristics of the materials. The Brunauer–Emmett–Teller (BET) surface area and Barrett–Joyner–Halenda (BJH) pore size and pore volume were determined. Prior to the analysis, samples were degassed in a vacuum at 115 °C for 4 h. Nitrogen sorption tests were performed at -196 °C. The surface area was derived from multipoint BET adsorption characteristics at a relative pressure (p/p0) between 0.05 and 0.3. The BJH pore volume and pore size were determined at a relative pressure (p/p0) exceeding 0.35 (UBEYITOGULLARI et al., 2016).

##### 7.2.2.8.3 Water Solubility

The water solubility of aerogels was measured by dissolving 1.0±0.02 g of the sample in 100 mL of distilled water. The solution was heated to 60 °C and held at that temperature for 10 min. Subsequently, the mixture was centrifuged at 670 g for 20 min. The resulting supernatant evaporated at 103 °C until a constant weight was reached. The solubility was determined as the percentage by weight of the solids dissolved in the supernatant compared to the weight of the initial sample (UBEYITOGULLARI et al., 2016).

#### 7.2.2.9 Determination of total phenolic content

The phenolic compounds were extracted from 0.100 g of aerogels in 10 mL of

60% ethanol for 24 h, and the suspensions were centrifuged at 3100g and 0 °C for 20 min. The extracts were collected in 40 mL brown glass vials, flushed with nitrogen, and stored at -20 °C until further analyses (AHMADZADEH, HETTIARACHCHY, et al., 2023). Total phenolic content (TPC) was quantified using the Folin-Ciocalteu method, as detailed by DE BARROS et al. (2024). Briefly, 100 µL of the extract was mixed with 500 µL of 0.2 N Folin-Ciocalteu's phenol reagent, which initiated a reaction for 5 min at room temperature (23 °C). Following this, 400 µL of 0.7 M sodium carbonate solution was added, and the mixture was incubated for 2 h at the same temperature. TPC was measured using a Milton Roy Spectronic 1201 UV/Vis spectrophotometer (PA, USA), referencing a gallic acid standard curve (0–200 ppm) at 760 nm with an $R^2$ value of 0.99. All analyses were performed in triplicate, and the TPC results were expressed as milligrams of gallic acid equivalent (GAE) per 100 grams.

#### 7.2.2.10 Quantification and identification ofanthocyanins

The total monomeric anthocyanins were determined according to CAROLINE PAZ GONÇALVES et al. (2024), with slight modifications. The phenolic extracts were analyzed using a spectrophotometer at 535 nm for anthocyanins. The standard curve (R2 = 0.99) was prepared using cyanidin-3-glucoside (0 to 1000 ppm) for total anthocyanins, and the results were expressed in mg of cyanidin-3-glucoside (C3G) per 100g. Additionally, the identification of anthocyanins was carried out with HPLC/UV-Vis (SPD-20AV UV/VIS detector, Shimadzu Corp., Japan) and HPLC-ESI-MS using an HP 1000 series HPLC and a Bruker Esquire 2000 quadrupole ion trap mass spectrometer equipped with a binary pump, vacuum degasser, auto-sampler, and thermostatic column compartment. The analyses were executed according to our previous study (DE BARROS et al., 2024). A 250 × 4.6 mm Symmetry C18 column (Waters Corp., MA, USA) was employed for the chromatographic separation. The HPLC analysis was performed using a binary mobile phase composed of solvent A (5% formic acid in water) and solvent B (methanol). The separation was achieved under a linear gradient elution from 2% to 60% B over 60 min, with a constant flow rate of 1.0 mL/min. Anthocyanin peaks were optimized by UV-Vis at 510 nm and identified with mass spectrometry (MS). The following conditions of capillary voltage at -4.1 kV, nebulizer gas pressure at 32 psi, and dry gas flow at 12 L/min were used to condition the system. The tandem mass spectrometry (MS/MS) system was carried out in positive ion mode, and multiple reaction monitoring (MRM) mode was used for acquisition.

#### 7.2.2.11 Determination of antioxidant activity

##### 7.2.2.11.1 DPPH radical scavenging activity

The DPPH radical scavenging activity was conducted according to (KAUR, & UBEYITOGULLARI, 2024). Briefly, 150 µL of extracts were mixed with 200 µL of 0.15 mM DPPH solution in ethanol and kept at a constant temperature of 25 °C for 30 min. After this incubation period, the absorbance was recorded at 517 nm. To establish a calibration curve ($R^2$=0.99), various concentrations of Trolox (0 to 150 ppm) were used. The findings were expressed as milligrams of Trolox equivalents (TEV) per gram.

##### 7.2.2.11.2 ABTS radical scavenging activity assay

The ABTS assay was conducted following the procedure by DE BARROS et al. (2024). To prepare the ABTS radical cation (ABTS+) solution, a 7 mM ABTS+ stock solution was mixed with 2.45 mM potassium persulfate in a 1:2 volume ratio. This reaction was allowed to take place for 8 h before being used. The solution was then diluted with ethanol to achieve an initial absorbance of 0.700±0.02 at 734 nm. Next, 2 mL of the ABTS+ solution was combined with 100 mL of the extracts and incubated in the dark at room temperature (23 °C) for 10 min. The absorbance was then measured at 734 nm, and the results were expressed as milligrams of Trolox equivalent antioxidant capacity (TEAC) per gram.

##### 7.2.2.11.3 Ferric reducing antioxidant power (FRAP) assay

The FRAP assay of extracts was carried out accordingly AHMADZADEH and UBEYITOGULLARI (2023). The FRAP solution was prepared by combining acetate buffer, TPTZ (2,4,6-Tris(2-pyridyl)-s-triazine) solution, and FeCl3 solution in a ratio of 10:1:1 (v/v/v). To create the acetate buffer, sodium acetate trihydrate was mixed with acetic acid in deionized water until the pH reached 3.6. The TPTZ solution was prepared by dissolving 10 mM TPTZ in a 40 mM hydrochloric acid solution and 20 mM FeCl3 solution was prepared (TUNNISA et al., 2022). The FRAP solution was first placed in a water bath and incubated for 30 min at 37 °C while stirring at 100 rpm. Next, 150 µL of the extract was added to 2,850 µL of the FRAP solution and mixed thoroughly using a vortex. The combined solution was then kept away from the light at room temperature (23 °C) for another 30 min. Finally, the absorbance was measured at a wavelength of 593 nm. Gallic acid solutions ranging from 0 to 50 ppm ($R^2$ = 0.99) created a standard curve, and the results were expressed as milligrams of gallic acid equivalent (GAE) per gram.

#### 7.2.2.11.4 Oxygen radical absorbance capacity (ORAC) assay

The antioxidant capacity was determined using the ORAC assay according to PICOS-SALAS et al. (2024) with slight modifications. The aerogels were dissolved in a 75 mM phosphate buffer and adjusted to a pH of 7.0 to maintain stability. A fluorescein solution (0.5 nM) was prepared by diluting a 0.1 µM stock solution in the same phosphate buffer. Additionally, 14.63 mM AAPH (2,2'-azobis(2-amidinopropane) dihydrochloride) solution was formulated in the same buffer. In a black 96-well microplate, 50 µL of extract or a Trolox standard was combined with 50 µL of the fluorescein solution. This mixture was incubated at 37°C for 15 min. After incubation, 25 µL of the AAPH solution was added to initiate the reaction, generating free radicals that interact with the antioxidants in the samples. Fluorescence was continuously monitored for 60 min using a Biotek Synergy HT microplate reader set to an excitation wavelength of 485 nm and an emission wavelength of 520 nm. The antioxidant capacity of the aerogels was quantified and expressed as millimoles of Trolox equivalents (TE) per gram of sample, achieved by comparing the area under the curve (AUC) of each sample to that of a previously established Trolox standard curve according to the equation (1):

$$ORAC_{auc} = \frac{AUC_{sample} - AUC_o}{AUC_{trolox} - AUC_o} xf\ x + [Trolox] \qquad (1)$$

Where:

The AUC (Area Under the Curve) represents the integrated fluorescence signal over time in the presence of the tested aerogel extract, reflecting its antioxidant activity. The $AUC_0$ (Blank) corresponds to the control sample containing only fluorescein and AAPH, without any antioxidant, and serves as the baseline to correct for non-specific oxidation. The AUC_Trolox refers to the area under the curve for Trolox, a well-established antioxidant standard used to benchmark the antioxidant capacity of the sample. The dilution factor ($f$) accounts for the ratio between the total reaction volume and the volume of extract added, ensuring the antioxidant capacity is normalized for concentration. The [Trolox] term represents the molar concentration of the Trolox standard, allowing the results to be expressed in Trolox Equivalents (TE).

## 7.3. Results and discussion

### 7.3.1 Physicochemical properties of PSP

The PSP's color parameters (L* = 39.65, a* = 20.47, b* = 1.23) indicated its distinctively dark purple hue with red and yellow, reflects the high anthocyanin content in the PSP samples. Additionally, the pH of the PSP (pH 5.7) is another characteristic that influences the aerogels' structural formation and stability. A slightly acidic environment is beneficial for preserving anthocyanins, which are prone to degradation under neutral or alkaline conditions (CHEN et al., 2019). The Brix value of 18.26° Brix and the lipid content of 1.46% offer valuable insights into the sugar and fat levels in the PSP. These factors can significantly influence the textural properties of the aerogels, highlighting the importance of separating the polar and non-polar components during the extraction processes and the formation of aerogels (TUHANIOGLU et al., 2022). In this study, we focused on a high-amylose corn starch to use as a copolymer because of its capability to create dense, cohesive gels due to an amylose content, which is essential for producing aerogels that boast enhanced mechanical stability and refined pore structures (LV et al., 2021).

### 7.3.2 Viscosity

Fig. 14 presents the viscosity behavior of four different formulations with varying CS and PSPP ratios at shear rates between 0.1 to 100 $s^{-1}$. The water content in all PSPP/CS formulations was maintained at 20% (w/w) to ensure consistent hydration conditions. In the PSPP75-CS25 formulations, viscosity is relatively lower, indicating that the mixture struggles to form a stable gel network. The low starch concentration limits its ability to act as the primary thickening agent, weakening gelation. Although the PSPP phenolic contents were higher, the high anthocyanin content hindered its effectiveness in improving gel formation. Anthocyanins, being hydrophilic, bind to water molecules, reducing the water available for starch granule hydration (LI et al., 2025). This leads to incomplete starch swelling and weak gel formation. Polyphenols such as anthocyanins can also disrupt starch crystallinity, further weakening the gel network and reducing overall viscosity (JÖBSTL et al., 2004; WANG et al., 2020; YONG et al., 2018).

In contrast, the PSPP50-CS50 formulations showed improved gel properties. The increased CS concentration provided better gelatinization, allowing more starch to absorb water and form a robust gel network. This balance between starch and anthocyanin levels results in a stable gel without excessive interference

(AHMADZADEH, HETTIARACHCHY, et al., 2023). This formulation demonstrates that moderate anthocyanin levels promote gel stability by improving water retention and gel flexibility while maintaining a cohesive structure (NURDJANAH et al., 2022).

The PSPP75-CS25 and PSPP100-CS0 formulations further strengthen the gel, as the higher starch content enhances amylose release and granule hydration, resulting in a firmer and more stable gel structure (BOONKOR et al., 2022). The lower anthocyanin content also minimizes interference with starch network formation. The PSPP100-CS0 formulation exhibits the highest viscosity and has the most significant gel strength compared to all other formulations. As a result, this formulation exhibits the most substantial gelation properties with a dense and stable structure. As discussed above, anthocyanins can form complexes with amylose, reducing the amount of free amylose available for retrogradation, and impacting gel strength. This finding aligns with other studies on purple sweet potato and anthocyanin-rich starches, which report similar interactions that limit retrogradation and hinder the development of a crystalline gel structure (WANG et al., 2024). The results were consistent with studies SOHANY et al. (2021), particularly where high anthocyanin levels reduce gel stability and firmness.

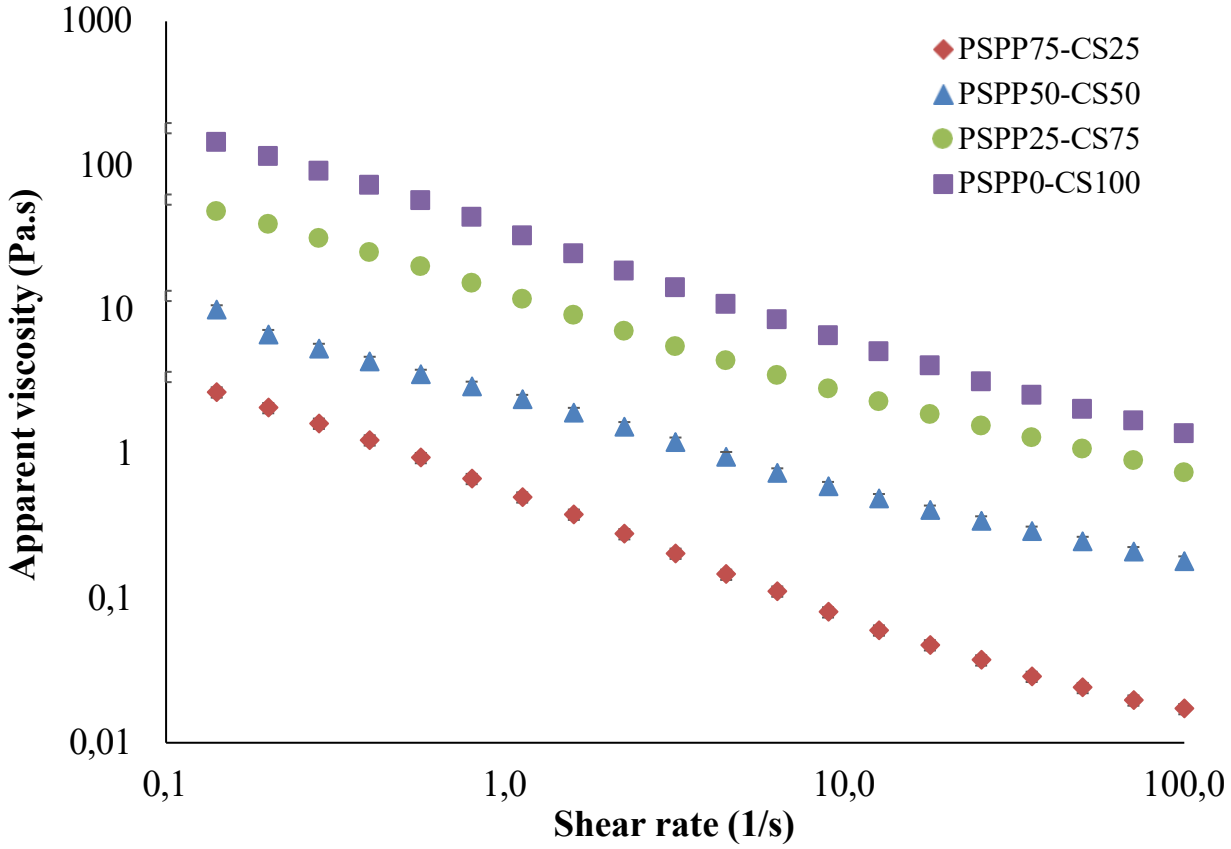


**Figure 14.** Relationship between apparent viscosity (Pa.s) and shear rate (1/s) for four different formulations containing varying concentrations of PSPP (25%; 50%; 75%; and 100%).

### 7.3.3 Hydrogel formation

Hydrogels generated using different concentrations of PSPP-CS (purple sweet potatoes and corn starch mixture) are depicted in Fig. 15. The PSPP0-CS100 sample, composed entirely of corn starch, showed a white, firm, uniform hydrogel. This demonstrates the typical behavior of pure corn starch, which is known to form strong gels due to its high amylose content, leading to an influential network of starch molecules after gelatinization (CEVALLOS-CASALS et al., 2003).

Additionally, a PSPP25-CS75 sample introduced a slight pigmentation from PSPP; the gel remained relatively stable, consistency appeared slightly softer than that of the PSPP0-CS100 sample. The PSPP50-CS50 anthocyanin retention and structural stability (Fig. 15). Hydrogels at PSPP50-CS50 and PSPP75-CS25 demonstrated a notable shift in behavior. Both samples exhibited darker colors due to the higher anthocyanin content, but their structural integrity was significantly compromised. The high concentration of PSPP had the darkest color and the weakest gel. This condition

altered the starch's water absorption capacity and reduced its swelling ability, making it difficult for the residue to gelatinize and form a stable hydrogel fully. This sample's poor structural formation was consistent with retrograded starch's behavior, which often failed to develop a strong gel network due to its limited hydration potential (MOJO-QUISANI et al., 2024). In contrast, the behavior observed with PSPP75-CS25 is markedly different, as the sample exhibited rapid paste formation. This phenomenon led to an excessive increase in the viscosity of the hydrogels, ultimately resulted in a failure to establish a cohesive network. Research on other high-starch hydrogels, such as those made from cassava or potato starch, has shown similar behavior where exceeding a critical starch concentration inhibit proper gelation due to excessive viscosity buildup and poor water distribution (AHMADZADEH, & UBEYITOGULLARI, 2023; HAN et al., 2019; LV et al., 2021).

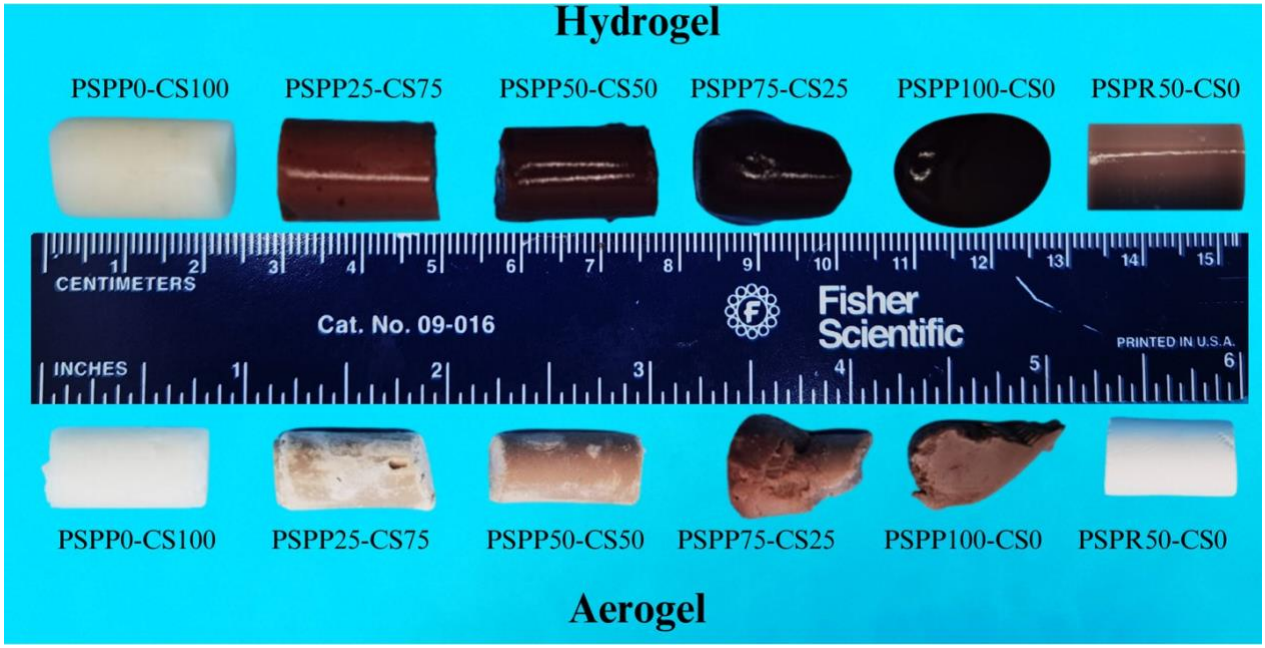


**Figure 15.** Hydrogels and aerogels formed with the mixture of PSPP and CS mixture (PSPP0-CS100; PSPP25-CS75; PSPP50-CS50; PSPP75-CS25; PSPP100-CS0; and PSPR50-CS0. PSPP: purple sweet potatoes powder. CS: corn starch. Fonte: elaborado pelo autor, 2025

In addition to the PSPP, the (PSPR) after anthocyanins extraction was also utilized for generating hydrogels. At a concentration of PSPR25-CS0, the hydrogel showed weak structural integrity and incomplete gelatinization (Fig. 16). In contrast, at PSPR50-CS0, the hydrogel exhibited optimal water absorption and swelling, resulting in

a stable gel network (Fig. 16). However, at PSPR75-CS0, the formation of the hydrogel faced challenges due to rapid paste formation, which led to excessive viscosity. Consequently, creating a gel network at 90% PSPR-CS0 was not feasible. Similar behavior has been observed in other

starchy residues, such as cassava and potato (HAN et al., 2019; REN et al., 2024).
The anthocyanin extraction process may have further altered the starch properties, particularly affecting its water-holding capacity and the ratio of amylose to amylopectin, which were crucial for proper gel formation (AHMADZADEH, HETTIARACHCHY, et al., 2023). These structural changes likely contributed to the challenges in forming stable hydrogels at higher concentrations (UBEYITOGULLARI et al., 2016). The evaluation showed that the ability of PSPR to form hydrogels was concentration-dependent, with PSPR50 being identified as the optimal treatment (Fig. 16).

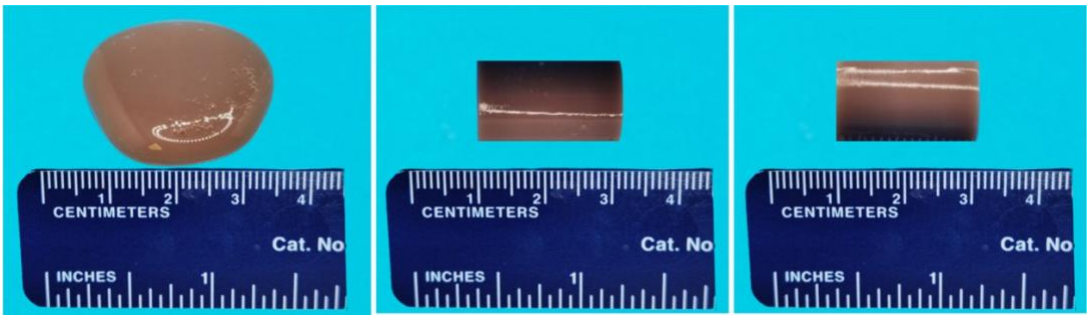


**PSPR25-CS0** **PSPR50-CS0** **PSPR75-CS0**

**Figure 16.** Impact of the gelatinization process on hydrogels prepared from PSPR at varying polymer concentrations (25%, 50%, and 75%) after anthocyanins extraction. PSPR: purple sweet potatoes residue (i.e., spent purple sweet potatoes after anthocyanins extraction). Source: Designed by the Author, 2025.

### 7.3.4. Aerogel formation

Generally, PSPR50-CS0, PSPP25-CS75, and PSPP100-CS0 (Fig. 15) showcased the critical interplay between starch concentrations and anthocyanins or other bioactive compounds (LIN et al., 2020). This condition can be verified after SC-CO2 drying in aerogels, with irregular shape formation in PSPP75-CS25 and PSPP100-CS0, which differed from other polymer concentrations (Fig. 16). The aerogels exhibited unique structural characteristics following the SC-CO2 drying process. The PSPP0-CS100 sample, composed solely of corn starch, maintained a smooth and uniform structure due to its robust gelation properties. The aerogels achieved a stable and porous form of PSPP25-CS75 and PSPP50-CS50 hydrogels, balancing structural integrity with anthocyanin retention. However, the aerogels displayed irregular shapes (e.g., PSPP75-

CS25 and PSPP100-CS0) and fragile textures at higher concentrations (e.g., PSPP25-CS75 and PSPP0-CS100).

The study also explored varying concentrations of corn starch combined with (PSPP0-CS100, PSPP25-CS75, PSPP50-CS50, PSPP75-CS25) and PSPR50-CS0, influencing color retention and structural properties of aerogels impregnating anthocyanins (Fig. 17). Before impregnation, water in the aerogel pores was replaced with ethanol to improve pore accessibility for anthocyanin loading. This step was crucial to prevent structural disruption and enhance anthocyanin distribution within the matrix. Ethanol's lower polarity facilitated better interaction with the internal pore surfaces, ensuring efficient impregnation and maintaining aerogel integrity. (AHMADZADEH, & UBEYITOGULLARI, 2023; HATAMI et al., 2024; KAUR et al., 2024; UBEYITOGULLARI et al., 2016).

The outer layers of the aerogels showcased a noticeable progression in color intensity as the concentration of PSPP increased (Fig. 17). The sample with PSPP0-CS100-ANT, which consisted entirely of corn starch, appeared white, indicating that minimal anthocyanins were retained during the impregnation process (Fig. 17) (OLADZADABBASABADI et al., 2022). When PSPP25-CS75-ANT was introduced, it added a subtle yet visually appealing hue to the gel, suggesting that this concentration effectively encapsulated the anthocyanins (MOHD NAWI et al., 2015). Furthermore, the higher concentrations PSPP, as in PSPP50-CS50-ANT and PSPP75-CS25-ANT, resulted in deeper color intensity but did not significantly enhance structural stability (Fig. 16). Interestingly, the PSPR50-CS0-ANT sample exhibited a rich color, similar to the PSPP50-CS50-ANT sample, but slightly less intense, indicating that PSPR-CS0 could be a viable alternative for pigmentation (Figs. 16 and 17). When examining the inner layers (i.e., cross-section), additional distinctions between treatments were apparent. The PSPP25-CS75 sample revealed moderate and uniform pigmentation, signifying optimal anthocyanin encapsulation and even color distribution throughout the matrix. At PSPP75-CS25-ANT, the cross-section became less uniform, suggesting that higher concentrations may disrupt the starch matrix and compromise internal cohesion (LIN et al., 2020). The PSPR50-CS0-ANT achieved a pigmentation level between the PSPP25-CS75-ANT and PSPP50-CS50-ANT, indicating effective anthocyanin integration without destabilizing the structure (Fig. 17).

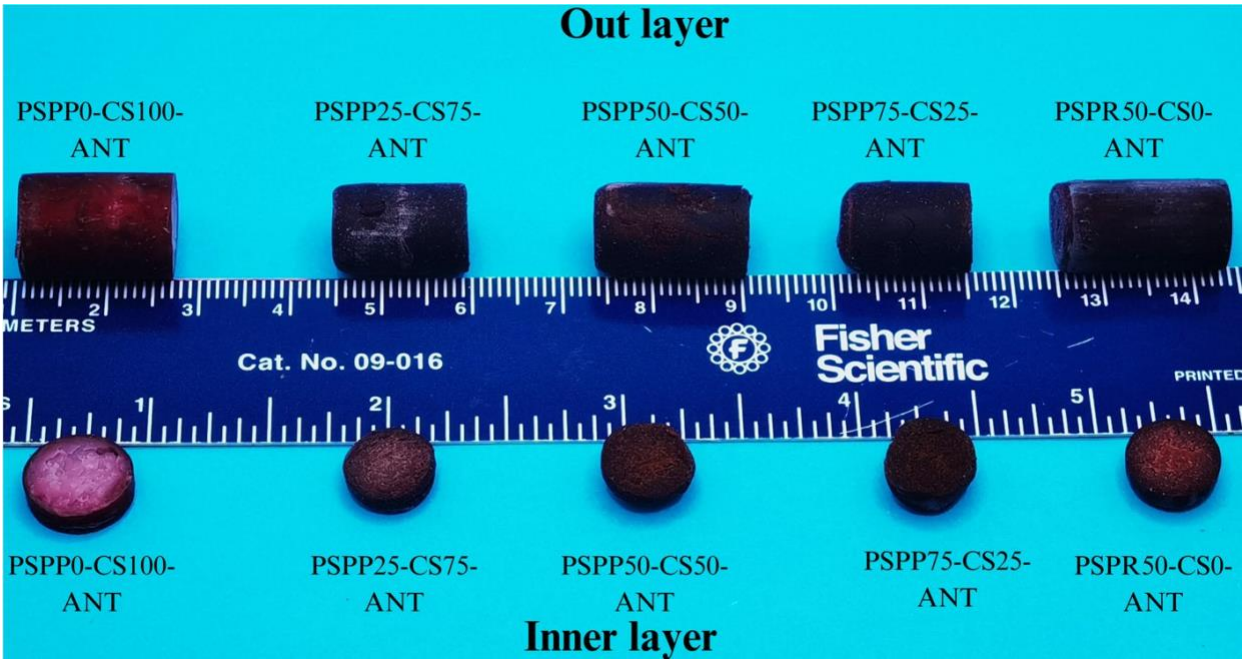


**Figure 17.** The outer and cross-section layers of aerogels infused with anthocyanins in samples from a mixture of PSPP and CS mixture at various concentrations (PSPP0-CS100-ANT; PSPP25-CS75-ANT; PSPP50-CS50-ANT; PSPP75-CS25-ANT; and PSPR50-CS0-ANT), dried using SC-CO2 at 40 ◦C and 10 MPa with a flow rate of 0.5 L/min. PSPP: purple sweet potato powder. CS: corn starch. ANT: Anthocyanins extract. PSPR: purple sweet potato residue after extraction. Source: Designed by the Author, 2025.

### 7.3.5. Aerogels Characterization

#### 7.3.5.1 Morphology

The structures of the aerogels are shown in Fig. 18. As the PSPP concentrations increase from 0% to 100% (PSPP0-CS100, PSPP25-CS75, PSPP50-CS50, PSPP75-CS25, and PSPP100-CS0), the surface drastically changed. PSPP0-CS100 had a very compact and uniform surface with few visible pores, indicating a dense structure. As the concentration of PSPP increased, larger pores and a less compact structure were observed (Fig. 18). The observed alteration was attributed to the incorporation of PSPP, which disrupted the continuity of the starch matrix, thereby resulting in the formation of voids within the aerogel structure (KASTER et al., 2024).

It is important to note that these SEM images represent unloaded (empty) aerogels. Although anthocyanin-loaded samples were not analyzed morphologically in this study, previous research suggests that the loading of bioactive compounds may alter aerogel microstructure by affecting porosity, surface collapse, and network homogeneity

(AHMADZADEH et al., 2024; HATAMI et al., 2024).

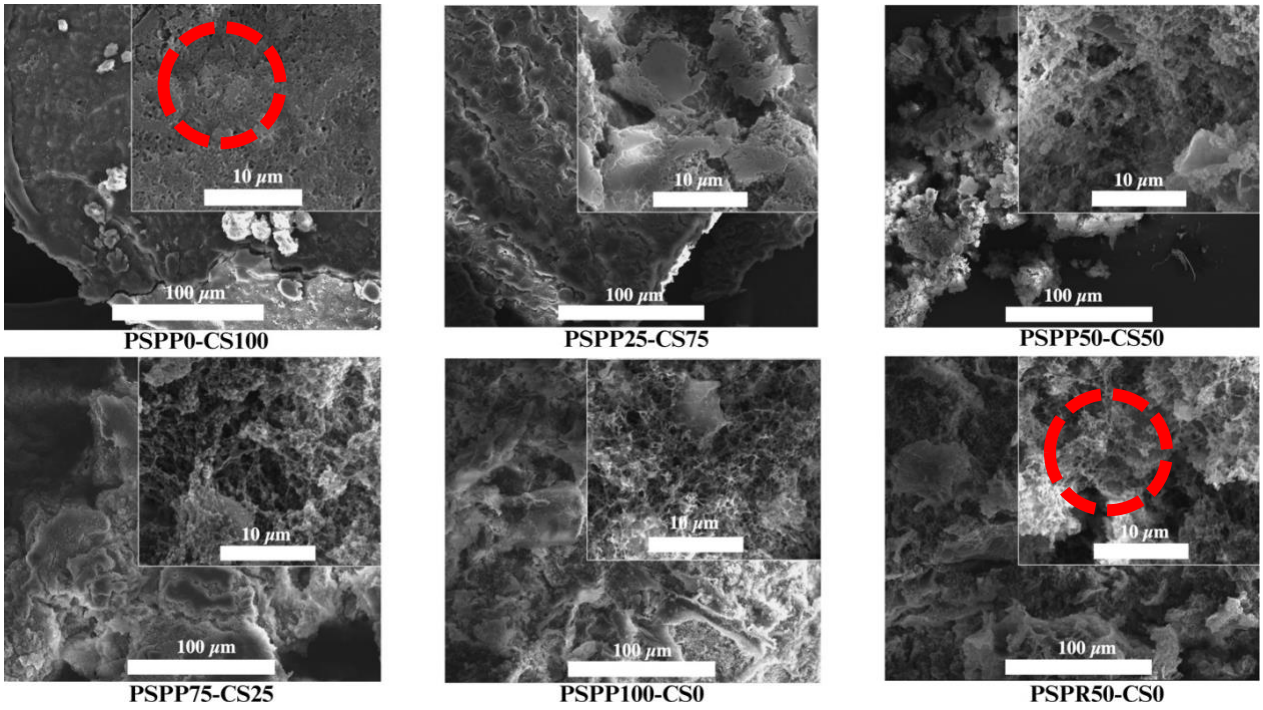


**Figure 18.** SEM micrographs of empty aerogels from PSPP, PSPR, and CS mixture (PSPP0-CS100-CS100; PSPP25-CS75; PSPP50-CS50; PSPP75-CS25; PSPP100-CS0; and PSPR50-CS0. PSPP: purple sweet potatoes powder. CS: corn starch. PSPR: purple sweet potatoes residue after extraction.

### 7.3.5.2 Surface area, pore size, and pore volume

The PSPP0-CS100 aerogel had the highest surface area (129.36 $m^2\ g^{-1}$), while the PSPP100-CS0 showed the lowest (12.68 $m^2\ g^{-1}$), indicating a denser network as PSPP concentration increases (Table 2). Pore sizes varied among samples, with PSPP50-CS0 having the largest pore size (56.81 nm) and PSPP100-CS0 the smallest (3.11 nm). Intermediate samples, like PSPP25-CS75 and PSPP50-CS50, had moderate to relatively high pore sizes (24.75 nm and 15.53 nm), while PSPP75-CS25 had a relatively large pore size (25.23 nm). These trends in pore volume align with the observed pore sizes (HORVAT et al., 2022). The PSPP25-CS75 aerogel exhibited the highest pore volume (0.96 $cm^3\ g^{-1}$), followed by the PSPR50-CS0 sample (0.58 $cm^3\ g^{-1}$) and the PSPP50-CS50 (0.85 $cm^3\ g^{-1}$). The PSPR sample's combination of moderate surface area (75.2 $m^2\ g^{-1}$) and arge pore size suggests it forms a highly open structure, likely due to its composition and distinct processing. Conversely, the PSPP100-CS0 aerogel forms a dense network that limits porosity with its smallest pore size (3.11 nm) and lowest pore volume (3.11 nm and 0.10 $cm^3\ g^{-1}$, respectively) (Table 1).

**Table 2.** Textural properties of aerogels prepared with varying proportions of purple sweet potato powder (PSPP), corn starch (CS), and purple sweet potato residue (PSPR).*

| Sample | Surface Area ($m^2/g$) | Pore Size (nm) | Pore Volume ($cm^3/g$) |
|---|---|---|---|
| PSPP0-CS100 | 129.36±1.69[a] | 7.0±0.42d | 0.32±0.001c |
| PSPP25-CS75 | 91.3±0.62b | 24.75±1.03b | 0.96±0.001a |
| PSPP50-CS50 | 80.3±0.59c | 15.53±0.75c | 0.85±0.004a |
| PSPP75-CS25 | 61.4±0.32d | 25.23±1.78b | 0.70±0.000b |
| PSPP100-CS0 | 12.68±0.49e | 3.11±0.13d | 0.10±0.003c |
| PSPR50-CS0 | 75.2±0.79c | 64.62±2.68a | 0.58±0.002b |

*Means in the same column that do not share a common letter are significantly different ($p < 0.05$) using tukey Test.

The 10% and PSPP75-CS25 aerogels were the most effective candidates for anthocyanin loading (Fig. 17). These samples provide an optimal combination of moderate pore size (15.53 nm and 25.23 nm) and significant pore volume (0.85 $cm^3\ g^{-1}$ and 0.71 $cm^3\ g^{-1}$, respectively). This balance suggests that the matrix structure at these concentrations supports effective anthocyanin encapsulation, likely due to sufficient porosity without compromising structural integrity. Furthermore, the moderate surface areas of the PSPP50-CS50 (80.3 $m^2\ g^{-1}$) and PSPP75-CS25 (61.4 $m^2\ g^{-1}$) samples enhance accessibility for bioactive compound retention, making them ideal for industrial applications (KAKOLI et al., 2023).

### 7.3.5.3. Water solubility

Fig. 19 reveals the solubility of the aerogels increasing with the addition of PSPP, with the PSPP0-CS100-ANT sample having the lowest solubility (approximately 55%) and the solubility reaching around 80% in the PSPP50-CS50-ANT, PSPP75-CS25-ANT, and PSPR50-CS0-ANT samples. The lowest water solubility observed in the PSPP0-CS100-ANT sample can be attributed to its compact and cohesive structure, as mentioned in the previous session (3.4.2), which is only composed of corn starch. At 25% concentration (PSPP25-CS75-ANT) also provides more surface area and hydrophilic sites for water interaction, contributing to higher solubility (LI et al., 2022).

Interestingly, the PSPR50-CS0-ANT concentration also showed a solubility of

around 80%, similar to the PSPP50-CS50-ANT and PSPP75-CS25-ANT samples. The PSPR may contain partially degraded starch and PSPP components, exposing additional hydrophilic sites or irregularities that facilitate water absorption (WU et al., 2024). The similar solubility to the 50%-75% PSPP samples suggests that the PSPR retains enough hydrophilic compounds and porous structure to promote high solubility, though it may have less structural regularity.

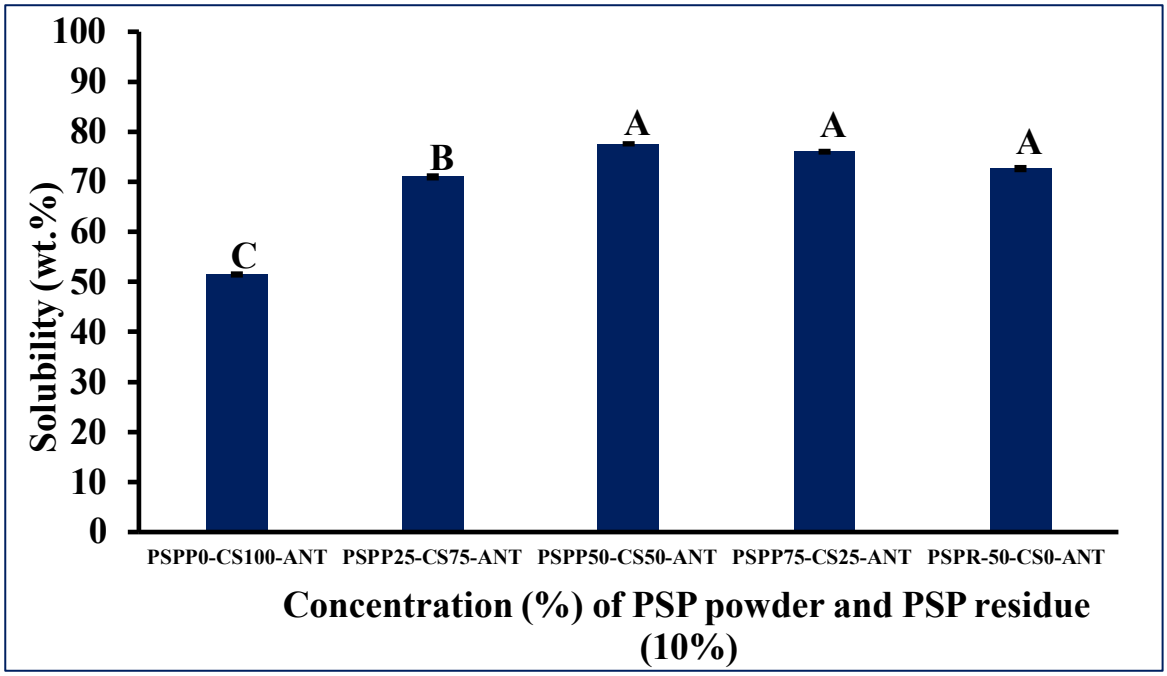


**Figure 19.** The water solubility (wt.%) of aerogels from a mixture of PSPP, PSPR, and CS mixtures at various concentrations (PSPP0-CS100-CS100; PSPP25-CS75; PSPP50-CS50; PSPP75-CS25; PSPP100-CS0; and PSPR50-CS0).. PSPP: purple sweet potato powder. CS: corn starch. ANT: Anthocyanins extract. PSPR: purple sweet potato residue after extraction.

### 7.3.6. Total phenolic content and total anthocyanins before loading

The total phenolic content (TPC) in aerogels showed a significant positive correlation between the amount of PSP added. The levels of TPC were measured (Fig. 20a). The control aerogel (PSPP0-CS100) exhibited the lowest TPC value of 2.06 ± 0.90 mg of GAE/100g, establishing a baseline for subsequent comparisons (Fig. 20a). When PSPP was systematically increased, there was a notable elevation in TPC levels across the samples. For instance, aerogels incorporating PSPP25-CS75 attained a TPC of 194.84 ± 2.00 mg of GAE/100g. This trend continued with samples containing 10% PSPP, demonstrating a TPC of 531.55 ± 14.16 mg of GAE/100g. With an increase to

PSPP75-CS25, the TPC reached 577.38 ± 17.75 mg of GAE/100g.

Eventually, aerogels enriched with PSPP100-CS0 exhibited the highest recorded TPC value of 1316.18 ± 24.94 mg of GAE/100g. The consistent rise in TPC underscores the efficacy of PSPP as a rich source of phenolic compounds, contributing significantly to the functional properties of the aerogels (CUNHA JÚNIOR et al., 2024; LIAO et al., 2021; XU et al., 2018). The aerogel made with PSPR50-CS0 showed a notably lower TPC of just 69.97 ± 2.50 mg of GAE/100g. This indicates that the phenolic compounds in the PSPR were reduced during the anthocyanin extraction process. Other than that, results from PSPP25-CS75 to PSPP100-CS0 found in our work belong to the interval described CEVALLOS-CASALS et al. (2003) when studying the stoichiometric and kinetic phenolic antioxidants from andean purple corn and red-fleshed sweet potato; the lowest value in wet basis was 1756± 64 mg of GAE/100g, and 945 ± 82 mg of GAE/100g, for purple corn and sweet potatoes, respectively. In contrast, the TPC in the pure corn starch and PSPR50-CS0 aerogels were lower than CEVALLOS-CASALS et al. (2003).

However, it is high compared to the minimum value found by INSANU et al. (2022) when evaluating the potential antioxidative activity of waste products of purple sweet potato (2.059g of GAE/100g). Additionally, aerogels made with 0% purple sweet potatoes are higher than the study developed, ARAUJO et al. (2023) which found 0.462 mg of GAE/100g of TPC after impregnation polyphenols from passion fruit residue in corn starch aerogels. In contrast, aerogels made with PSPR, a byproduct of anthocyanin extraction, show much lower TPC (69.97±2.50 mg of GAE/100g) due to phenolic depletion during extraction. This difference in TPC aligns with findings from INSANU et al. (2022) PSPP waste products, which also had lower antioxidant potential compared to the whole PSPP.

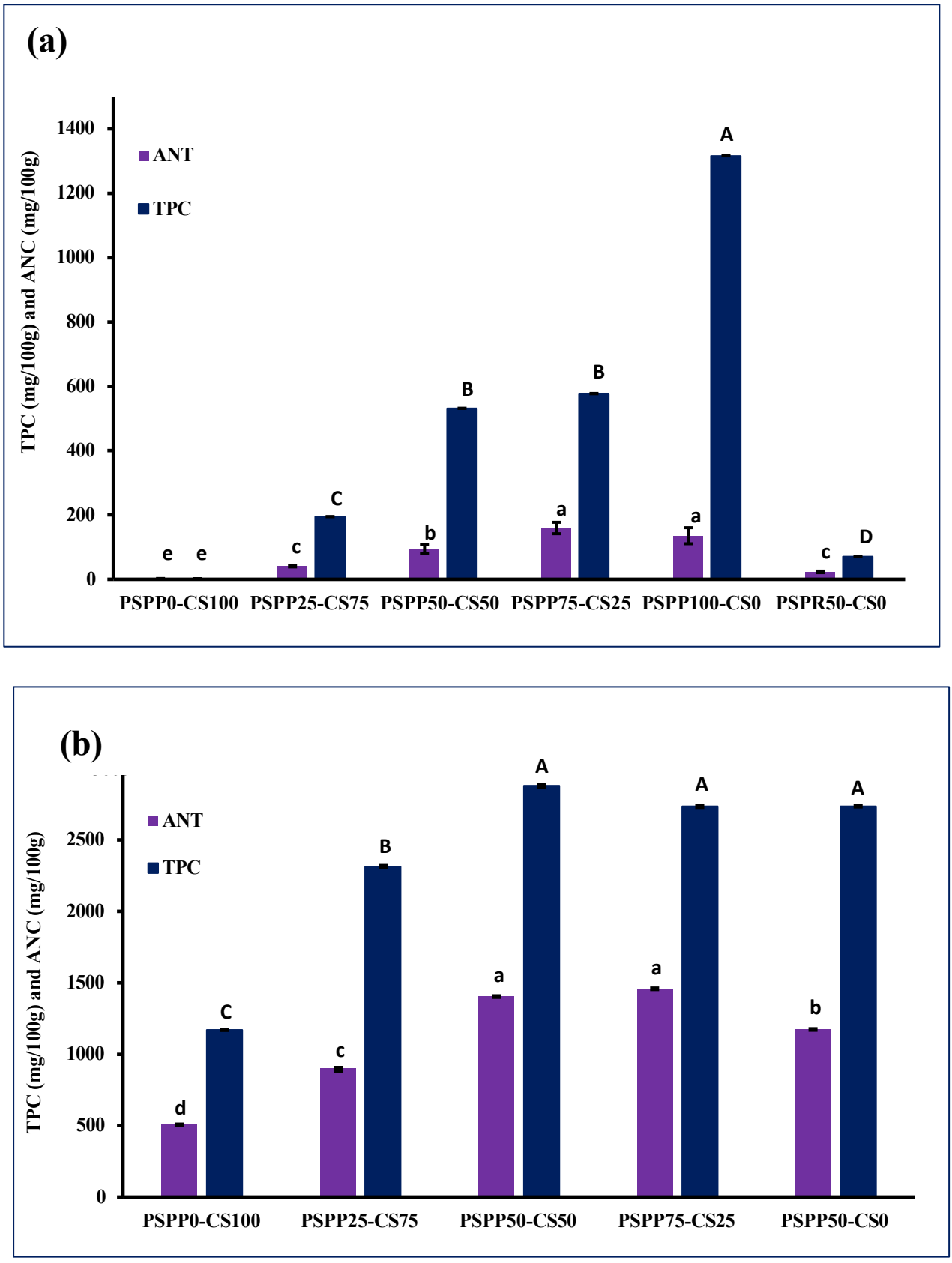


**Figure 20.**Total phenolic compounds (TPC) and anthocyanins (ANT) in aerogels made from a mixture of PSPP and corn starch mixture at various concentrations (PSPP0-CS100, PSPP25-CS75, PSPP50-CS50, PSPP75-CS25, PSPP100-CS0, and PSPR50-CS0 (a) before and (b) after loading.

### 7.3.7. Total phenolic content and total anthocyanins after loading

Fig. 20b shows the TPC in aerogels after loading, where a substantial increase in TPC was observed in formulations containing higher levels of PSPP. An increase exceeding 100% in TPC values was recorded when anthocyanins were loaded into the aerogel matrix. Notably, the aerogel sample PSPP50-CS50-ANT exhibited the highest TPC (2880.26±5.90 mg of GAE/100g) (Figure 20b). In contrast, the sample containing PSPP0-CS100 showed the lowest TPC, with a value of 1168.68 ± 4.93 mg of GAE/100g. The result emphasized the crucial role of PSPP in contributing phenolic compounds to the aerogel matrix. By comparison, the PSPP50-CS50-ANT yielded a TPC of 2313.85 ± 12.00 mg of GAE/100g.

For samples PSPP0-CS100-ANT and PSPP25-CS75-ANT, anthocyanin encapsulation significantly increased TPC, indicating their key role when natural phenolics were low ($p>0.05$). However, at higher PSP concentrations (PSPP50-CS50-ANT and PSPP75-CS25-ANT), anthocyanin loading did not significantly affect TPC ($p>0.05$), suggesting a saturation point in the aerogel matrix limited further phenolic binding or stabilization (ALZATE-ARBELAEZ et al., 2022; LI et al., 2025; LIN et al., 2020). The results indicated that PSPP significantly enhanced the TPC of aerogels, particularly at the PSPP50-CS50-ANT formulation. The observed saturation effect at higher PSP levels suggests that exceeding certain concentrations may not yield additional TPC benefits (ARAUJO et al., 2023).

Total ANT has been studied after loading (Fig. 20b). The control sample (PSPP0-CS100) exhibited a minimal anthocyanin content, recording a baseline value of 506.43 ± 2.70 mg of GAE/100g after loading. When the PSPP concentration was increased to 25%, the anthocyanin content rose to 897.63 ± 8.22 mg of GAE/100g, indicating a notable enhancement in anthocyanins even with a relatively low concentration of PSPP. Raising the PSPP concentration to 50% resulted in an anthocyanin content of 1403.36 ± 9.70 mg/100g, reflecting another significant increase. Nevertheless, there was no statistical difference ($p>0.05$) in anthocyanin levels between the PSPP50-CS50-ANT and PSPP75-CS25-ANT, as the PSPP75-CS25-ANT measured 1457.83 ± 8.05 mg of GAE/100g, implying that the anthocyanin content reached its peak around the 50% concentration level.

The 50% PSPR maintained a detectable ANT of 1173.02 ± 4.83 mg C-3-G/100g, which, while lower than that of PSPP50-CS50-ANT and PSPP75-CS25-ANT, was still significantly higher than the control (PSPP0-CS100-ANT) ($p<0.05$). Additionally, the high anthocyanin content in the PSPR-ANT highlights an opportunity for using PSP by-products not only as functional food ingredients or natural colorants but also in advanced

applications such as active packaging. Anthocyanins, due to their pH-sensitive colorimetric properties and antioxidant activity, can be incorporated into biodegradable films to serve as freshness indicators or to extend shelf life by reducing oxidative degradation. These multifunctional applications support sustainable practices by reducing food waste and promoting the valorization of agricultural by-products (INSANU et al., 2022; LI et al., 2023; ZHAO et al., 2022). (INSANU et al., 2022). Although this study demonstrates the potential of PSP as an anthocyanin source, further research is recommended to evaluate the stability of these pigments under different processing and storage conditions, as anthocyanins are sensitive to factors such as pH, light, and extended storage times (LI et al., 2023; ZHAO et al., 2022).

### 7.3.8. Antioxidant activities before loading

The DPPH demonstrated a steady increase in antioxidant activity as PSPP concentration increased from PSPP0-CS100 to PSPP75-CS25, with values rising from 0.06 ± 0.03 mg TEV/g at PSPP0-CS100 to 3.50 ± 0.03 mg TEV/g in PSPP75-CS25 (Fig. 21a). However, in PSPP100-CS0 concentration, the DPPH activity (3.51 ± 0.02 mg/100g) was not significantly higher than the PSPP75-CS25 sample ($p > 0.05$), suggesting that the aerogel matrix reaches a maximum stabilization. This level effect indicates that beyond PSPP75-CS25, the corn starch matrix may no longer support effective integration or release of additional anthocyanins and phenolics, likely due to saturation and limited solubility in the DPPH assay environment (CHEN et al., 2024; DIEP et al., 2020; LI et al., 2019). These findings are consistent with MOHD NAWI et al. (2015), indicating that starch matrices can encapsulate anthocyanins effectively up to a specific concentration, beyond which anthocyanins may either aggregate or become trapped in the aerogel structure, reducing their accessibility to DPPH radicals (INSANU et al., 2022).

The ABTS assay decisively demonstrated its superiority in detecting a wider range of antioxidant compounds, as evidenced by the substantial increase in activity with escalating PSPP concentrations. The assay results rose dramatically from 0.06 ± 0.00 mg TEV/g at 0% PSP to 1.08 ± 0.00 mg TEV/g at PSPP100-CS0 (Fig. 21a). Notably, unlike the DPPH results, ABTS activity at 100% surpassed that of PSPP75-CS25.

The ABTS assay's continued response at 100% (PSPP100-CS0) suggests that additional phenolic compounds are accessible in the assay environment, contributing to the increased antioxidant potential at this concentration (SILVA et al., 2023). The PSPR sample, containing 50% post-extraction PSPP, showed moderate antioxidant activity, with values of 0.78 ± 0.12 mg TEV/g for DPPH and 0.15 ± 0.00 mg TEV/g for ABTS. Statistically distinct from all PSPP concentrations, the PSPR50-CS0 activity indicates

that some phenolic compounds remained active in the sample after anthocyanin extraction.

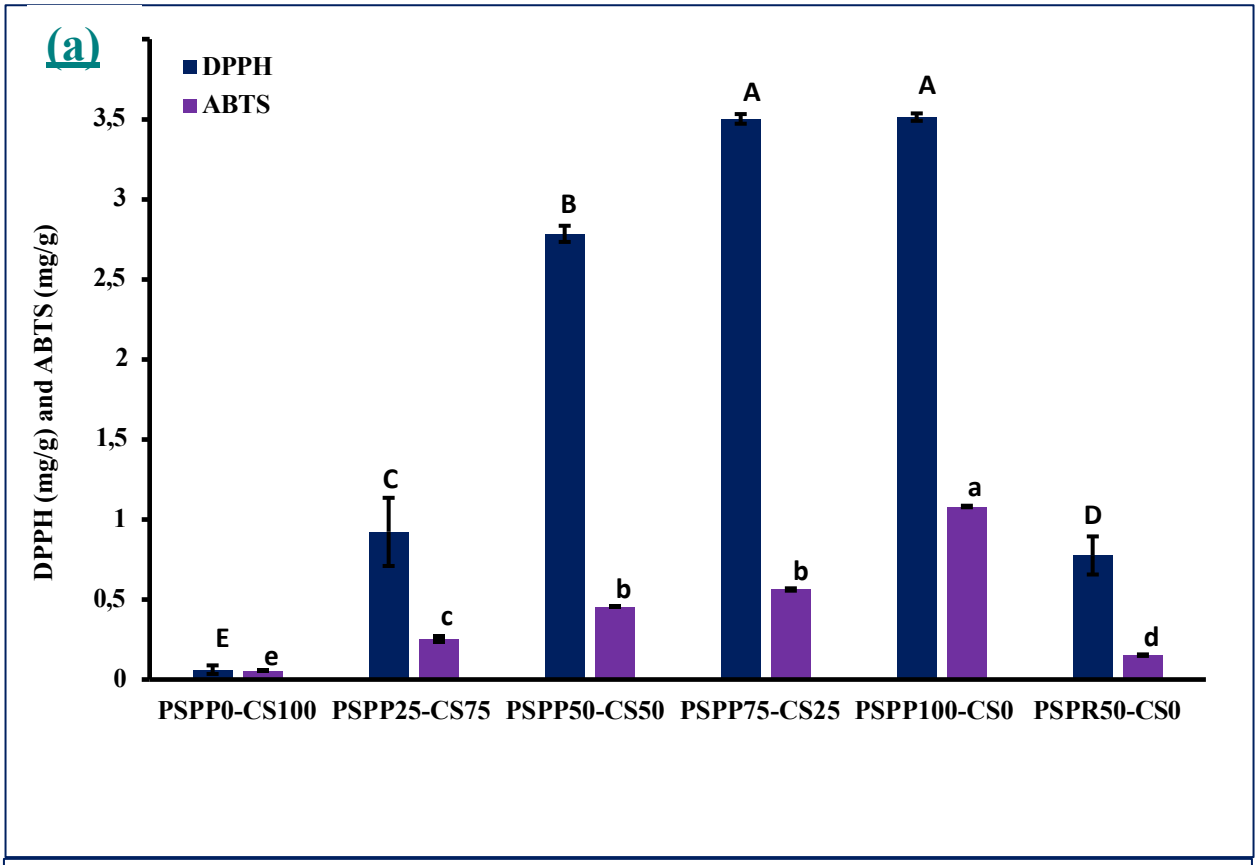


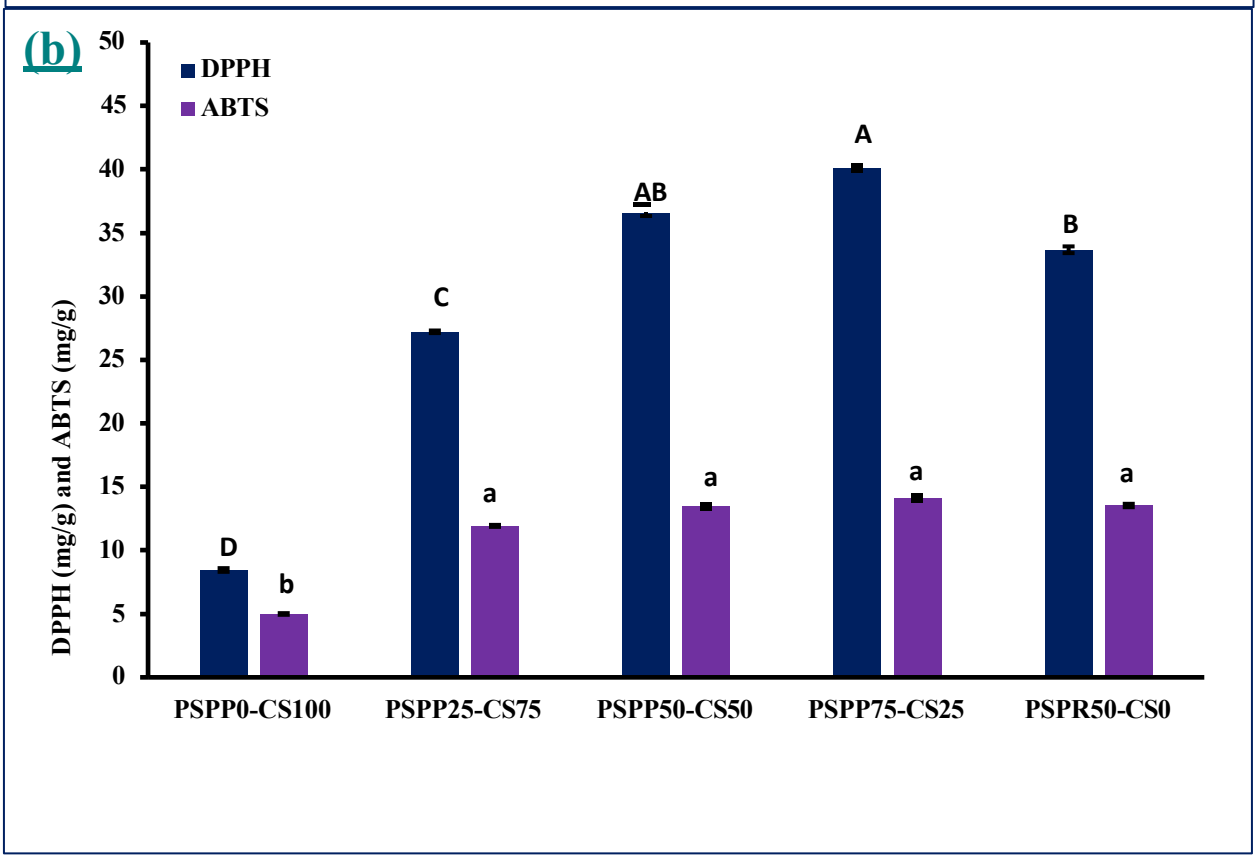

**Figure 21.** Antioxidant properties of corn starch-based aerogels with different levels of (PSPP0-CS100, PSPP25-CS75, PSPP50-CS50, PSPP75-CS25, PSPP100-CS0, and PSPR50-CS0) using DPPH and ABTS assays before (a) and after (b) encapsulation.

### 7.3.9. Antioxidant activities after loading

The antioxidant properties of the samples PSPP25-CS75-ANT, PSPP50-CS50-ANT, PSPP50-RS50-ANT, and PSPP75-CS25-ANT were assessed using DPPH and ABTS assays (Fig. 21b).

#### 7.3.9.1 DPPH

The DPPH values indicated a notable increase in antioxidant capacity with higher PSPP, ranging from 8.46 ± 0.15 mg TEV/g for the PSPP0-CS100 control to 40.14 ± 0.20 mg TEV/g for PSPP75-CS25-ANT aerogel. Significant differences ($p < 0.05$) were observed across treatments, illustrating a dose-dependent relationship. Additionally, the PSPR50-CS0-ANT aerogel displayed substantial antioxidant activity at 33.68 ± 0.26 mg TEV/g, indicating that PSPR can retain significant bioactive compounds when paired with anthocyanins. These findings align well with ROSELL et al. (2024) the PSP, which has been shown to possess significantly higher antioxidant potential than other sweet potato varieties due to its rich ANT and phenolic acids composition. The high antioxidant capacity of PSP is primarily due to anthocyanins (such as cyanidin and peonidin derivatives) and its ability to donate hydrogen atoms to neutralize reactive oxygen species (ROS) (DE BARROS et al., 2024). This characteristic makes PSPP an ideal functional ingredient for enhancing antioxidant capacity in food products (DE OLIVEIRA et al., 2024; ROSELL et al., 2024). Compared with similar studies, the DPPH values observed in this study (Fig. 21b) were consistent with the upper range of antioxidant activity reported by CEVALLOS-CASALS et al. (2003) (1.56mg/mL TE/g sample mg TEV/g) for red fresh potatoes, studying stoichiometric and kinetic studies of phenolic antioxidants from Andean purple corn and red-fleshed sweet potato. The PSPP75-CS25-ANT aerogel revealed antioxidant activity of 40.14 ± 0.20 mg TEV/g, reinforcing the high antioxidant potential of PSP compared with other sources, mainly when processed into functional food ingredients (HARASYM et al., 2020; LIAO et al., 2021; XU et al., 2018). In addition, the DPPH values found in our work was higher than those reported by CHEN et al. (2019); CHEN et al. (2024); DE BARROS et al. (2024) using purple sweet potatoes in their experiments (18.2 mg TEV/g dry PSP, 333 TEV/g, 356 TEV/g, respectively). These results highlight the importance of loading anthocyanins in aerogels for antioxidant

effects, especially in DPPH. Another unique aspect of this study was the application of anthocyanin-loaded starch aerogels incorporated in aerogels produced by PSPR (Figure 17).

#### 7.3.9.2 ABTS

PSPP-CS and PSPR-based aerogels were assessed using ABTS assay. The ABTS values obtained for the aerogels were as follows: 4.99 ± 0.06 mg TEV/g sample for the control (PSPP0-CS100), 11.93 ± 0.08 mg TEV/g sample for PSPP25-CS75, 13.49 ± 0.16 mg TEV/g sample for PSPP50-CS50-ANT, 14.13 ± 0.16 mg TEV/g sample for PSPP75-CS25-ANT, and 13.53 ± 0.13 mg TE/g sample for the PSPP50-CS50-ANT ($p < 0.05$). The control group exhibited the lowest antioxidant activity, while the PSPP50-CS50-ANT and PSPP75-CS25-ANT samples had the highest values with no significant difference between them. The PSPR50-CS0-ANT and PSPP25-CS75-ANT samples had intermediate activity, significantly higher than the control. Notably, the PSPP75-CS25-ANT sample showed a high ABTS value (14.13 ± 0.16 mg TEV/g), highlighting the radical-scavenging potential of anthocyanins in starch-based aerogels. The similar antioxidant activity of PSPR50-CS0-ANT (13.53 ± 0.13 mg TEV/g) and PSPP50-CS50-ANT (13.49 ± 0.16 mg TEV/g). The ABTS values observed in the PSPP0-CS100 were consistent with KUAN et al. (2016) (4.82 mg TEV/g). The comparable ABTS activity of the PSPR50-CS0-ANT and PSPP25-CS75-ANT samples reinforces the value of PSP byproducts as sustainable alternatives to fresh PSPP, even as a byproduct of extraction, PSPR (Fig. 21b).

#### 7.3.9.3 FRAP

The antioxidant capacity, measured as FRAP, varied significantly across treatments, ranging from 895.12 mg GAE/100g for the control (PSPP0-CS100) to 3685.23 mg GAE/100g for the PSPP50-CS50-ANT treatment ($p < 0.05$). In addition, PSPP25-CS75-ANT and PSPP75-CS25-ANT treatments, as well as the PSPR-ANT, showed moderate antioxidant capacities, significantly higher than the control but lower than the PSPP50-CS50-ANT treatment (Fig. 22a). The rise in FRAP values by 4.12 times from PSPP0-CS100-ANT to the PSPP50-CS50-ANT indicates that incorporating PSPP enhances antioxidant capacity up to a certain optimal level. This observation aligns with previous studies that report increased antioxidant activities in aerogels fortified with anthocyanin-rich powders, as anthocyanins contribute significantly to reducing $Fe^{3+}$ ions in the FRAP assay (AMAROWICZ et al., 2019).

Notably, studies on PSP extracts indicate that anthocyanin-rich aerogels generally

produce higher FRAP values than starch-based aerogels without PSP concentration (PSPP75-CS25-ANT). For instance, a slight decrease in antioxidant activity could suggest a saturation effect or potential interference from high starch content affecting the $Fe^{3+}$ to $Fe^{2+}$ reduction efficiency (Fig. 22). This pattern has been observed in similar studies, where an excessive amount of matrix material, such as starch, can hinder optimal interactions between antioxidants and $Fe^{3+}$ ions. This is evident from the FRAP value of the matrix alone (0.564 mg TE/g), which is lower compared to the impregnation of polyphenols from passion fruit PSPR in corn starch aerogels (ARAUJO et al., 2023).

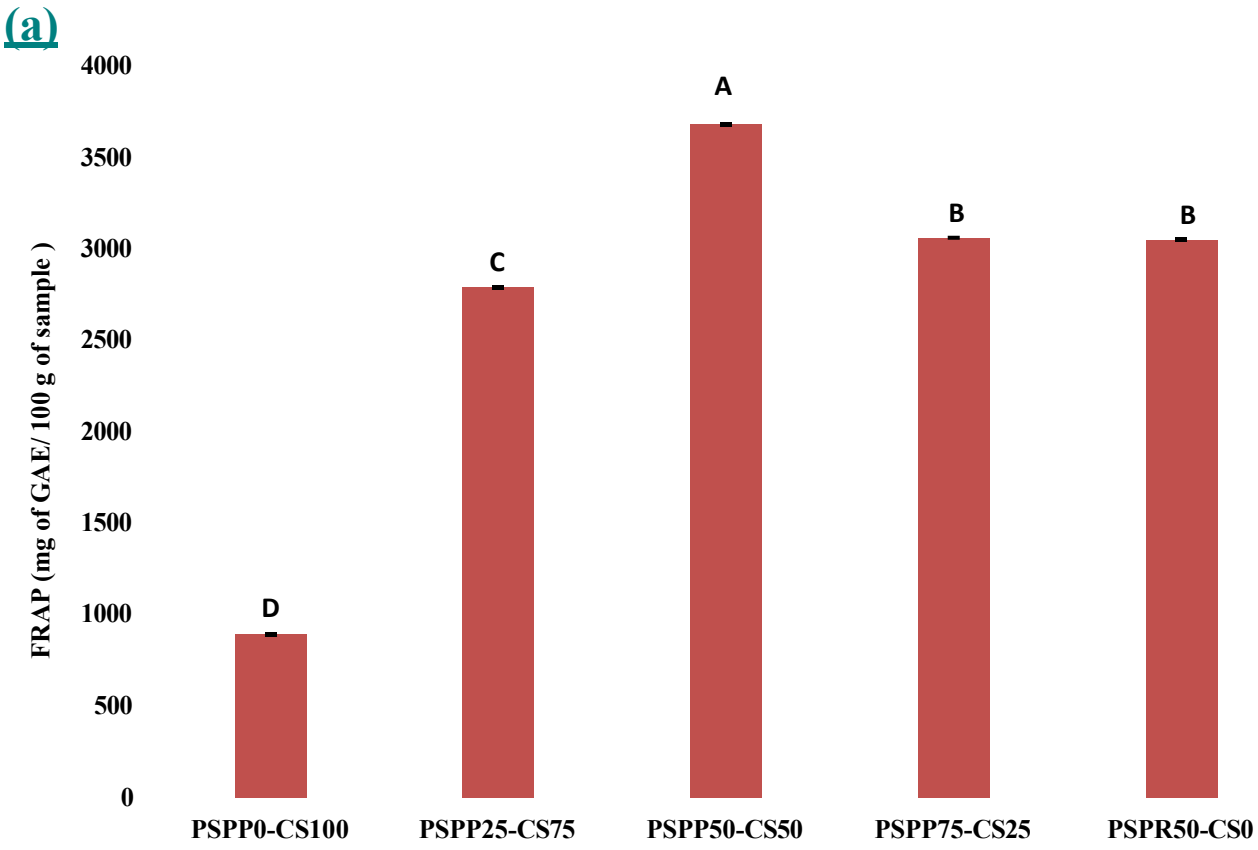

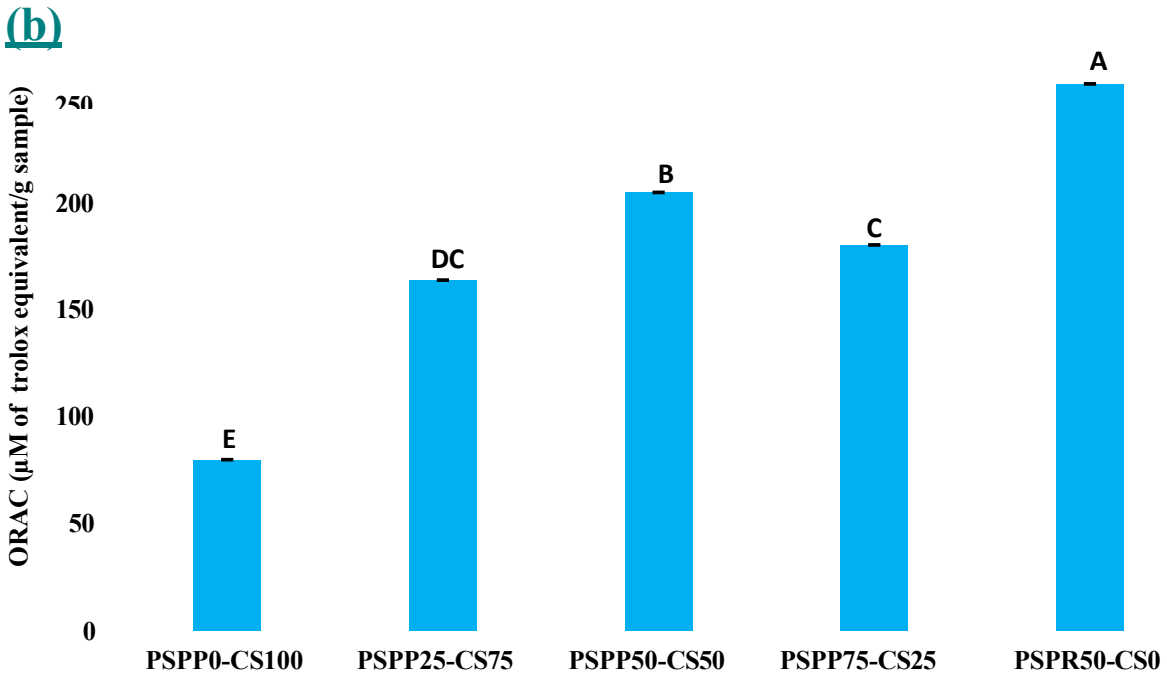


**Figure 22.** FRAP (a) and ORAC (b) assay of aerogels made from a mixture of PSPP-corn starch mixture at various concentrations (PSPP0-CS100, PSPP25-CS75, PSPP50-CS50, PSPP75-CS25, PSPP100-CS0, and PSPR50-CS0) after loading.

In Fig. 22b, the ORAC antioxidant capacities of the samples are reported. PSPP50-CS50-ANT treatment exhibited the highest antioxidant capacity (204.76 µM TE/g), followed by the PSPP75-CS25-ANT (180.21 µM TE/g) and PSPP25-CS75 (163.79 µM TE/g) treatments. As shown in Fig. 22b, PSPP50-CS50-ANT aerogel reached a 156% increase in ORAC value compared to the control. In addition, PSPP25-CS75-ANT aerogel exhibited a 25% higher antioxidant capacity, while the PSPP75-CS25-ANT treatment showed a 12% reduction relative to the PSPP50-CS50-ANT aerogel. This trend suggests that PSPP50-CS50-ANT provides the optimal anthocyanin-to-matrix ratio, while higher concentrations (PSPP75-CS25-ANT) may reduce radical accessibility due to matrix effects (SMIRNOVA et al., 2017). On the other hand, the lower antioxidant activity at PSPP25-CS75-ANT (163.79 µM TE/g), 20% less than the PSPP50-CS50-ANT aerogel, reflects insufficient anthocyanin loading and reinforcing the importance of achieving an appropriate balance in the formulation (BURATTO et al., 2019).

The PSPR demonstrated the highest antioxidant capacity (221.44 µM TE/g), with a 7.5%

greater activity than the PSPP50-CS50-ANT aerogel and a 177% increase compared to the control (Fig. 22b). Previously, WU et al. (2012) reported ORAC values of 200–300 μM TE/g in purple-fleshed sweet potatoes, aligning closely with the PSPP50-CS50-ANT aerogel (204.76 μM TE/g).

### 7.3.10. Anthocyanin Profiling by HPLC

High-performance liquid chromatography (HPLC) analysis revealed 18 anthocyanins in the PSPP and PSPR aerogels. The predominant compounds identified were peonidin 3-sophoroside-5-glucoside (peak 3) and peonidin 3-O-(6-O-coumaroyl-6-O-p-hydroxybenzoyl sophoroside)-5-O-glucoside (peak 13) (fig.22 and Table 2), both consistently detected across treatments. This indicates a decrease in anthocyanins compared to our earlier findings, which identified 23 in untreated purple sweet potato samples (DE BARROS et al., 2024).

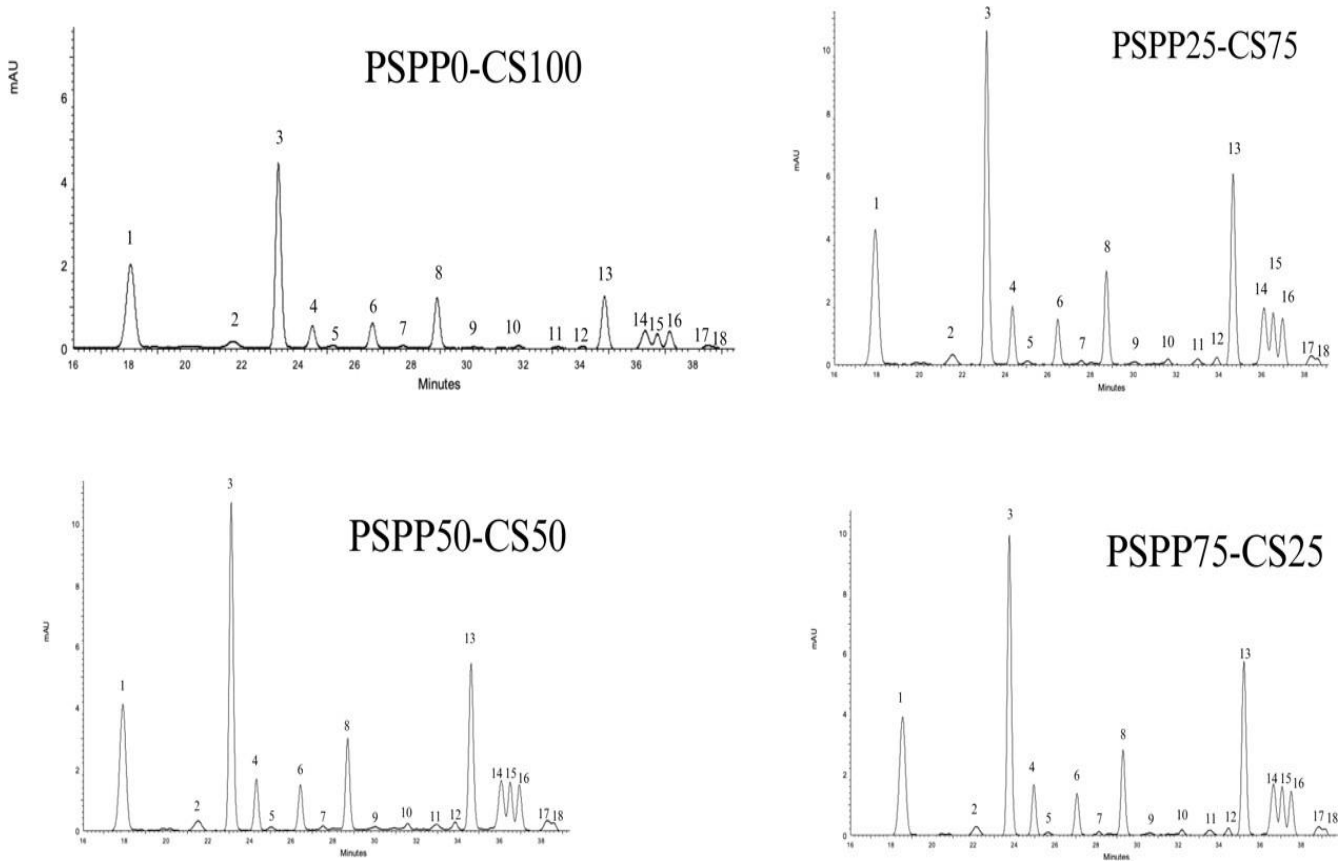

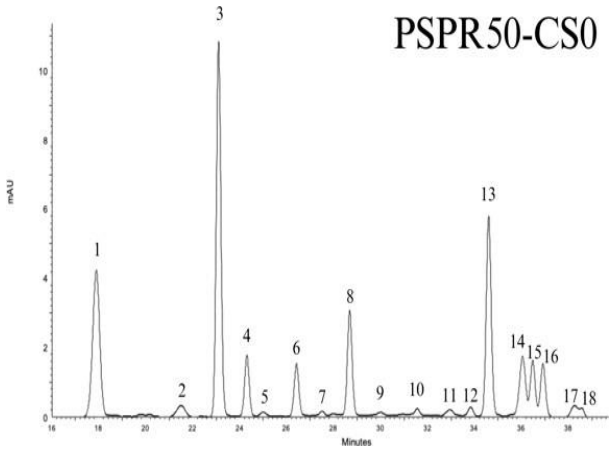


**Figure 23.** HPLC/UV-Vis MS chromatograms for aerogels obtained from a mixture PSPP and corn starch at various concentrations (PSPP0-CS100, PSPP25-CS75, PSPP50-CS50, PSPP75-CS25, and PSPR50-CS0) after anthocyanin loading.

**Table 2.** Peak assignment, mass (M+), and ion fragmentation (MS/MS) of anthocyanins aerogels from purple sweet potato (PSP).

| Peak no. | Anthocyanin Type | $M^+$ (*m/z*) | MS/MS (*m/z*) |
|---|---|---|---|
| **1** | Cyanidin 3-O-rutinoside | 595.2 | 287 |
| **2** | Cyanidin 3-caffeoyl-p-hydroxybenzoyl sophoroside-5-glucoside | 1055.9 | 893, 449, 287 |
| **3** | Peonidin 3-sophoroside-5-glucoside | 787.22 | 625, 463, 301 |
| **4** | Delfinidin 3-glucoside | 465.1 | 302.9 |
| **5** | Cyanidin-3-p-hydroxybenzoylsophoroside-5-glucoside | 893.5 | 731, 449, 287 |
| **6** | Delphinidin 3-sambubioside-5-glucoside ?? | 759.3 | 391, 177 |
| **7** | Peonidin-3-p-hydroxybenzoylsophoroside-5-glucoside | 907.5 | 745, 463, 301 |
| **8** | Peonidin-3-caffeoyl-p-hydroxybenzoylsophoroside-5-glucoside | 1069.5 | 907, 463, 301 |
| **9** | Peonidin derivative | 1067.4 | ---------- |
| **10** | Cyanidin 3-xylosyl(sinapoylglucosyl)galactoside | 949.47 | 449, 787, 287 |
| **11** | Delfinidin 3-glucoside | 465.1 | 302.9 |
| **12** | Peonidin 3-O-(6”-O-feruloyl -6”’-O- caffeoyl sophoroside)-5-O-glucoside | 1125.5 | 963,463, 301 |

| | | | | |
|---|---|---|---|---|
| **13** | Peonidin 3-O-(6-O-coumaroyl-6-O-p-hydroxybenzoyl sophoroside)-5-O-glucoside | 1053.45 | 893, 287 | 449, |
| **14** | Peonidin-3-(6″-feruloylsophoroside)-5-glucoside | 963.4 | 801, 301 | 463, |
| **15** | Peonidin 3-(feruloyl-p-coumaroyl sophoroside)-5-glucoside | 1109.4 | 947, 301 | 463, |
| **16** | Peonidin 3-O-(6-O-caffeoyl-6-O-vaniloyl sophoroside)-5-O-glucoside | 1099.4 | 935, 301 | 463, |
| **17** | Cyanidin-3-diferuloyldiglucoside-5-glucoside | 1125.4 | 287, 963 | 449, |
| **18** | Peonidin -3-(6″-caffeoyl-6‴-p-hydroxybenzoylsoph)-5-glucoside | 1069.4 | 907, 301 | 463, |

The noted reduction can be linked to the multistep processing involved in aerogel production extraction, concentration, and loading, as well as the established sensitivity of anthocyanins to factors like temperature, pH, light, and oxygen (GHASSEMPOUR et al., 2008; LAO et al., 2016; ZHAO et al., 2021). These findings confirm the selective retention of more stable anthocyanins, especially peonidin derivatives, under rigorous processing conditions.

## 7.4. Conclusions

This study demonstrated the potential of PSPP as a rich source of bioactive compounds for aerogel generation using SC-$CO_2$ drying. The PSPP50-CS50-ANT aerogel exhibited the best formulation with highest anthocyanin content (1403.36 ± 9.70 C3G/100 g). TPC of PSPP50-CS50-ANT aerogel after anthocyanin loading was 2313.85 ± 12.00 mg GAE/100g, highlighting its high phenolic compound retention capacity. Further, HPLC analysis revealed a total of 18 anthocyanins in the aerogels, with peonidin 3- sophoroside-5-glucoside and peonidin 3-O-(6-O-coumaroyl-6-O-p-hydroxybenzoyl sophoroside)-5-O-glucoside as the dominant compounds. This emphasizes the stability of anthocyanins during SC-$CO_2$ drying, maintaining their structural integrity and functional properties. The antioxidant potential of PSPP aerogels was confirmed through various assays, resulting in PSPP75-CS25-ANT aerogel with the highest DPPH radical scavenging activity (40.14 ± 0.20 mg TEV/g) and ABTS activity (14.13 ± 0.16 mg TEV/g), reflecting substantial free radical neutralization. The PSPP50-CS50-ANT aerogel excelled in reducing power, achieving the highest FRAP value (3685.23 mg GAE/100g), while the PSPR50-CS0-ANT aerogel recorded the highest ORAC value (221.44 μM TE/g), highlighting the significance of PSPRs in antioxidant applications. Additionally, the PSPR50-CS0-ANT aerogel demonstrated its potential as a sustainable, cost-effective alternative, retaining substantial bioactive properties even after anthocyanin extraction. Its high-water solubility further broadens its applicability, suggesting promising uses as a natural exudate in functional beverages or supplements, as well as in the development of active packaging systems that can release bioactive compounds to enhance food preservation and extend shelf life.

### 7.5. Circular economy

The circular economy pathway illustrated in Figure 24 finds strong support in the results obtained for the PSPR50–CS0 treatment (Table 1). This formulation, developed from purple sweet potato residue, combined favorable structural properties with good levels of anthocyanins and antioxidant activity, confirming its potential as a functional carrier system. As shown in Figure 15, both aerogels and hydrogels derived from PSPR50–CS0 exhibited consistent bioactive retention, reinforcing the versatility of this treatment in different matrix formats. Furthermore, Figure 17 provides visual confirmation of the aerogel after anthocyanin encapsulation, highlighting its structural integrity and demonstrating how the porous architecture effectively supports pigment stabilization. This approach consolidates the zero-waste perspective that underpins the thesis and offers a clear example of how circular economy principles can be applied in food systems to generate innovation, sustainability, and added functionality.


**Figure 24.** Circular economy process applied to purple sweet potato: (1) raw material; (2) pre-treatment; (3) anthocyanin extraction; (4) post-extraction residue; (5) aerogel production; (6) anthocyanin encapsulation in aerogels. Souce: Designed by the Author, 2025.

# 8 GENERAL CONCLUSION

The findings across the three studies provide converging evidence for the effectiveness of a systematic, multidisciplinary approach to valorizing anthocyanin-rich plant matrices, aligning with circular economy principles.

The morpho-anatomical characteristics of plant tissues play a decisive role in the efficiency and outcome of anthocyanin extraction. By mapping structural features such as cell wall composition and organ-specific distribution of compounds, a decision-tree model was successfully developed and validated with blackberry and purple sweet potato.

The application of SC–$CO_2$ technology, particularly when modified with a low-ratio ethanol water cosolvent system, demonstrated strong potential as a green alternative to traditional solvent-based extraction. Under optimized conditions, it achieved comparable phenolic and anthocyanin yields to those of high methanol methods, while operating at lower temperatures and eliminating toxic residues. The antioxidant capacity remained satisfactory, and the structural disruption observed at the cellular level confirmed effective solubilization of bioactives. These results support the broader adoption of SC–$CO_2$ systems for food-grade extractions where compound preservation and environmental impact.

The final phase of the study explored the development of aerogels from both purple sweet potato powder and post-extraction residues. The aerogels not only retained high levels of anthocyanins and phenolics, as confirmed by spectrophotometric and HPLC analyses, but also exhibited antioxidant properties across samples. Their composition enabled them to act as protective matrices, preserving anthocyanin integrity against environmental stressors, including oxidation and pH shifts. Furthermore, the encapsulated aerogels reduced waste and enhanced sustainability in food systems.

This thesis illustrates a comprehensive framework for enhancing the recovery, stability, and functionality of plant-based bioactives through informed method selection, green processing, and circular design. It offers valuable contributions to the fields of food science and bioactive delivery, while also providing scalable, environmentally conscious alternatives for industrial applications. Future research should investigate the integration of these systems into food matrices and evaluate their performance under realistic storage and digestion conditions to ensure functional viability in consumer products.

## REFERENCIAS

AHMADZADEH, S., & UBEYITOGULLARI, A. (2022). **Fabrication of Porous Spherical Beads from Corn Starch by Using a 3D Food Printing System.** FOODS, 11(7), 913. https://www.mdpi.com/2304-8158/11/7/913

AHMADZADEH, S., & UBEYITOGULLARI, A. (2023). **Generation of porous starch beads via a 3D food printer: The effects of amylose content and drying technique.** Carbohydrate Polymers, 301, 120296. https://doi.org/https://doi.org/10.1016/j.carbpol.2022.120296

AHMADZADEH, S., & UBEYITOGULLARI, A. (2024). **Lutein encapsulation into dual-layered starch/zein gels using 3D food printing: Improved storage stability and in vitro bioaccessibility.** International Journal of Biological Macromolecules, 266, 131305. https://doi.org/https://doi.org/10.1016/j.ijbiomac.2024.131305

AKOGOU, F. U., KAYODÉ, A. P., DEN BESTEN, H. M., & LINNEMANN, A. R. (2018). **Extraction methods and food uses of a natural red colorant from dye sorghum.** JOURNAL OF THE SCIENCE OF FOOD AND AGRICULTURE, 98(1), 361-368. https://doi.org/https://doi.org/10.1002/jsfa.8479

ALBUQUERQUE, B. R., PINELA, J., BARROS, L., OLIVEIRA, M. B. P. P., & FERREIRA, I. C. F. R. (2020). A**nthocyanin-rich extract of jabuticaba epicarp as a natural colorant: Optimization of heat- and ultrasound-assisted extractions and application in a bakery product.** Food Chemistry, 316, 126364. https://doi.org/https://doi.org/10.1016/j.foodchem.2020.126364

ALIBADE, A., LAKKA, A., BOZINOU, E., LALAS, S. I., CHATZILAZAROU, A., & MAKRIS, D. P. (2021). **Development of a Green Methodology for Simultaneous Extraction of Polyphenols and Pigments from Red Winemaking Solid Wastes (Pomace) Using a Novel Glycerol-Sodium Benzoate Deep Eutectic Solvent and Ultrasonication Pretreatment.** Environments, 8(9). https://doi.org/10.3390/environments8090090

ALIOTTA, L., GIGANTE, V., COLTELLI, M. B., CINELLI, P., & LAZZERI, A. (2019). **Evaluation of Mechanical and Interfacial Properties of Bio-Composites Based on Poly(Lactic Acid) with Natural Cellulose Fibers.** Int J Mol Sci, 20(4). https://doi.org/10.3390/ijms20040960

ALZATE-ARBELAEZ, A. F., CORTÉS, F. B., & ROJANO, B. A. (2022). A**ntioxidants from Hyeronima macrocarpa Berries Loaded on Nanocellulose: Thermal and Antioxidant Stability**. Molecules, 27(19), 6661. https://www.mdpi.com/1420-3049/27/19/6661

AMAROWICZ, R., & PEGG, R. B. (2019). Chapter One - Natural antioxidants of plant origin. In I. C. F. R. Ferreira & L. Barros (Eds.), **Advances in Food and Nutrition Research** (Vol. 90, pp. 1-81). Academic Press. https://doi.org/https://doi.org/10.1016/bs.afnr.2019.02.011

ARAUJO, E. J. S., SCOPEL, E., REZENDE, C. A., & MARTÍNEZ, J. (2023). **Supercritical impregnation of polyphenols from passion fruit residue in corn starch aerogels: Effect of operational parameters.** Journal of Food Engineering, 343, 111394. https://doi.org/https://doi.org/10.1016/j.jfoodeng.2022.111394

ARRUDA, H. S., SILVA, E. K., PEIXOTO ARAUJO, N. M., PEREIRA, G. A., PASTORE, G. M., & MAROSTICA JUNIOR, M. R. (2021). **Anthocyanins Recovered from Agri-Food By-Products Using Innovative Processes: Trends, Challenges, and Perspectives for Their** Application in Food Systems. Molecules, 26(9). https://doi.org/10.3390/molecules26092632

BABOVA, O., OCCHIPINTI, A., CAPUZZO, A., & MAFFEI, M. E. (2016). **Extraction of bilberry (Vaccinium myrtillus) antioxidants using supercritical/subcritical CO2 and ethanol as co-solvent.** Journal of Supercritical Fluids, 107, 358-363. https://doi.org/10.1016/j.supflu.2015.09.029

BARROS, G. L. d., PIO, R., RIBEIRO, C. H. M., FAZENDA, L. H. V., SILVA, A. D. d., & PECHE, P. M. (2023). **Management of blackberry pruning to extend harvest seasonality.** Pesquisa Agropecuária Brasileira, 58.

BENUCCI, I., LOMBARDELLI, C., MAZZOCCHI, C., & ESTI, M. (2022). **Natural colorants from vegetable food waste: Recovery, regulatory aspects, and stability-A review.** Compr Rev Food Sci Food Saf, 21(3), 2715-2737. https://doi.org/10.1111/1541-4337.12951

BOONKOR, P., SAGIS, L. M. C., & LUMDUBWONG, N. (2022). **Pasting and Rheological Properties of Starch Paste/Gels in a Sugar-Acid System**. Foods, 11(24), 4060. https://www.mdpi.com/2304-8158/11/24/4060

BORDA, M. G., RAMÍREZ-VÉLEZ, R., BOTERO-RODRIGUEZ, F., PATRICIO-BALDERA, J., DE LUCIA, C., POLA, I., BARRETO, G. E., KHALIFA, K., BERGLAND, A. K., KIVIPELTO, M., CEDERHOLM, T., ZETTERBERG, H., ASHTON, N. J., BALLARD, C., SIOW, R., AARSLAND, D., & NJ, F. (2025). Ant**hocyanin supplementation in adults at risk for dementia: a randomized controlled trial on its cardiometabolic and anti-inflammatory biomarker effects**. Geroscience. https://doi.org/10.1007/s11357-025-01669-8

BURATTO, R. T., HOYOS, E. G., COCERO, M. J., & MARTÍN, Á. (2019). I**mpregnation of açaí residue extracts in silica-aerogel. The Journal of Supercritical Fluids,** 146, 120-127. https://doi.org/https://doi.org/10.1016/j.supflu.2018.12.004

CAO, X. Y., HAO, W. H., PAN, W. Q., GAO, X. L., XIE, J. W., & DU, L. J. (2024). **A vacuolar protein MaSCPL1 mediates anthocyanin acylation modifications in blue-flowered grape hyacinth.** Plant Science, 349, Article 112273. https://doi.org/10.1016/j.plantsci.2024.112273

CAROLINE PAZ GONÇALVES, G., LIZANDRA GOMES ROSAS, A., CARNEIRO DE SOUSA, R., REGINA RODRIGUES VIEIRA, T., CÉSAR DE ALBUQUERQUE SOUSA, T., RAMIRES, T., FERREIRA FERREIRA DA SILVEIRA, T., BARROS, L., PADILHA DA SILVA, W., RENATO GUERRA DIAS, Á., DA ROSA ZAVAREZE, E., & DILLENBURG MEINHART, A. (2024). **A green method for anthocyanin extraction from Clitoria ternatea flowers cultivated in southern Brazil: Characterization, in vivo toxicity, and biological activity.** FOOD CHEMISTRY, 435, 137575. https://doi.org/https://doi.org/10.1016/j.foodchem.2023.137575

CEVALLOS-CASALS, B. A., & CISNEROS-ZEVALLOS, L. (2003). **Stoichiometric and kinetic studies of phenolic antioxidants from Andean purple corn and red-fleshed sweetpota**to. J Agric Food Chem, 51(11), 3313-3319. https://doi.org/10.1021/jf034109c

CHEN, B. J., XIANG, L. R., ZHAO, D. Y., LIU, Z. Y., & JIA, F. (2025). **Unraveling Nature's Color Palette: The Chemistry, Biosynthesis and Applications in Health Promotion of Anthocyanins-A Comprehensive Review.** Food Reviews International, 41(2), 491-520. https://doi.org/10.1080/87559129.2024.2404471

CHEN, C.-C., LIN, C., CHEN, M.-H., & CHIANG, P.-Y. (2019). **Stability and Quality of Anthocyanin in Purple Sweet Potato Extracts.** FOODS, 8(9), 393. https://www.mdpi.com/2304-8158/8/9/393

CHEN, H. W., WANG, M. M., ZHANG, L. J., REN, F. X., LI, Y. T., CHEN, Y., LIU, Y. Q., ZHANG, Z. W., & ZENG, Q. Q. (2024). **Anthocyanin profiles and color parameters of fourteen grapes and wines from the eastern foot of Helan Mountain in Ningxia.** Food Chemistry-X, 24, Article 102034. https://doi.org/10.1016/j.fochx.2024.102034

CHEN, Z., WANG, J., LU, Y., WU, Q., LIU, Y., LIU, Y., KUMAR, S., ZHU, G., & ZHU, Z. (2024). **Pre-Treatment, Extraction Solvent, and Color Stability of Anthocyanins from Purple Sweetpotato.** FOODS, 13(6), 833. https://www.mdpi.com/2304-8158/13/6/833

CORTEZ, R., LUNA-VITAL, D. A., MARGULIS, D., & GONZALEZ DE MEJIA, E. (2017). **Natural Pigments: Stabilization Methods of Anthocyanins for Food Applications.** Compr Rev Food Sci Food Saf, 16(1), 180-198. https://doi.org/10.1111/1541-4337.12244

COSTA, A. F. d. S., DE AMORIM, J. D. P., ALMEIDA, F. C. G., DE LIMA, I. D., DE PAIVA, S. C., ROCHA, M. A. V., VINHAS, G. M., & SARUBBO, L. A. (2019). **Dyeing of bacterial cellulose films using plant-based natural dyes. International Journal of Biological Macromolecules,** 121, 580-587. https://doi.org/https://doi.org/10.1016/j.ijbiomac.2018.10.066

CUI, H. P., ZHAO, S. X., JI, Y., & YANG, J. T. (2025). **Effect of L-proline on stability and in vitro digestive antioxidant capacity of mulberry anthocyanins in model beverages.** Lwt-Food Science and Technology, 215, Article 117210. https://doi.org/10.1016/j.lwt.2024.117210

CUNHA JÚNIOR, P. C. d., SILVA, M. T. d. C., BARBOSA, M. I. M. J., & FERREIRA, E. H. d. R. (2024). **Application of lyophilized purple-fleshed sweet potato powder as a multifunctional ingredient in Greek yogurt.** Ciência Rural, 54.

ĆURKO, N.; TOMAŠEVIĆ, M.; BUBALO, M. C.; GRACIN, L.; REDOVNIKOVIĆ, I. R.; GANIĆ, K. K. **Extraction of Proanthocyanidins and Anthocyanins from Grape Skin by Using Ionic Liquids.** Food Technol. And Biotechnol. 2017, 55(3), 429–437. DOI: 10.17113/ftb.55.03.17.5200.

DARABI, A., JESSOP, P. G., & CUNNINGHAM, M. F. (2016). **CO2-Responsive Polymeric Materials: Synthesis, Self-Assembly, and Functional Applications**. Chem. Soc. Rev., 45, 4391.

DE BARROS, TUHANIOGLU, A., KAUR, S., NORA, L., & UBEYITOGULLARI, A. (2024). **Extraction of anthocyanins from purple sweet potato using supercritical carbon dioxide and conventional approaches.** Applied Food Research, 4(2), 100505. https://doi.org/https://doi.org/10.1016/j.afres.2024.100505

DE BARROS, G. L., SILVA, F. T. S., TEIXEIRA, R. S., WAGNER, J. G., ROMBALDI, C. V., VIZZOTTO, M., UBEYITOGULLARI, A., & NORA, L. (2024). **Anthocyanin extraction methods: synthesis of morpho-anatomical knowledge for decision-making based on decision-tree.** International Journal of Food Properties, 27(1), 1315-1346. https://doi.org/10.1080/10942912.2024.2409893

DE OLIVEIRA, Z. B., SILVA DA COSTA, D. V., DA SILVA DOS SANTOS, A. C., DA SILVA JÚNIOR, A. Q., DE LIMA SILVA, A., DE SANTANA, R. C. F., COSTA, I. C. G., DE SOUSA RAMOS, S. F., PADILLA, G., & DA SILVA, S. K. R. (2024). **Synthetic Colors in Food: A Warning for Children's Health.** Int J Environ Res Public Health, 21(6). https://doi.org/10.3390/ijerph21060682

DIEP, T., POOK, C., & YOO, M. (2020). **Phenolic and Anthocyanin Compounds and Antioxidant Activity of Tamarillo (Solanum betaceum Cav.).** Antioxidants (Basel), 9(2). https://doi.org/10.3390/antiox9020169

DONG, J. J., LV, Y. T., ZHAO, C. L., SHI, Y. R., TANG, R. M., HE, L. H., FAN, R. W., & JIA, X. Y. (2025). **Extraction of anthocyanins from purple sweet potato: evaluation of anti-inflammatory effects in a rheumatoid arthritis animal model, mechanistic studies on inflammatory cells, and development of exosome-based delivery for enhanced targeting.** Frontiers in Immunology, 16, Article 1559874. https://doi.org/10.3389/fimmu.2025.1559874

DONG, Y. W. X. H. L. B. J. H. C. E.-O. E. G. L. W. M. T. P. R. o. D. A. i. I. V. E. C. S., & PREVENTING CARDIOVASCULAR, D. (2022). **Nutrients**, 14(14).

DOWNHAM, A., & COLLINS, P. (2000). **Colouring our foods in the last and next millennium.** International Journal of Food Science & Technology, 35(1), 5-22. https://doi.org/https://doi.org/10.1046/j.1365-2621.2000.00373.x

EREN, H. A., AVINC, O., & EREN, S. (2017). **Supercritical Carbon Dioxide for Textile Applications and Recent Developments.** IOP Conf. Ser.: Mater. Sci. Eng., 254, 82011.

EVANS, W. C., & EVANS, D. (2009). Chapter 41 - Plant description, morphology and anatomy. In W. C. Evans & D. Evans (Eds.), **Trease and Evans' Pharmacognosy (Sixteenth Edition)** (pp. 541-550). W.B. Saunders. https://doi.org/https://doi.org/10.1016/B978-0-7020-2933-2.00041-1

FARIAS, C. A. A., MORAES, D. P., NEUENFELDT, N. H., ZABOT, G. L., EMANUELLI, T., BARIN, J. S., BALLUS, C. A., & BARCIA, M. T. (2022). **Microwave hydrodiffusion and gravity model with a unique hydration strategy for exhaustive extraction of anthocyanins from strawberries and raspberries.** FOOD CHEMISTRY, 383, 132446. https://doi.org/https://doi.org/10.1016/j.foodchem.2022.132446

FEITOSA, B. F., DECKER, B. L. A., DE BRITO, E. S., MARQUES, M. C., RODRIGUES, S., & MARIUTTI, L. R. B. (2025). **Stability of anthocyanins from fruits associated with microencapsulation: A 21st-century bibliometric approach**. Food Research International, 214, Article 116621. https://doi.org/10.1016/j.foodres.2025.116621

FENG, Y. P., QIAO, B. Q., LU, X., XIAO, J. H., YU, L. L., & NIU, L. Y. (2024). **Wheat Protein Hydrolysates Improving the Stability of Purple Sweet Potato Anthocyanins under Neutral pH after Commercial Sterilization at 121 °C.** Foods, 13(6), Article 843. https://doi.org/10.3390/foods13060843

FERNANDEZ-AULIS, F., HERNANDEZ-VAZQUEZ, L., AGUILAR-OSORIO, G., ARRIETA-BAEZ, D., & NAVARRO-OCANA, A. (2019). **Extraction and Identification of Anthocyanins in Corn Cob and Corn Husk from Cacahuacintle Maize.** JOURNAL OF FOOD SCIENCE, 84(5), 954-962. https://doi.org/https://doi.org/10.1111/1750-3841.14589

FERREIRA, M. V. S., CAPPATO, L. P., SILVA, R., ROCHA, R. S., GUIMARAES, J. T., BALTHAZAR, C. F., ESMERINO, E. A., FREITAS, M. Q., RODRIGUES, F. N., GRANATO, D., NETO, R. P. C., TAVARES, M. I. B., SILVA, P. H. F., RAICES, R. S. L., SILVA, M. C., & CRUZ, A. G. (2019). **Ohmic heating for processing of whey-raspberry flavored beverage.** FOOD CHEMISTRY, 297, Article 125018. https://doi.org/10.1016/j.foodchem.2019.125018

FERREIRA, M. V. S., CAPPATO, L. P., SILVA, R., ROCHA, R. S., GUIMARÃES, J. T., BALTHAZAR, C. F., ESMERINO, E. A., FREITAS, M. Q., RODRIGUES, F. N., GRANATO, D., NETO, R. P. C., TAVARES, M. I. B., SILVA, P. H. F., RAICES, R. S. L., SILVA, M. C., & CRUZ, A. G. (2019). **Ohmic heating for processing of whey-raspberry flavored beverage.** Food Chemistry, 297, 125018. https://doi.org/https://doi.org/10.1016/j.foodchem.2019.125018

FORGHANI, S., & ALMASI, H. (2025). **Halochromic aerogels with Ca2+-induced tailored porosity based on alginate/gellan integrated with Echium amoenum anthocyanins: Characterization and application for freshness monitoring of rainbow trout fillet.** Food Hydrocolloids, 160, Article 110826. https://doi.org/10.1016/j.foodhyd.2024.110826

FROND, A. D., IUHAS, C. I., STIRBU, I., LEOPOLD, L., SOCACI, S., ANDREEA, S., AYVAZ, H., ANDREEA, S., MIHAI, S., DIACONEASA, Z., & CARMEN, S. (2019). **Phytochemical Characterization of Five Edible Purple-Reddish Vegetables: Anthocyanins, Flavonoids, and Phenolic Acid Derivatives.** Molecules, 24(8), 1536. https://www.mdpi.com/1420-3049/24/8/1536

GHASSEMPOUR, A., HEYDARI, R., TALEBPOUR, Z., FAKHARI, A. R., RASSOULI, A., DAVIES, N., & ABOUL-ENEIN, H. Y. (2008). **Study of New Extraction Methods for Separation of Anthocyanins from Red Grape Skins: Analysis by HPLC and LC-MS/MS.** Journal of Liquid Chromatography & Related Technologies, 31(17), 2686-2703. https://doi.org/10.1080/10826070802353247

GONZÁLEZ-LÁZARO, M., DE URTURI, I. S., ROMÁN, S. M. S., MURILLO-PEÑA, R., PÉREZ-ALVAREZ, E. P., & GARDE-CERDÁN, T. (2024). **Effects of foliar applications of methyl jasmonate alone or with urea on anthocyanins content during grape ripening.** Scientia Horticulturae, 338, Article 113782. https://doi.org/10.1016/j.scienta.2024.113782

GRILLO, G., GUNJEVIĆ, V., RADOŠEVIĆ, K., REDOVNIKOVIĆ, I. R., & CRAVOTTO, G. (2020). **Deep Eutectic Solvents and Nonconventional Technologies for Blueberry-Peel Extraction: Kinetics, Anthocyanin Stability, and Antiproliferative Activity.** Antioxidants, 9(11), 1069. https://www.mdpi.com/2076-3921/9/11/1069

GUAN, Y. L., ZHU, H. X., LIN, M. H., ZHANG, Y. X., HE, Q., & PAN, J. R. (2025). **Preparation and stability evaluation of flexible nanoliposomes co-encapsulated with black wolfberry anthocyanins and EGCG.** Lwt-Food Science and Technology, 217, Article 117402. https://doi.org/10.1016/j.lwt.2025.117402

GULATI, M., MURTHY, P. S. K., DASALKAR, A. H., YANNAM, S. K., & REDDY, J. P. (2025). **Development of Spray-Dried Microparticles Encapsulating Onion Peel Extract Containing Anthocyanin: Optimization, Characterization, and Storage Stability.** Acs Food Science & Technology, 5(6), 2123-2138. https://doi.org/10.1021/acsfoodscitech.4c00998

HAN, H., HOU, J., YANG, N., ZHANG, Y., CHEN, H., ZHANG, Z., SHEN, Y., HUANG, S., & GUO, S. (2019). I**nsight on the changes of cassava and potato starch granules during gelatinization.** Int J Biol Macromol, 126, 37-43. https://doi.org/10.1016/j.ijbiomac.2018.12.201

HARASYM, J., SATTA, E., & KAIM, U. (2020). **Ultrasound Treatment of Buckwheat Grains Impacts Important Functional Properties of Resulting Flour.** Molecules, 25(13), 3012. https://www.mdpi.com/1420-3049/25/13/3012

HASHEMI GAHRUIE, H., PARASTOUEI, K., MOKHTARIAN, M., ROSTAMI, H., NIAKOUSARI, M., & MOHSENPOUR, Z. (2020). **Application of innovative processing methods for the extraction of bioactive compounds from saffron (Crocus sativus) petals**. JOURNAL OF APPLIED RESEARCH ON MEDICINAL AND AROMATIC PLANTS, 19, 100264. https://doi.org/https://doi.org/10.1016/j.jarmap.2020.100264

HASSOUN, A., CROPOTOVA, J., TRIF, M., RUSU, A. V., BOBIS, O., NAYIK, G. A., JAGDALE, Y. D., SAEED, F., AFZAAL, M., MOSTASHARI, P., KHANEGHAH, A. M., & REGENSTEIN, J. M. (2022). **Consumer acceptance of new food trends resulting from the fourth industrial revolution technologies: A narrative review of literature and future perspectives.** Front Nutr, 9, 972154. https://doi.org/10.3389/fnut.2022.972154

HATAMI, T., JARLES SANTOS DE ARAÚJO, E., LUIZ BAIÃO DIAS, A., HELENA INNOCENTINI MEI, L., & MARTÍNEZ, J. (2024). **Mechanism of multicyclic β-carotene impregnation into corn starch aerogels via supercritical CO(2) with mathematical modeling.** Food Res Int, 178, 114002. https://doi.org/10.1016/j.foodres.2024.114002

HAYES, D.J., ROSS, J., HAYES, M.H.B. and Fitzpatrick, S. (2008) **The Biofine Process: Production of Levulinic Acid, Furfural and Formic Acid from Lignocellulosic Feedstocks.** In: Biorefineries-Industrial Processes and Products: Status Quo and Future Directions, Wiley VCH, Weinheim.

HE, Y.; WEN, L. K.; DU, Y. J.; WANG, Z. T.; LIN, K. **Comparison of Different Extraction Methods of Antioxidant Anthocyanins in Zuoyouhong Vitis Amurensis.** Oxid. Commun. 2016, 39(4–I), 2928–2937.

HENDERSON, R. K., JIMÉNEZ-GONZÁLEZ, C., CONSTABLE, D. J. C., ALSTON, S. R., INGLIS, G. G. A., FISHER, G., SHERWOOD, J., BINKS, S. P., & CURZONS, A. D. (2011). **Expanding GSK's Solvent Selection Guide – Embedding Sustainability Into Solvent Selection Starting at Medicinal Chemistry.** Green Chem., 13, 854.

HORVAT, G., PANTIĆ, M., KNEZ, Ž., & NOVAK, Z. (2022). **A Brief Evaluation of Pore Structure Determination for Bioaerogels.** Gels, 8(7), 438. https://www.mdpi.com/2310-2861/8/7/438

HUANG, Y. J., KOU, P., LUO, J., CHEN, C. L., LI, J. M., LAI, Z. X., MIAO, L. X., & CHEN, Y. T. (2024). **Effect of Storage Temperature on Fruit Hardness and Anthocyanin**

**Biosynthesis in Red Peeled Banana (Musa acuminata Hongmeiren)**. Hortscience, 59(11), 1667-1673. https://doi.org/10.21273/hortsci18192-24

INSANU, M., AMALIA, R., & FIDRIANNY, I. (2022). **Potential Antioxidative Activity of Waste Product of Purple Sweet Potato (Ipomoea batatas Lam.)**. Pak J Biol Sci, 25(8), 681-687. https://doi.org/10.3923/pjbs.2022.681.687

JESUS, M. S. C. d., SANTIAGO, M. C. P. d. A., PACHECO, S., GOUVÊA, A. C. M. S., NASCIMENTO, L. d. S. d. M. d., BORGUINI, R. G., GUERRA, J. G. M., ESPINDOLA, J. A. A., & GODOY, R. L. d. O. (2021). **Acylated anthocyanins from organic purple-fleshed sweet potato (Ipomoea batatas (L.) Lam) produced in Brazil**. Scientia Agricola, 78(4). https://doi.org/10.1590/1678-992x-2019-0309

JIANG, Y., LI, X. S., ZHANG, Y. L., WU, B. Y., LI, Y. X., TIAN, L. M., SUN, J. X., & BAI, W. B. (2024). **Mechanism of action of anthocyanin on the detoxification of foodborne contaminants-A review of recent literature.** Comprehensive Reviews in Food Science and Food Safety, 23(1), 1-33. https://doi.org/10.1111/1541-4337.13259

JIN, S., BYRNE, F., MCELROY, C. R., SHERWOOD, J., CLARK, J. H., & HUNT, A. J. (2017). **Challenges in the Development of Bio-Based Solvents: A Case Study on methyl(2,2-Dimethyl-1,3-Dioxolan-4-Yl)methyl Carbonate as an Alternative Aprotic Solvent**. Faraday Discuss., 202, 157.

JÖBSTL, E., O'CONNELL, J., FAIRCLOUGH, J. P. A., & WILLIAMSON, M. P. (2004). **Molecular Model for Astringency Produced by Polyphenol/Protein Interactions**. Biomacromolecules, 5(3), 942-949. https://doi.org/10.1021/bm0345110

KAKOLI, D., & ROSALIN, N. (2023). **Application of Colorimetry in Food Industries.** In S. Ashis Kumar (Ed.), Advances in Colorimetry (pp. Ch. 5). IntechOpen. https://doi.org/10.5772/intechopen.112099

KASTER, J. B., CRUZ, E. P. D., SILVA, F. T. D., HACKBART, H., SIEBENEICHLER, T. J., CAMARGO, T. M., RADÜNZ, M., FONSECA, L. M., & ZAVAREZE, E. D. R. (2024). **Bioactive aerogels based on native and phosphorylated potato (Solanum tuberosum L.) starches incorporated with star fruit extract (Averrhoa carambola L.)**. Int J Biol Macromol, 272(Pt 2), 132907. https://doi.org/10.1016/j.ijbiomac.2024.132907

KAUR, D., YOUSUF, B., & QADRI, O. S. (2024). **Syzygium cumini anthocyanins: recent advances in biological activities, extraction, stability, characterisation and utilisation in food systems**. Food Production Processing and Nutrition, 6(1), Article 34. https://doi.org/10.1186/s43014-023-00177-6

KAUR, S., CHEN, J., & UBEYITOGULLARI, A. (2024). **Formation of nanoporous aerogels from defatted rice bran via supercritical carbon dioxide drying** [10.1039/D3FB00069A]. Sustainable Food Technology, 2(1), 152-161. https://doi.org/10.1039/D3FB00069A

KAUR, S., & UBEYITOGULLARI, A. (2023). **Extraction of phenolic compounds from rice husk via ethanol-water-modified supercritical carbon dioxide**. Heliyon, 9(3), e14196. https://doi.org/https://doi.org/10.1016/j.heliyon 2023.e14196

KAUR, S., & UBEYITOGULLARI, A. (2024). **In vitro digestion of starch and protein aerogels generated from defatted rice bran via supercritical carbon dioxide drying**.

Food Chemistry, 455, 139833. https://doi.org/https://doi.org/10.1016/j.foodchem.2024.139833

KIM, H., JUNG, Y. S., SONG, N. E., YOO, M., SEO, D. H., KIM, H. S., & NAM, T. G. (2024). **Ultrasound-assisted extraction of major anthocyanins in Korean black raspberries (Rubus coreanus Miquel) using natural deep eutectic solvents.** Lwt-Food Science and Technology, 199, Article 116121. https://doi.org/10.1016/j.lwt.2024.116121

KLINGER, E., SALMINEN, H., BAUSE, K., & WEISS, J. (2024). **Interactions between lipid oxidation and anthocyanins from black carrots in ω-3 fatty acid-rich flaxseed oil-in-water emulsions.** European Food Research and Technology, 250(12), 2973-2987. https://doi.org/10.1007/s00217-024-04604-x

KUAN, L.-Y., THOO, Y.-Y., & SIOW, L.-F. (2016). **Bioactive components, ABTS radical scavenging capacity and physical stability of orange, yellow and purple sweet potato (pomoea batatas) powder processed by convection- or vacuum-drying methods.** International Journal of Food Science & Technology, 51(3), 700-709. https://doi.org/https://doi.org/10.1111/ijfs.13023

KUANG, T. R., MI, H. Y., FU, D. J., JING, X., CHEN, B. Y., MOU, W. J., & PENG, X. F. (2015). **Fabrication of Poly(lactic Acid)/graphene Oxide Foams with Highly Oriented and Elongated Cell Structure via Unidirectional Foaming Using Supercritical Carbon Dioxide**. Ind. Eng. Chem. Res., 54, 758.

KUMAR, M., DAHUJA, A., SACHDEV, A., KAUR, C., VARGHESE, E., SAHA, S., & SAIRAM, K. V. S. S. (2019). **Valorisation of black carrot pomace: microwave assisted extraction of bioactive phytoceuticals and antioxidant activity using Box–Behnken design.** Journal of Food Science and Technology, 56(2), 995-1007. https://doi.org/10.1007/s13197-018-03566-9
KUMKUM, R., ASTON-MOURNEY, K., MCNEILL, B. A., HERNÁNDEZ, D., & RIVERA, L. R. (2024). **Bioavailability of Anthocyanins: Whole Foods versus Extracts.** Nutrients, 16(10), Article 1403. https://doi.org/10.3390/nu16101403

KUTLU, N., ISCI, A., SAKIYAN, O., & YILMAZ, A. E. (2021). Extraction of Phenolic Compounds from Cornelian Cherry (Cornus mas L.) **Using Microwave and Ohmic Heating Assisted Microwave Methods.** Food and Bioprocess Technology, 14(4), 650-664. https://doi.org/10.1007/s11947-021-02588-0

LAILA, U., YULIYANTO, P., HARIYADI, S., JULIGANI, B., INDRIANINGSIH, A. W., KRISTANTI, D., ARIANI, D., HERAWATI, E. R. N., IWANSYAH, A. C., ANWAR, M., GINTING, E., PANGESTU, A., ANDRIANA, Y., PURWANINGSIH, H., INDRASARI, S. D., NURMAHMUDI, N., HARIADI, H., HOO, A. W., & WARDHANI, R. (2025). I**ncorporation of low-pH purple-fleshed sweet potato (Ipomoea batatas L.) anthocyanin extract into a sucrose matrix: Characterization and application in powdered beverage.** Food and Bioproducts Processing, 151, 172-188. https://doi.org/10.1016/j.fbp.2025.03.008

LAKSHMIKANTHAN, M., MUTHU, S., KRISHNAN, K., ALTEMIMI, A. B., HAIDER, N. N., GOVINDAN, L., SELVAKUMARI, J., ALKANAN, Z. T., CACCIOLA, F., & FRANCIS, Y. M. (2024). **A comprehensive review on anthocyanin-rich foods: Insights into extraction, medicinal potential, and sustainable applications**. Journal of Agriculture and Food Research, 17, Article 101245. https://doi.org/10.1016/j.jafr.2024.101245

LAO, F., & GIUSTI, M. M. (2016). **Quantification of Purple Corn (Zea mays L.) Anthocyanins Using Spectrophotometric and HPLC Approaches: Method Comparison and Correlation.** Food Analytical Methods, 9(5), 1367-1380. https://doi.org/10.1007/s12161-015-0318-0

LEICHTWEIS, M. G., PEREIRA, C., PRIETO, M. A., BARREIRO, M. F., BARALDI, I. J., BARROS, L., & FERREIRA, I. C. F. R. (2019). U**ltrasound as a Rapid and Low-Cost Extraction Procedure to Obtain Anthocyanin-Based Colorants from Prunus spinosa L. Fruit Epicarp: Comparative Study with Conventional Heat-Based Extraction.** Molecules, 24(3), 573. https://www.mdpi.com/1420-3049/24/3/573

LEONARSKI, E., KUASNEI, M., DOS SANTOS, E. H., BENVENUTTI, L., MORAES, P. A. D., CESCA, K., DE OLIVEIRA, D., & ZIELINSKI, A. A. F. (2025). **Ultrasound and microwave-assisted extractions as green and efficient approaches to recover anthocyanin from black rice bran. Biomass Conversion and Biorefinery**, 15(5), 7251-7264. https://doi.org/10.1007/s13399-024-05479-4

LI, A., XIAO, R., HE, S., AN, X., HE, Y., WANG, C., YIN, S., WANG, B., SHI, X., & HE, J. (2019). **Research Advances of Purple Sweet Potato Anthocyanins: Extraction, Identification, Stability, Bioactivity, Application, and Biotransformation.** Molecules, 24(21), 3816. https://www.mdpi.com/1420-3049/24/21/3816

LI, F. F., SUN, Q. C., CHEN, L., ZHANG, R. J., & ZHANG, Z. P. (2025). **Unlocking the health potential of anthocyanins: a structural insight into their varied biological effects**. Critical Reviews in Food Science and Nutrition, 65(11), 2134-2154. https://doi.org/10.1080/10408398.2024.2328176

LI, L., ZHOU, C., XU, Y., ZHENG, X., WU, Y., YAN, B., ZHONG, K., & GAO, H. (2025). **An intelligent biomass aerogel label loaded with anthocyanin from wasted peanut seed coat for monitoring chilled chicken freshness.** Food Hydrocolloids, 160, 110731. https://doi.org/https://doi.org/10.1016/j.foodhyd.2024.110731

LI, L., ZHOU, C. M., XU, Y. J., ZHENG, X., WU, Y. P., YAN, B., ZHONG, K., & GAO, H. (2025). **An intelligent biomass aerogel label loaded with anthocyanin from wasted peanut seed coat for monitoring chilled chicken freshness**. Food Hydrocolloids, 160, Article 110731. https://doi.org/10.1016/j.foodhyd.2024.110731

LI, P., YANG, C., XU, X., MIAO, C., HE, T., JIANG, B., & WU, W. (2022). **Preparation of Bio-Based Aerogel and Its Adsorption Properties for Organic Dyes**. Gels, 8(11), 755. https://www.mdpi.com/2310-2861/8/11/755

LI, Q., ZHANG, F., WANG, Z., FENG, Y., & HAN, Y. (2023). **Advances in the Preparation, Stability, Metabolism, and Physiological Roles of Anthocyanins: A Review**. FOODS, 12(21). https://doi.org/10.3390/foods12213969

LIAO, L., HUIHUI, L., & WU, W. (2021). **Processability and physical-functional properties of purple sweet potato powder as influenced by explosion puffing drying.** JOURNAL OF FOOD MEASUREMENT AND CHARACTERIZATION, 15(1), 944-952. https://doi.org/10.1007/s11694-020-00688-7

LIDIKOVÁ, J., CERYOVÁ, N., MUSILOVÁ, J., VOLLMANNOVÁ, A., TÓTH, T., GRYGORIEVA, O., & BRINDZA, J. (2025). **Antioxidant activity, polyphenol, and anthocyanin content of black chokeberry (Aronia melanocarpa l.).** Journal of

Microbiology Biotechnology and Food Sciences, 14(4). https://doi.org/10.55251/jmbfs.11620

LIN, X., LI, S., YIN, J., CHANG, F., WANG, C., HE, X., HUANG, Q., & ZHANG, B. (2020). **Anthocyanin-loaded double Pickering emulsion stabilized by octenylsuccinate quinoa starch: Preparation, stability and in vitro gastrointestinal digestion.** Int J Biol Macromol, 152, 1233-1241. https://doi.org/10.1016/j.ijbiomac.2019.10.220

LIU, C., XUE, H., SHEN, L., LIU, C., ZHENG, X., SHI, J., & XUE, S. (2019). **Improvement of anthocyanins rate of blueberry powder under variable power of microwave extraction**. Separation and Purification Technology, 226, 286-298. https://doi.org/https://doi.org/10.1016/j.seppur.2019.05.096

LIU, H., LIN, S., FENG, Y., & THEATO, P. (2017). **CO2-Responsive Polymer Materials**. Polym. Chem., 8, 12.
LIU, R., ZHANG, P., ZHANG, S., YAN, T., XIN, J., & ZHANG, X. (2016). **Ionic Liquids and Supercritical Carbon Dioxide: Green and Alternative Reaction Media for Chemical Processes.** Rev. Chem. Eng., 32(6), 587.

LÓPEZ, C. J., CALEJA, C., PRIETO, M. A., BARREIRO, M. F., BARROS, L., & FERREIRA, I. C. F. R. (2018). **Optimization and comparison of heat and ultrasound assisted extraction techniques to obtain anthocyanin compounds from Arbutus unedo L. Fruits.** Food Chemistry, 264, 81-91. https://doi.org/https://doi.org/10.1016/j.foodchem.2018.04.103

LU, Z. G., WANG, X. W., LIN, X. Y., MOSTAFA, S., ZOU, H. L., WANG, L., & JIN, B. (2024). **Plant anthocyanins: Classification, biosynthesis, regulation, bioactivity, and health benefits.** Plant Physiology and Biochemistry, 217, Article 109268. https://doi.org/10.1016/j.plaphy.2024.109268

LV, X., HONG, Y., ZHOU, Q., & JIANG, C. (2021). **Structural Features and Digestibility of Corn Starch With Different Amylose Content**. Front Nutr, 8, 692673. https://doi.org/10.3389/fnut.2021.692673

MAAZ, M., SULTAN, M. T., NOMAN, A. M., ZAFAR, S., TARIQ, N., HUSSAIN, M., IMRAN, M., MUJTABA, A., YEHUALA, T. F., MOSTAFA, E. M., SELIM, S., AL JAOUNI, S. K., ALSAGABY, S. A., & AL ABDULMONEM, W. (2025). **Anthocyanins: From Natural Colorants to Potent Anticancer Agents.** Food Science & Nutrition, 13(5), Article e70232. https://doi.org/10.1002/fsn3.70232

MACHADO, A. P. D. F., PASQUEL-REÁTEGUI, J. L., BARBERO, G. F., & MARTÍNEZ, J. (2015). **Pressurized liquid extraction of bioactive compounds from blackberry (Rubus fruticosus L.) residues: a comparison with conventional methods.** Food Research International, 77, 675-683. https://doi.org/10.1016/j.foodres.2014.12.042

MAITY, S. K. (2015). **Opportunities, Recent Trends and Challenges of Integrated Biorefinery: Part II.** Renewable Sustainable Energy Rev., 43, 1446.

MALEKI, H., DURAES, L., & PORTUGAL, A. (2015). **Synthesis of Mechanically Reinforced Silica Aerogels via Surface-Initiated Reversible Addition-Fragmentation Chain Transfer (RAFT) Polymerization.** J. Mater. Chem. A, 3, 1594.

MANOUSI, N., SARAKATSIANOS, I., & SAMANIDOU, V. (2019). **Extraction Techniques of Phenolic Compounds and Other Bioactive Compounds From**

**Medicinal and Aromatic Plants**. In Engineering Tools in the Beverage Industry (pp. 283-314). https://doi.org/10.1016/b978-0-12-815258-4.00010-x

MATOS, Í. T. S. R.; MOTA, M. L. F.; Carmo, E. J. D. **Using Purple Amerindian Yam (Cará Roxo, Dioscorea Trifida L.) as Brewing Adjunct: Technical and Sensorial Analysis**. Ciência e Tecnologia de Alimentos 2022, 42, e48521. DOI: 10.1590/fst.4852.

MENGIST, M. F., ABID, M. A., GRACE, M. H., SETH, R., BASSIL, N., KAY, C. D., DARE, A. P., CHAGNÉ, D., ESPLEY, R., NEILSON, A., LILA, M. A., FERRUZZI, M., & IORIZZO, M. (2025). **Identification and functional characterization of BAHD acyltransferases associated with anthocyanin acylation in blueberry.** Horticulture Research, 12(5), Article uhaf041. https://doi.org/10.1093/hr/uhaf041

MEREGALLI, M. M., PUTON, B. M. S., CAMERA, F. D. M., AMARAL, A. U., ZENI, J., CANSIAN, R. L., MIGNONI, M. L., & BACKES, G. T. (2020). **Conventional and ultrasound-assisted methods for extraction of bioactive compounds from red araçá peel (Psidium cattleianum Sabine)**. Arabian Journal of Chemistry, 13(6), 5800-5809. https://doi.org/https://doi.org/10.1016/j.arabjc.2020.04.017

MIRMOEINI, S. S., MORADI, M., TAJIK, H., ALMASI, H., & GAMA, F. M. (2023). **Cellulose/Salep-based intelligent aerogel with red grape anthocyanins: Preparation, characterization and application in beef packaging.** Food Chemistry, 425, 136493. https://doi.org/https://doi.org/10.1016/j.foodchem.2023.136493

MOHAMMADI, Z., NIKKHOU, S., SARABI-AGHDAM, V., CHOOBKAR, N., & AKHAVAN-MAHDAVI, S. (2025). **Development of Anthocyanin-Enriched Pastilles Using Aerogels From Eggplant Skin Extracts.** Journal of Food Processing and Preservation, 2025(1), Article 9952019. https://doi.org/10.1155/jfpp/9952019

MOHD NAWI, N., MUHAMAD, II, & MOHD MARSIN, A. (2015). **The physicochemical properties of microwave-assisted encapsulated anthocyanins from Ipomoea batatas as affected by different wall materials.** Food Sci Nutr, 3(2), 91-99. https://doi.org/10.1002/fsn3.132

MOJO-QUISANI, A., LICONA-PACCO, K., CHOQUE-QUISPE, D., CALLA-FLOREZ, M., LIGARDA-SAMANEZ, C. A., MAMANI-CONDORI, R., FLOREZ-HUARACHA, K., & HUAMANÍ-MELENDEZ, V. J. (2024). **Physicochemical properties of starch of four varieties of native potatoes.** Heliyon, 10(16), e35809. https://doi.org/10.1016/j.heliyon.2024.e35809

MONTES, L., ROSELL, C. M., & MOREIRA, R. (2022). **Rheological Properties of Corn Starch Gels With the Addition of Hydroxypropyl Methylcellulose of Different Viscosities** [Original Research]. FRONTIERS IN NUTRITION, 9. https://doi.org/10.3389/fnut.2022.866789

MORAES, D. P., MACHADO, M. L., FARIAS, C. A. A., BARIN, J. S., ZABOT, G. L., LOZANO-SÁNCHEZ, J., FERREIRA, D. F., VIZZOTTO, M., LEYVA-JIMENEZ, F. J., DA SILVEIRA, T. L., RIES, E. F., & BARCIA, M. T. (2020). **Effect of Microwave Hydrodiffusion and Gravity on the Extraction of Phenolic Compounds and Antioxidant Properties of Blackberries (Rubus spp.): Scale-Up Extraction**. Food and Bioprocess Technology, 13(12), 2200-2216. https://doi.org/10.1007/s11947-020-02557-z

MUANGRAT, R., PONGSIRIKUL, I., & BLANCO, P. H. (2018). **Ultrasound assisted extraction of anthocyanins and total phenolic compounds from dried cob of purple waxy corn using response surface methodology.** Journal of Food Processing and Preservation, 42(2), e13447. https://doi.org/https://doi.org/10.1111/jfpp.13447

NGUYEN, H. T., & TRAN, P. H. (2016). **An Extremely Efficient and Green Method for the Acylation of Secondary Alcohols, Phenols and Naphthols with a Deep Eutectic Solvent as the Catalyst.** RSC Adv., 6, 98365.

NGUYEN, T. K., TIEN, N. N. T., VO, H. T. D., VU, L. T. K., & LE, N. L. (2024). **Comparison between anthocyanins from roselle and mulberry as pH indicators in development of intelligent films**. Journal of Food Measurement and Characterization, 18(8), 6973-6985. https://doi.org/10.1007/s11694-024-02708-2

NOMAN, A. M., SULTAN, M. T., MAAZ, M., MAZHAR, A., TARIQ, N., IMRAN, M., HUSSAIN, M., MUJTABA, A., ABDELGAWAD, M. A., MOSTAFA, E. M., GHONEIM, M. M., SELIM, S., & AL JBAWI, E. (2025). **Nutraceutical Potential of Anthocyanins: A Comprehensive Treatise.** Food Science & Nutrition, 13(5), Article e70164. https://doi.org/10.1002/fsn3.70164

NUNES MATTOS, G., PESSANHA DE ARAÚJO SANTIAGO, M. C., SAMPAIO DORIA CHAVES, A. C., ROSENTHAL, A., VALERIANO TONON, R., & CORREA CABRAL, L. M. (2022). **Anthocyanin Extraction from Jaboticaba Skin (Myrciaria cauliflora Berg.) Using Conventional and Non-Conventional Methods**. Foods, 11(6).

NURDJANAH, S., NURDIN, S. U., ASTUTI, S., & MANIK, V. E. (2022). **Chemical Components, Antioxidant Activity, and Glycemic Response Values of Purple Sweet Potato Products**. Int J Food Sci, 2022, 7708172. https://doi.org/10.1155/2022/7708172

OLADZADABBASABADI, N., MOHAMMADI NAFCHI, A., GHASEMLOU, M., ARIFFIN, F., SINGH, Z., & AL-HASSAN, A. A. (2022). **Natural anthocyanins: Sources, extraction, characterization, and suitability for smart packaging.** Food Packaging and Shelf Life, 33, 100872. https://doi.org/https://doi.org/10.1016/j.fpsl.2022.100872

OLIVEIRA, H. F. A. F. B. N. M. N. d. F. V. F. I. A. a. A. A. I. V., In silico approaches of, p., & therapeutic, E. (2020). **Molecules**, 25(17).

OTTO, S., KRASOWSKA, M., MACWILLIAMS, S., BEATTIE, D., & BLENCOWE, A. (2024). **The solid-state stability of anthocyanins under various conditions and the implications for storage and shelf-life**. Dyes and Pigments, 231, Article 112367. https://doi.org/10.1016/j.dyepig.2024.112367

PAGE, M. J., MCKENZIE, J. E., BOSSUYT, P. M., BOUTRON, I., HOFFMANN, T. C., MULROW, C. D., SHAMSEER, L., TETZLAFF, J. M., AKL, E. A., BRENNAN, S. E., CHOU, R., GLANVILLE, J., GRIMSHAW, J. M., HRÓBJARTSSON, A., LALU, M. M., LI, T., LODER, E. W., MAYO-WILSON, E., MCDONALD, S., . . . MOHER, D. (2021). **The PRISMA 2020 statement: an updated guideline for reporting systematic reviews**. BMJ, 372, n71. https://doi.org/10.1136/bmj.n71

PALENCIA-ARGEL, M., RODRÍGUEZ-VILLAMIL, H., BERNAL-CASTRO, C., DÍAZ-MORENO, C., & FUENMAYOR, C. A. (2025). **Development of a Plant-Based Beverage with Synbiotic Potential Using Anthocyanin-Rich Fruits**. Journal of

Culinary Science & Technology, 23(3), 600-626. https://doi.org/10.1080/15428052.2024.2325922

PATNI, N. (2024). **An improved supply of anthocyanin dye for creation of effective dye-sensitized solar cells grounded on natural dyes**. International Journal of Materials Research, 115(9), 734-741. https://doi.org/10.1515/ijmr-2024-0076

PEI, Z. Q., HUANG, Y. F., NI, J. B., LIU, Y., & YANG, Q. S. (2024). **For a Colorful Life: Recent Advances in Anthocyanin Biosynthesis during Leaf Senescence**. Biology-Basel, 13(5), Article 329. https://doi.org/10.3390/biology13050329

PEREIRA, R. N., COELHO, M. I., GENISHEVA, Z., FERNANDES, J. M., VICENTE, A. A., PINTADO, M. E., & TEIXEIRA, e. J. A. (2020). **Using Ohmic Heating effect on grape skins as a pretreatment for anthocyanins extraction.** FOOD AND BIOPRODUCTS PROCESSING, 124, 320-328. https://doi.org/https://doi.org/10.1016/j.fbp.2020.09.009

PICOS-SALAS, M. A., LEYVA-LÓPEZ, N., BASTIDAS-BASTIDAS, P. J., ANTUNES-RICARDO, M., CABANILLAS-BOJÓRQUEZ, L. A., ANGULO-ESCALANTE, M. A., HEREDIA, J. B., & GUTIÉRREZ-GRIJALVA, E. P. (2024). **Supercritical CO(2) extraction of naringenin from Mexican oregano (Lippia graveolens): its antioxidant capacity under simulated gastrointestinal digestion.** Sci Rep, 14(1), 1146. https://doi.org/10.1038/s41598-023-50997-2

QIU, K. H., WANG, Y. J., CHENG, K. L., JIANG, L. Q., LI, X., & ZHANG, J. L. (2025). **Preparation, characterization and analysis of anthocyanin arbutin co-amorphous complexes and evaluation of the inhibition of tyrosinase.** International Journal of Biological Macromolecules, 311, Article 143600. https://doi.org/10.1016/j.ijbiomac.2025.143600

RAJ, R., SHEIKH, S. A., SINGH, S. A., & SHETTY, N. P. (2024). **Improvement of storage stability and bioaccessibility of microencapsulated black carrot ( Daucus Carota ssp. sativus ) anthocyanins using maltodextrin and sericin protein combinations as wall material.** Food Bioscience, 61, Article 104666. https://doi.org/10.1016/j.fbio.2024.104666

REMEDIO, L. N., & QUINAYÁ, C. P. (2024). I**ntelligent Packaging Systems with Anthocyanin: Influence of Different Polymers and Storage Conditions.** Polymers, 16(20), Article 2886. https://doi.org/10.3390/polym16202886

REN, F., LIU, X., XIE, F., & WANG, S. (2024). **Phase transition and gel properties of chemically modified cassava starch in choline acetate and water mixtures**. Carbohydr Polym, 345, 122560. https://doi.org/10.1016/j.carbpol.2024.122560

REZENDE, Y., NOGUEIRA, J. P., & NARAIN, N. (2017). **Comparison and optimization of conventional and ultrasound assisted extraction for bioactive compounds and antioxidant activity from agro-industrial acerola (Malpighia emarginata DC) residue**. Lwt-Food Science and Technology, 85, 158-169. https://doi.org/10.1016/j.lwt.2017.07.020

RODRIGUES, L. M., ROMANINI, E. B., SILVA, E., PILAU, E. J., DA COSTA, S. C., & MADRONA, G. S. (2020). **Camu-camu bioactive compounds extraction by ecofriendly sequential processes (ultrasound assisted extraction and reverse**

**osmosis).** ULTRASONICS SONOCHEMISTRY, 64, 105017. https://doi.org/https://doi.org/10.1016/j.ultsonch.2020.105017

ROJAS-OCAMPO, E., TORREJON-VALQUI, L., MUNOZ-ASTECKER, L. D., MEDINA-MENDOZA, M., MORI-MESTANZA, D., & CASTRO-ALAYO, E. M. (2021). **Antioxidant capacity, total phenolic content and phenolic compounds of pulp and bagasse of four Peruvian berries.** Heliyon, 7(8), e07787. https://doi.org/10.1016/j.heliyon 2021.e07787

ROSELL, M. d. l. Á., QUIZHPE, J., AYUSO, P., PEÑALVER, R., & NIETO, G. (2024). **Proximate Composition, Health Benefits, and Food Applications in Bakery Products of Purple-Fleshed Sweet Potato (Ipomoea batatas L.) and Its By-Products: A Comprehensive Review**. Antioxidants, 13(8), 954. https://www.mdpi.com/2076-3921/13/8/954

SADAF, N., TUHANIOGLU, A., HETTIARACHCHY, N., & UBEYITOGULLARI, A. (2024). **Effect of a novel drying method based on supercritical carbon dioxide on the physicochemical properties of sorghum proteins** [10.1039/D3RA07426A]. RSC Advances, 14(9), 5851-5862. https://doi.org/10.1039/D3RA07426A

SAINI, R. K., KHAN, M. I., SHANG, X. M., KUMAR, V., KUMARI, V., KESARWANI, A., & KO, E. Y. (2024). **Dietary Sources, Stabilization, Health Benefits, and Industrial Application of Anthocyanins-A Review.** Foods, 13(8), Article 1227. https://doi.org/10.3390/foods13081227

SÁNCHEZ-VICENTE, Y., STEVENS, L. A., PANDO, C., JOSÉ, M., SNAPE, C. E., DRAGE, T. C., & CABAÑAS, A. (2015). **A New Sustainable Route in Supercritical CO2 to Functionalize Silica SBA-15 with 3-Aminopropyltrimethoxysilane as Material for Carbon Capture.** Chem. Eng. J., 264, 886.

SENDRI, N., & BHANDARI, P. (2024). **Anthocyanins: a comprehensive review on biosynthesis, structural diversity, and industrial applications**. Phytochemistry Reviews, 23(6), 1913-1974. https://doi.org/10.1007/s11101-024-09945-9

SENEVIRATHNA, N., HASSANPOUR, M., O'HARA, I., & KARIM, A. (2024). **Extraction, Isolation, Identification, and Characterization of Anthocyanin from Banana Inflorescence by Liquid Chromatography-Mass Spectroscopy and Its pH Sensitivity**. Biomimetics, 9(11), Article 702. https://doi.org/10.3390/biomimetics9110702

SHI, C. Y., GUO, C. T., WANG, S., LI, W. X., ZHANG, X., LU, S., NING, C., & TAN, C. (2024). **The mechanism of pectin in improving anthocyanin stability and the application progress of their complexes: A review.** Food Chemistry-X, 24, Article 101955. https://doi.org/10.1016/j.fochx.2024.101955

SIGURDSON, G. T., TANG, P., & GIUSTI, M. M. (2017). **Natural Colorants: Food Colorants from Natural Sources.** Annual Review of Food Science and Technology, 8(Volume 8, 2017), 261-280. https://doi.org/https://doi.org/10.1146/annurev-food-030216-025923

SILVA, F. T., FONSECA, L. M., BRUNI, G. P., CRIZEL, R. L., OLIVEIRA, E. G., ZAVAREZE, E. D. R., & DIAS, A. R. G. (2023). **Absorbent bioactive aerogels based on germinated wheat starch and grape skin extract.** Int J Biol Macromol, 249, 126108. https://doi.org/10.1016/j.ijbiomac.2023.126108

SMIRNOVA, I., & GURIKOV, P. (2017). **Aerogels in Chemical Engineering: Strategies Toward Tailor-Made Aerogels.** Annu Rev Chem Biomol Eng, 8, 307-334. https://doi.org/10.1146/annurev-chembioeng-060816-101458

SOARE, R., DINU, M., BABEANU, C., & SOARE, M. (2020). **Evaluation and comparison of antioxidant activity and biochemical compounds in some coloured potato cultivars.** Plant, Soil and Environment, 66(No. 6), 281-286. https://doi.org/10.17221/202/2020-pse

SOHANY, M., TAWAKKAL, I. S. M. A., ARIFFIN, S. H., SHAH, N. N. A. K., & YUSOF, Y. A. (2021). **Characterization of Anthocyanin Associated Purple Sweet Potato Starch and Peel-Based pH Indicator Films.** FOODS, 10(9), 2005. https://www.mdpi.com/2304-8158/10/9/2005

SOHRABI, N., ALMASI, H., & MORADI, M. (2024). **Controlled porosity intelligent aerogel based on chitosan nanofiber, anthocyanins and starch nanoparticles: Preparation, characterization and application in monitoring food spoilage**. Food Hydrocolloids, 156, Article 110261. https://doi.org/10.1016/j.foodhyd.2024.110261

SONG, A. N., WU, Y. L., & LI, C. W. (2025). D**evelopment and application of a time-temperature hydroxyethyl cellulose ink based on Clitoria ternatea L. blue petals anthocyanin and N-Hydroxyphthalimide for food freshness monitoring.** International Journal of Biological Macromolecules, 299, Article 140060. https://doi.org/10.1016/j.ijbiomac.2025.140060

STANCA, L., BILTEANU, L., BUJOR, O. C., ION, V. A., PETRE, A. C., BADULESCU, L., GEICU, O. I., PISOSCHI, A. M., SERBAN, A. I., & GHIMPETEANU, O. M. (2024). **Development of Functional Foods: A Comparative Study on the Polyphenols and Anthocyanins Content in Chokeberry and Blueberry Pomace Extracts and Their Antitumor Properties**. Foods, 13(16), Article 2552. https://doi.org/10.3390/foods13162552

SUDHAKARAN, G. (2024). **Artificial food dyes are toxic: Neurobehavioral implications in children**. Brain and Spine, 4, 102869. https://doi.org/https://doi.org/10.1016/j.bas.2024.102869

SURESH, S., & VELLAPANDIAN, C. (2024). **Assessment of oral toxicity and safety profile of cyanidin: acute and subacute studies on anthocyanin.** Future Science Oa, 10(1), Article Fso982. https://doi.org/10.2144/fsoa-2023-0322

TAN, J., LI, Q., XUE, H., & TANG, J. (2020). **Ultrasound-assisted enzymatic extraction of anthocyanins from grape skins: optimization, identification, and antitumor activity**. JOURNAL OF FOOD SCIENCE, 85(11), 3731-3744. https://doi.org/https://doi.org/10.1111/1750-3841.15497

TANG, S. Y., SI, X., ZANG, Z. H., GUI, H. L., XIE, X., WANG, L., HE, Y., YANG, B. R., & LI, B. (2024). **Mildly preheating induced conformational changes of soy protein isolates contributed to the binding interaction with blueberry anthocyanins for stabilization**. Food Hydrocolloids, 155, Article 110209. https://doi.org/10.1016/j.foodhyd.2024.110209

TUHANIOGLU, A., & UBEYITOGULLARI, A. (2022). **Extraction of High-Value Lipids and Phenolic Compounds from Sorghum Bran via a Sequential Supercritical**

**Carbon Dioxide Approach.** ACS Food Science & Technology, 2(12), 1879-1887. https://doi.org/10.1021/acsfoodscitech.2c00266

TUNNISA, F., NUR FARIDAH, D., AFRIYANTI, A., ROSALINA, D., ANA SYABANA, M., DARMAWAN, N., & DEWI YULIANA, N. (2022). **Antioxidant and antidiabetic compounds identification in several Indonesian underutilized Zingiberaceae spices using SPME-GC/MS-based volatilomics and in silico methods**. Food Chemistry: X, 14, 100285. https://doi.org/https://doi.org/10.1016/j.fochx.2022.100285

UBEYITOGULLARI, A., & CIFTCI, O. N. (2016). **Formation of nanoporous aerogels from wheat starch.** Carbohydrate Polymers, 147, 125-132. https://doi.org/https://doi.org/10.1016/j.carbpol.2016.03.086

UBEYITOGULLARI, A., MOREAU, R., ROSE, D. J., ZHANG, J., & CIFTCI, O. N. (2019). **Enhancing the Bioaccessibility of Phytosterols Using Nanoporous Corn and Wheat Starch Bioaerogels**. European Journal of Lipid Science and Technology, 121(1), 1700229. https://doi.org/https://doi.org/10.1002/ejlt.201700229

WANG, H., YANG, Q., FERDINAND, U., GONG, X., QU, Y., GAO, W., IVANISTAU, A., FENG, B., & LIU, M. (2020). **Isolation and characterization of starch from light yellow, orange, and purple sweet potatoes.** Int J Biol Macromol, 160, 660-668. https://doi.org/10.1016/j.ijbiomac.2020.05.259

WANG, J., LIU, Z., LI, X., LIU, G., & ZHAO, J. (2023). **Elucidating structure of pectin in ramie fiber to customize enzyme cocktail for high-efficiency enzymatic degumming.** Carbohydrate Polymers, 314, 120954. https://doi.org/https://doi.org/10.1016/j.carbpol.2023.120954

WANG, L., YANG, S., YANG, Y., JIANG, H., HUANG, W., BIAN, Y., & LI, B. (2024). **Effects of endogenous anthocyanins from purple corn on the quality, physicochemical properties and antioxidant capacity of bread.** JOURNAL OF FOOD MEASUREMENT AND CHARACTERIZATION, 18(6), 4678-4691. https://doi.org/10.1007/s11694-024-02523-9

WEISS, V., OKUN, Z., & SHPIGELMAN, A. (2024). **Ternary anthocyanin-iron ion-pectin interactions: Structure-dependent formation and spectral properties as potential Tools for more stable blue colorants.** Food Hydrocolloids, 153, Article 110035. https://doi.org/10.1016/j.foodhyd.2024.110035

WU, T. Y., TSAI, C. C., HWANG, Y. T., & CHIU, T. H. (2012). **Effect of Antioxidant Activity and Functional Properties of Chingshey Purple Sweet Potato Fermented Milk by Lactobacillus acidophilus, L. delbrueckii subsp lactis, and L. gasseri Strains.** JOURNAL OF FOOD SCIENCE, 77(1), M2-M8. https://doi.org/10.1111/j.1750-3841.2011.02507.x

WU, Y., LI, B.-h., CHEN, M.-m., & LIU, B. (2024). **An aerogel-based intelligent active packaging with the dual functions of spoilage detection and freshness preservation. Food Hydrocolloids,** 156, 110160. https://doi.org/https://doi.org/10.1016/j.foodhyd.2024.110160

XU, A., GUO, K., LIU, T., BIAN, X., ZHANG, L., & WEI, C. (2018). **Effects of Different Isolation Media on Structural and Functional Properties of Starches from Root Tubers of Purple, Yellow and White Sweet Potatoes.** Molecules, 23(9), 2135. https://www.mdpi.com/1420-3049/23/9/2135

XUE, H. K., ZHAO, J. D., WANG, Y., SHI, Z. M., XIE, K. F., LIAO, X. J., & TAN, J. Q. (2024). **Factors affecting the stability of anthocyanins and strategies for improving their stability: A review.** Food Chemistry-X, 24, Article 101883. https://doi.org/10.1016/j.fochx.2024.101883

YAN, M. H., HUANG, X. X., XIE, N. C., ZHAO, T. Y., ZHU, M. Z., LI, J., & WANG, K. B. (2024). **Advances in Purple Tea Research: Chemical Compositions, Anthocyanin Synthesis and Regulation, Processing, and Health Benefits.** Horticulturae, 10(1), Article 50. https://doi.org/10.3390/horticulturae10010050

YANG, L., LI, S., CHEN, Y., WANG, M., YU, J. J., BAI, W. Q., & HONG, L. (2024). **Combined Metabolomics and Network Pharmacology Analysis Reveal the Effect of Rootstocks on Anthocyanins, Lipids, and Potential Pharmacological Ingredients of Tarroco Blood Orange (Citrus sinensis L. Osbeck).** Plants-Basel, 13(16), Article 2259. https://doi.org/10.3390/plants13162259

YI, J., QIU, M., ZHU, Z., DONG, X., ANDREW DECKER, E., & MCCLEMENTS, D. J. (2021). **Robust and recyclable magnetic nanobiocatalysts for extraction of anthocyanin from black rice.** Food Chemistry, 364, 130447. https://doi.org/https://doi.org/10.1016/j.foodchem.2021.130447

YIN, M., XIE, J., XIE, C., LUO, M., & YANG, X. (2022). **Extration, identification and stability ananlysis of anthocyanins from organic Guizhou blueberries in China.** Food Science and Technology, 42. https://doi.org/10.1590/fst.33520

YONG, H., WANG, X., SUN, J., FANG, Y., LIU, J., & JIN, C. (2018). C**omparison of the structural characterization and physicochemical properties of starches from seven purple sweet potato varieties cultivated in China**. Int J Biol Macromol, 120(Pt B), 1632-1638. https://doi.org/10.1016/j.ijbiomac.2018.09.182

YUN, D. W., YONG, H. M., XU, F. F., LI, N., GUAN, T. Z., & LIU, J. (2025). **Purple sweet potato anthocyanin-g-dialdehyde locust bean gum: An innovative polymeric colorant with good stability and application potential in food intelligent packaging**. Food Hydrocolloids, 163, Article 111121. https://doi.org/10.1016/j.foodhyd.2025.111121

ZANNOU, O., & KOCA, I. (2022). **Greener extraction of anthocyanins and antioxidant activity from blackberry (Rubus spp) using natural deep eutectic solvents.** LWT, 158, 113184. https://doi.org/https://doi.org/10.1016/j.lwt.2022.113184

ZHANG, K., LI, Z. H., ZHAO, W. Y., GUO, J., HASHIM, S. B. H., KHAN, S., SHI, J. Y., HUANG, X. W., & ZOU, X. B. (2024). **Aerogel colorimetric label sensors based on carboxymethyl cellulose/ sodium alginate with black goji anthocyanin for monitoring fish freshness.** International Journal of Biological Macromolecules, 265, Article 130466. https://doi.org/10.1016/j.ijbiomac.2024.130466

ZHANG, L., FAN, G., KHAN, M. A., YAN, Z., & BETA, T. (2020). **Ultrasonic-assisted enzymatic extraction and identification of anthocyanin components from mulberry wine residues.** Food Chemistry, 323, 126714. https://doi.org/https://doi.org/10.1016/j.foodchem.2020.126714

ZHANG, M., MA, J. B., BI, H. T., SONG, J. Y., YANG, H. X., XIA, Z. H., DU, Y. Z., GAO, T. T., & WEI, L. X. (2017). **Characterization and cardioprotective activity of**

**anthocyanins from Nitraria tangutorum Bobr. by-products.** Food & Function, 8(8), 2771-2782. https://doi.org/10.1039/c7fo00569e

ZHANG, S. K., ZENG, D., ZHANG, H., DING, L. W., GUO, D. Y., SUN, P. L., HAN, Z. M., QU, G. Z., SIQIN, T., & YOU, X. L. (2025). **Genome-wide identification and functional analysis of R2R3-MYB genes in Acer pseudosieboldianum: insights into low temperature stress response and anthocyanin biosynthesis.** Bmc Plant Biology, 25(1), Article 795. https://doi.org/10.1186/s12870-025-06782-6

ZHANG, S. S., LIN, S. H., ZHANG, J. H., & LIU, W. (2024). **Ultrasound-assisted natural deep eutectic solvent extraction of anthocyanin from Vitis davidii Foex. pomace: Optimization, identification, antioxidant activity and stability.** Heliyon, 10(12), Article e33066. https://doi.org/10.1016/j.heliyon.2024.e33066

ZHANG, Y. Q., WEI, X. C., & LONG, J. J. (2016). **Ecofriendly Synthesis and Application of Special Disperse Reactive Dyes in Waterless Coloration of Wool with Supercritical Carbon Dioxide.** J. Cleaner Prod., 133, 746.

ZHAO, L., LIU, Y., ZHAO, L., & WANG, Y. (2022). **Anthocyanin-based pH-sensitive smart packaging films for monitoring food freshness.** JOURNAL OF AGRICULTURE AND FOOD RESEARCH, 9, 100340. https://doi.org/https://doi.org/10.1016/j.jafr.2022.100340

ZHAO, S. S., LI, S., LUO, Z. H., ZHOU, Z. Q., LI, N., WANG, Y., YAO, X. S., & GAO, H. (2021). **Bioactive phenylpropanoid derivatives from the fruits of Lycium ruthenicum Murr.** Bioorganic Chemistry, 116, Article 105307. https://doi.org/10.1016/j.bioorg.2021.105307

ZHAO, Y. P., WANG, L., HUANG, Y., EVANS, P. C., LITTLE, P. J., TIAN, X. Y., WENG, J. P., & XU, S. W. (2024). **Anthocyanins in Vascular Health and Disease: Mechanisms of Action and Therapeutic Potential.** Journal of Cardiovascular Pharmacology, 84(3), 289-302. https://doi.org/10.1097/fjc.0000000000001602

ZHENG, H., ZHANG, J., YAN, J., & ZHENG, L. (2016). **An Industrial Scale Multiple Supercritical Carbon Dioxide Apparatus and Its Eco-Friendly Dyeing Production**. J. CO2 Util., 16, 272.

ZHU, L. H., LIAO, Y. W., ZHANG, T. T., ZENG, Z. Y., WANG, J. Z., DUAN, L. J., CHEN, X., LIN, K., LIANG, X. Q., HAN, Z. W., HUANG, Y. K., WU, W. F., HU, H., XU, Z. F., & NI, J. (2024). **Reactive oxygen species act as the key signaling molecules mediating light-induced anthocyanin biosynthesis in Eucalyptus**. Plant Physiology and Biochemistry, 212, Article 108715. https://doi.org/10.1016/j.plaphy.2024.108715

ZOU, J. Q., HUANG, S. N., GAO, Y., FU, W., LIU, Z. Y., FENG, H., & ZHANG, M. D. (2024). **Mutation in BrFLS encoding flavonol synthase induced anthocyanin accumulation in Chinese cabbage.** Theoretical and Applied Genetics, 137(2), Article 44. https://doi.org/10.1007/s00122-024-04552-w

ZUIN, V. G. (2016). **Circularity in Green Chemical Products, Processes and Services: Innovative Routes Based on Integrated Eco-Design and Solution Systems.** Curr. Opin. Green Sus. Chem., 2, 40.